The Analyst

THE ANALYST

THE ANALYTICAL JOURNAL OF THE CHEMICAL SOCIETY

Summaries of Papers in this Issue

Background Emission in Carbon Furnace Atomic-emission Spectrometry

Investigations have shown that with careful optical design and alignment the continuous background emission signal from a carbon furnace can be reduced to a minimum. When no radiation from the furnace wall enters the monochromator directly, the background signal is a result of Rayleigh scattering of furnace-wall radiation by atoms or molecules in the vapour phase of the furnace. Methods for further reducing the continuous background signal, including optical and furnace design, are discussed.

D. LITTLEJOHN and J. M. OTTAWAY

Department of Pure and Applied Chemistry, University of Strathclyde, Cathedral Street, Glasgow, G1 1XL.

Indirect Determination of Uranium by Atomic-absorption Spectrophotometry Using an Air - Acetylene Flame

An indirect method has been developed for the determination of uranium by atomic-absorption spectrophotometry using an air - acetylene flame. Use is made of the reduction of copper(II) by uranium(IV) followed by complex formation of the copper(I) ions so produced with neocuproine (2,9-dimethyl-1,10-phenanthroline) and finally the determination of copper in this complex by atomic-absorption spectrophotometry. The results show that the method can be recommended, provided that care is taken to ensure the complete reduction of uranium(VI) to uranium(IV). The sensitivity of the method is 4.9 μg of uranium and the upper limit 500 μg without dilution.

J. F. ALDER and B. C. DAS

Department of Chemistry, Imperial College of Science and Technology, London, SW7 2AY.

Analytical Optoacoustic Spectrometry
Part IV. A Double-beam Optoacoustic Spectrometer for Use with Solid and Liquid Samples in the Ultraviolet, Visible and Near-infrared Regions of the Spectrum

The design, construction and performance characteristics of a double-beam optoacoustic spectrometer suitable for recording corrected spectra of small solid and liquid samples in the wavelength range 0.25–2.5 μm are described. Typical spectra obtained for rare earth oxides, titanium(IV) oxides, catalase, blood, cystine and kaolinite are presented in order to illustrate the performance of the instrument. The application of the spectrometer to record conventional solution transmittance spectra is also reported.

M. J. ADAMS, B. C. BEADLE and G. F. KIRKBRIGHT

Department of Chemistry, Imperial College of Science and Technology, London, SW7 2AY.

Determination of Residues of the Herbicides Bromacil, Lenacil and Terbacil in Soils by Gas Chromatography

A rapid and sensitive procedure for the determination of residue levels of three uracil herbicides in soils is described. After addition of calcium hydroxide and Celite to the soil the herbicides are eluted from columns with water. After acidification of the eluate and partition into chloroform these herbicides are determined by gas chromatography using a nitrogen-selective detector. Recoveries from a range of soil types are better than 80%, with a sensitivity limit of 20 μg kg^{-1}.

Keywords: *Uracil herbicide determination*; *soils*; *gas chromatography*

DAVID J. CAVERLY

Ministry of Agriculture, Fisheries and Food, Agricultural Development and Advisory Service, Olantigh Road, Wye, Ashford, Kent, TN25 5EL.

and RONALD C. DENNEY

School of Chemistry, Thames Polytechnic, Woolwich, London, SE18 6PF.

Determination of Ronidazole in Pig and Turkey Feeding Stuffs by Gas - Liquid Chromatography

A gas - liquid chromatographic method with flame-ionisation detection has been developed for the determination of ronidazole in complete feeding stuffs. The method is based on the formation of a volatile silyl derivative of ronidazole by reaction with *NO*-bis(trimethylsilyl)acetamide. Recoveries of ronidazole at the level of 60 mg kg^{-1} were about 95%. No interference was observed from grass meal, fish meal or other drugs.

Keywords: *Ronidazole determination*; *animal feeding stuffs*; *prophylactics*; *gas - liquid chromatography*; *silylation*

J. R. HARRIS, P. G. BAKER and GERALDINE ALLISTON

Laboratory of the Government Chemist, Cornwall House, Stamford Street, London, SE1 9NQ.

Acetylation as a Means of End-point Indication in the Catalytic Thermometric Titration of Bases

The acid-catalysed acetylation of alcohols and phenols with acetic anhydride is used to indicate the end-point in the titration of tertiary amines and metal carboxylates with 0.1, 0.01 and 0.001 M perchloric acid in acetic acid.

Mixtures of acetic anhydride with butan-1-ol, 2-methylpropan-2-ol, 4-hydroxy-4-methylpentan-2-one, 3,5-dimethylphenol, pyrocatechol, hydroquinone or quinhydrone are all satisfactory end-point indicators for the determination of pyridine and quinoline derivatives, tertiary aliphatic amines and metal carboxylates, but the acetic anhydride - quinhydrone mixture is superior to the other mixtures for the determination of the very weak bases, antipyrine, caffeine, theophylline and urea. A colour change occurs at the end-point when quinhydrone is the hydroxylic component.

The sharpness of the end-point inflection can be improved by adding dichloromethane, nitromethane or propylene carbonate to the sample solution.

Sample sizes down to about 0.000 1 mequiv can be determined with 0.001 M titrant solution. Precisions are usually better than 0.5% with 0.1 M and 1.0% with 0.01 and 0.001 M titrants.

The influence of intra- and intermolecular hydrogen bonding of the hydroxyl groups in the alcohol and phenol reagents on end-point sharpness is discussed.

Keywords: *Tertiary amine determination*; *metal carboxylate determination*; *non-aqueous thermometric titration*; *alcohol and phenol acetylation*

E. J. GREENHOW

Department of Chemistry, Chelsea College, University of London, Manresa Road, London, SW3 6LX.

The Analyst

Background Emission in Carbon Furnace Atomic-emission Spectrometry

D. Littlejohn and J. M. Ottaway

Department of Pure and Applied Chemistry, University of Strathclyde, Cathedral Street, Glasgow, G1 1XL

Investigations have shown that with careful optical design and alignment the continuous background emission signal from a carbon furnace can be reduced to a minimum.   When no radiation from the furnace wall enters the monochromator directly, the background signal is a result of Rayleigh scattering of furnace-wall radiation by atoms or molecules in the vapour phase of the furnace. Methods for further reducing the continuous background signal, including optical and furnace design, are discussed.

> *Keywords: Atomic-emission spectrometry; carbon furnace atomisation; background emission*

Several recent publications have proposed the use of electrically heated carbon furnace atomisers as sources in atomic-emission spectrometry.[1-4]   Compared with carbon furnace atomic-absorption spectrometry, improved detection limits have been obtained for several elements[1,3] and, by using modified furnace tubes, acceptable detection limits have now also been achieved for a number of volatile elements.[2]   It is likely that the range of applications for which this technique is suitable[3,5-7] will increase rapidly as the advantages of sensitivity, simplicity and relative freedom from matrix and spectral interferences become more widely appreciated.[8]

One of the attractive features of the carbon furnace as an emission source is the nature of the background signal.   Although background molecular emissions from C_2 and CN have been observed,[9,10] the complexity of molecular spectra is very low compared with the complexity of emissions of these and other species from hydrocarbon flames, and it is unlikely that molecular emissions produced by the tube will constitute a serious interference on the important analytical line of any element.[10]   The major contribution to the background is therefore the continuous emission coming from the tube itself, and the magnitude of this signal will have a significant influence on the signal to background ratio and hence on the detection limit of the method.   During the atomisation stage the carbon tube is heated to temperatures in excess of 2 500 K and intense radiation is emitted from the tube wall that is black body in nature and has a higher intensity in the visible region than in the ultraviolet region.   In order for atomic-emission signals from gaseous atoms in the centre of the tube to be measured, the atomic emission must be optically separated from the background emission from the tube wall. The efficiency of this separation will determine the signal to background ratio and the detection limit for every element.

When carbon furnace atomisers were first introduced as alternative atom cells for atomic-absorption spectrometry, they were used in spectrometers designed for use with flames, and the optical alignment was often unsuited to furnace operation.   In a typical early system it was found to be impossible to measure calcium or barium by atomic absorption because tube-wall emission caused overloading of the photomultiplier in the visible region and no atomic-emission signals were observed, even at high concentrations of analyte.[11]   However, optical baffling in the Perkin-Elmer 306 atomic-absorption spectrometer allowed efficient masking of tube-wall emission and use of this spectrometer with commercial carbon furnaces allowed sensitive atomic-emission signals to be measured.[1,2,4]   With this instrument, a residual tube-wall emission signal is obtained[1,4] at all wavelengths, which constitutes the background signal.

One expression of the detection limit in emission spectrometry is that resulting from Harvey's concept of minimum detectability.[12]   In this definition, the concentration of an element giving a line plus background signal equal to $1\frac{1}{2}$ times the background signal is

described as the minimum detectable concentration.   Detection limits are more often defined statistically[1,4] and here both the magnitude and reproducibility of the background signal will be significant.   Even if a background correction technique, such as wavelength modulation, is used to remove the background automatically from the measured signal, the detection limit will be a function of the photon shot noise in the detector and this will increase as the square root of the carbon tube emission intensity.[3]

The residual background signal from the tube appears to be extremely stable and reproducible.   It increases with time during atomisation as the tube temperature increases and has a known variation with wavelength. It would obviously be advantageous to reduce the magnitude of this signal further, and attempts were made to achieve this end by additional baffling of the tube-wall radiation and by design and use of alternative optical systems.   These experiments were largely unsuccessful and have led to an investigation of the nature of the background emission signal measured in carbon furnace atomic-emission spectrometry.   The results of these investigations, which are described in this paper, suggest that, following the efficient removal of tube-wall radiation, further reductions in the magnitude of the background signal will be achieved by modification of the furnace system rather than by modification of the optical arrangement.

Experimental

Reagents

A stock 1 000 μg ml^{-1} lithium solution was prepared from lithium chloride dissolved in 10^{-2} M hydrochloric acid.   This solution was diluted as required with high-purity de-ionised water.

White spot nitrogen (99.9% purity), argon (99.996% purity) and helium (99.998% purity) as supplied by British Oxygen Company were used as purge gases.

Apparatus

An optical system, which would allow total removal of tube-wall emission from the measured emission signal, was designed and set up for operation with a Perkin-Elmer HGA-70 heated graphite atomiser.

The HGA-70 atomiser was mounted on the optical bar of a Hilger and Watts Monospek 1000 grating spectrometer - monochromator, which had a focal length of 1 m.   The monochromator was fitted with a 1 200 line mm^{-1} Bausch and Lomb plane grating in a Czerny - Turner Mount and had a reciprocal dispersion of 0.8 nm mm^{-1} at the blaze wavelength of 500 nm and an aperture of $f/10$.   The entrance and exit slits were variable from 0.01 to 3.0 mm and, by the use of slit baffles, the height of the slit could be varied from 1 to 20 mm.

An $f/11$ telephoto lens with a focal length of 20.3 cm was used to focus an image of the carbon tube on to the entrance slit of the monochromator.   By use of this lens it was possible to produce a sharply focused image of the carbon tube-wall emission as a ring on the entrance slits of the monochromator and this is illustrated in Fig. 1.   The telephoto lens was selected because of its ability to form an image in which radiations from all parts of the carbon tube surface are in focus.   Any lens that had a focal length four times or more longer than the carbon tube would suffice.   The image ring was both narrow and sharply defined, and greatly reduced the amount of tube-wall radiation reaching the monochromator during operation of the HGA-70. The size of the image depended on the object and image distances and these were selected in order to give image diameters of 6, 9 or 12 mm.   The internal diameter of the object, the HGA-70 carbon tube, was constant at 8.65 mm.   The slit baffles in front of the monochromator were adjusted to give observed heights of 4, 7 and 9 mm for image diameters of 6, 9 and 12 mm, respectively.   By reducing the entrance slit height in this way, it was possible to prevent totally the ring of tube-wall emisson from entering the monochromator. The entrance slit width was varied between 0.3 and 1.5 mm.   With this arrangement only radiation from the vapour phase in the centre of the carbon tube was allowed to pass through the entrance slits of the monochromator.

A monochromator exit slit of width 0.5 mm and height 20 mm was used throughout.   The radiation was detected by using an EMI 9592B photomultiplier connected to an a.c./d.c. pre-amplifier and coupled to a Servoscribe RE.541.20 potentiometric strip-chart recorder.   The applied photomultiplier voltage was varied between 0.3 and 0.7 kV.   Before entering the monochromator, the radiation was chopped using a Hilger and Watts Monospek 1000 chopper assembly mounted on the optical bar.
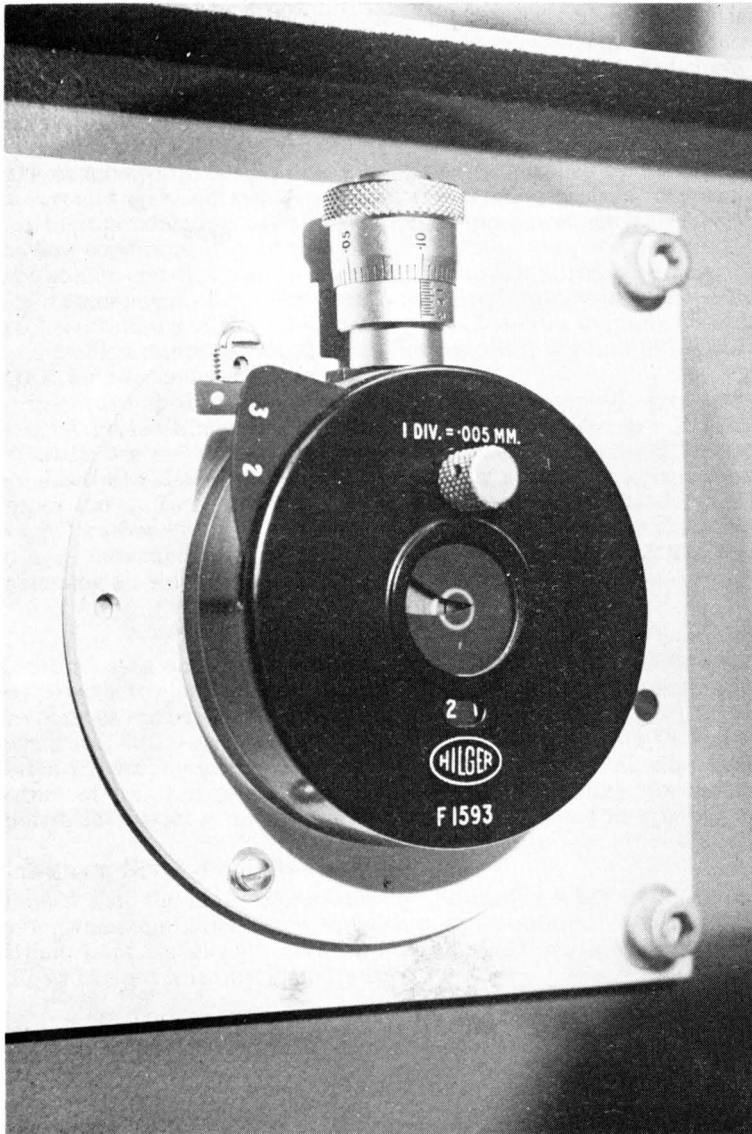
Fig. 1. View of the entrance slit of the Monospek 1000 showing clearly defined circle of tube-wall radiation from the HGA-70 focused by the telephoto lens.

Because of the variation in spectral efficiency of the optical system (grating, etc.) and the photomultiplier tube, intensities measured at different wavelengths are not directly comparable. The measurement system described above was therefore calibrated in the region 400–700 nm with a Hilger and Watts tungsten-filament lamp at a temperature of 2 550 K. Measurements of the emission intensity of the lamp were compared with the theoretical intensity distribution calculated from Planck's law and the spectral emissivity factors for tungsten,[13] and correction factors were calculated for the wavelength region of interest. The correction factors were then used to obtain the true spectral intensity distribution of the carbon furnace radiation by correction of the measurements obtained when using the Monospek 1000 - EMI 9592B system.

Argon, nitrogen and helium were used separately to provide an inert gas atmosphere within the carbon furnace, at a flow-rate of 1.5 l min^{-1} (40 lb in^{-2}), controlled by the HGA-70 power console. All background emission signals were measured using a clean, dry sample tube, which was heated to approximately 2 470 K at a maximum power setting of 10 V for 15 s under normal gas flow conditions.

Measurement of atomic-emission signals from graphite furnaces has been described previously.[1,4] For the measurement of lithium signals, the wavelength was adjusted by using a solution of high concentration and the detection limit was obtained by using 50-μl injections of a solution at a suitable lithium concentration. Samples were dried at 373 K for 45 s and atomised at 2 670 K for 10 s under gas stop conditions.

In addition to the above apparatus, several other commercial systems were used for comparative purposes. A Perkin-Elmer HGA-72 carbon furnace mounted in a PE 306 atomic-absorption spectrometer was used in an analogous manner. An Instrumentation Laboratory IL455 furnace atomiser was also used mounted in an IL151 atomic-absorption spectrometer and in the Monospek 1000. To reduce the tube emission reaching the photomultiplier in the IL151 system, a small washer with a hole of diameter 4 mm was placed over the entrance slits.

Temperatures were measured using an IRCON optical pyrometer and are reported as measured, *i.e.*, assuming an emissivity correction factor of unity.

Results and Discussion

With the apparatus based on a telephoto lens and a Hilger and Watts Monospek monochromator, it was possible to eliminate tube-wall emission completely when measuring atomic emission from the gaseous atmosphere in the centre of the tube. It was found, however, that a background signal was still measurable that had similar characteristics to wall radiation, *i.e.*, increase in intensity with temperature, low noise and an apparent maximum in the visible region. The nature of this background was investigated but, before the results can be correctly interpreted, the nature of the tube-wall emission itself must be appreciated.

The Carbon Tube as a Black-body Radiator

It is often assumed that the radiation emitted by the carbon tube, when heated to high temperatures during the atomisation stage, is black body in nature. If this is so, then the density of radiation, ρ, of wavelength between λ and $\lambda + d\lambda$, when the tube is heated to temperature T K, will be governed by Planck's law[14]:

$$\rho(\lambda,\ T) = \frac{8\pi hc}{\lambda^5} \times \frac{1}{\exp(hc/\lambda kT) - 1}\ d\lambda \quad \cdots \quad \cdots \quad \cdots \quad (1)$$

where $\rho(\lambda,\ T)$ J m^{-3} is the energy density per unit wavelength interval and the constants h, c and k have their usual meanings.

The flux of radiation in the waveband, $d\lambda$, emanating from a small hole of unit area into a unit solid angle defines the luminosity or brightness, B, and is given by

$$B_0(\lambda,\ T) = \frac{\rho(\lambda,\ T)c}{4\pi}\ d\lambda \quad \cdots \quad \cdots \quad \cdots \quad \cdots \quad (2)$$

Substituting for ρ from equation (1) yields

$$B_0(\lambda,\ T) = \frac{2hc^2}{\lambda^5} \times \frac{1}{\exp(hc/\lambda kT) - 1}\ d\lambda \cdots \quad \cdots \quad \cdots \quad \cdots \quad (3)$$

For the temperature range (2 000–2 700 K) and spectral region of interest (200–800 nm), equation (3) reduces to

$$B_0(\lambda,\ T) = \frac{2hc^2}{\lambda^5} \times \exp(-hc/\lambda kT) \qquad .. \qquad .. \qquad .. \qquad (4)$$

where B_0 is measured in W m^{-2} sr^{-1}. This equation is known as Wien's radiation law.

It is possible to test equation (4) experimentally for carbon tube-wall emission in two ways, *viz.*, with respect to temperature and wavelength. The brightness or intensity of radiation emitted by the hot graphite tube was measured with the apparatus described at tube temperatures between 2 200 and 2 700 K and at ten wavelengths between 530 and 620 nm near the wavelength of apparent maximum intensity (see Fig. 5). Tube-wall radiation was focused directly on to the slits of the monochromator and the gain of the photomultiplier was adjusted to give reasonable signals. Separate temperature measurements were made using the optical pyrometer and intensity readings were taken at times during atomisation at which the maximum tube temperature had been attained. Equation (4) predicts that a graph of ln (intensity) against the reciprocal of the absolute temperature should be linear, and this was observed at each wavelength. A typical graph is shown in Fig. 2 for results obtained at 560 nm for the temperature range between 2 300 and 2 600 K. A similar graph was reported by Adams and Kirkbright[15] under different experimental conditions.

If the temperature is maintained constant, then Wien's law would predict a linear relationship between ln $B_0\lambda^5$ and reciprocal wavelength for the carbon tube if it is behaving as a black-body radiator. When the intensity of tube-wall radiation is measured with respect to wavelength, a maximum is observed in the visible region which is a function of the spectral efficiency of the optical system and the spectral response of the photomultiplier tube. A typical graph obtained with the equipment described here is shown in Fig. 5 and is discussed later. Intensity measurements were therefore corrected using correction factors for the experimental system obtained for each wavelength by use of a tungsten filament lamp. The resulting Wien's law graph shows a linear relationship (Fig. 3) and confirms that the carbon tube behaves as an almost perfect black body. The slope of the line in Fig. 3 is equal to $-hc/kT$ [equation (4)]. When the value of the slope was used to calculate the black-body temperature, a value of 2 553 K was obtained, in reasonable agreement with the value of 2 603 K obtained with an optical pyrometer and assuming a carbon emissivity of unity. The slight deviation from linearity at the extremities of the line in Fig. 3 can be ascribed to the relatively low intensities at these wavelengths and the correspondingly large correction factors which magnify errors in measurement.
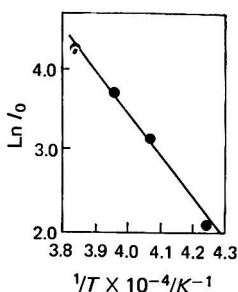
Fig. 2. Plot of logarithm of tube-wall radiation at 560 nm for the HGA-70 against reciprocal temperature.
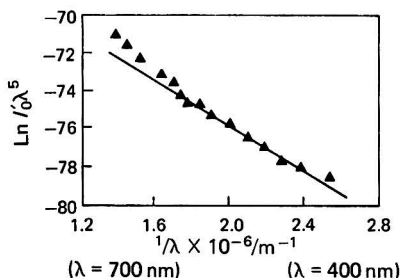
Fig. 3. Plot of ln $I_0'\lambda^5$ *versus* $1/\lambda$ for the HGA-70 at 2 603 K. Measured intensity values are arbitrary but self-consistent and are corrected for the variation in spectral efficiency of the measurement system.

Effect of Background Intensity on Detection Limits Obtained by Carbon Furnace Atomic-emission Spectrometry

Using the optical arrangement described under Experimental, it was expected that the relative magnitude of the background signal would be much less than in the HGA-72 - PE 306 system used previously[1,4] and that this would allow a significant improvement in detection

limits to be obtained by carbon furnace atomic-emission spectrometry. Only a slight improvement in the atomic emission to background emission ratio was achieved, despite the investigation of a wide variation in optical conditions on the Monospek 1000 spectrometer. Detection limits for lithium with these two systems are given in Table I, and are compared with those obtained with other furnace and optical systems available in our laboratory.

TABLE I

DETECTION LIMITS FOR LITHIUM AT 670.78 nm BY CARBON FURNACE ATOMIC-EMISSION SPECTROMETRY WITH DIFFERENT INSTRUMENT SYSTEMS

Furnace - spectrometer				Tube temperature/ K	Concentration of Li standard/ μg ml^{-1}	Detection limit*/ μg ml^{-1}
HGA-74 - PE 360	..	..	..	2 920	0.01	0.002 0
IL455 - IL151 ..	..	..	..	2 970	0.01	0.001 5
IL455 - Monospek 1000		..	..	2 970	0.005	0.000 5
HGA-74 - PE 306	..	..	..	2 920	0.002 5	0.000 30
HGA-72 - PE 306	..	..	..	2 770	0.002	0.000 24
HGA-70 - Monospek 1000	..		..	2 670	0.001	0.000 16

* Detection limit is defined as the concentration giving signals equal to the background plus two standard deviations; σ was measured from 10 injections of 50 μl (25 μl when using the IL455) of a solution of concentration approximately 10 times the detection limit shown in the last column.

Atomic-emission signals could only be measured with the IL455–IL151 system when a metal washer was placed over the entrance slits as described. The extent to which the background signal could be reduced by this device was limited, as the image of the tube-wall emission on the entrance slit of the spectrometer was blurred and this effect could not be eliminated. Optimum conditions were found to be a slit width of 0.04 mm and a photomultiplier voltage of 700 V. On the PE 360 spectrometer operated with the smaller diameter HGA-74 carbon furnace, a spectral band width of 0.2 nm was chosen to reduce the intensity of wall emission to a minimum. The detection limit was measured at the maximum temperature available and under gas stop conditions. As with the IL system, the image of the tube wall at the entrance slit appeared to be blurred and some tube-wall radiation reached the detector with all widths of the entrance slit. It seems possible that in both instruments there may be a contribution to the background from the reflection of light from the end windows of the furnace compartments.

In the HGA-72 - PE 306 system the image of the tube-wall radiation at the entrance slit is much less blurred and a comparatively wide entrance slit width of 0.3 mm can be used. Gas stop conditions were again used during atomisation. When the HGA-74 is used with the PE 306, the detection limit is almost as low as with the HGA-72, indicating that the effect of the end windows in the HGA-74 is minimal.

Using the HGA-70 with the Monospek 1000 the image is sharply defined and no tube-wall emission enters the monochromator. Although the HGA-70 furnace could reach only 2 670 K, the lowest temperature of the four furnaces, the detection limit was the lowest obtained but was only slightly better than that with the HGA-72 - PE 306 system. When the IL455 is used with the Monospek 1000, an improvement by a factor of three in the detection limit is obtained compared with the IL455 - IL151 unit, indicating the effect of inefficient optical baffling in this system.

With the HGA-70 - telephoto lens - Monospek 1000 system, optimum optical conditions giving the lowest detection limit were obtained for object and image distances of 0.5 and 0.34 m, respectively. The resulting magnification factor of 0.68 gave an image diameter of 6 mm, which was focused around the entrance slit of the monochromator as shown in Fig. 1. With this arrangement, an entrance slit width of 0.3 mm and height of 4 mm and an exit slit width of 0.5 mm and height of 20 mm were found to be optimum. The intensity of the atomic line recorded varies linearly with slit width but the continuum background intensity follows a square-law relationship with slit width. As entrance and exit slits are reduced, an increase in the signal to background ratio is therefore achieved until the system becomes noise limited.

With an entrance slit of 0.30 $\times$ 5 mm and an image diameter of 12 mm the variation in the
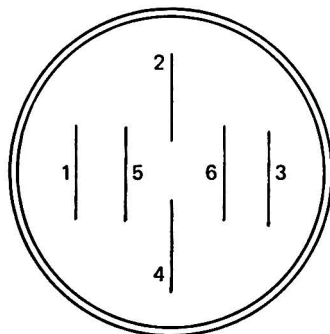
Fig. 4. Positions of the entrance slit of the monochromator with respect to the tube-wall image, used for the measurements given in Table II. Image diameter 12 mm, slit size 0.30 × 5 mm.

atomic-emission signal coming from different parts of the tube atmosphere cross-section was investigated. The position of the image ring was moved so that the entrance slit occupied six different positions, as shown in Fig. 4, and the background and atomic-emission signals were obtained at each position. The results are shown in Table II and indicate that although the background emission increases very slightly near the tube wall, atomic emission from lithium is the same from all parts of the tube.

TABLE II

VARIATION OF BACKGROUND AND LITHIUM ATOMIC-EMISSION SIGNALS FROM DIFFERENT PARTS OF THE CARBON TUBE AS SHOWN IN FIG. 4

HGA-70 - Monospek 1000 system. Temperature 2 670 K.

Slit position	Background emission, chart divisions	Atomic emission from 50 μl of 0.005 μg ml^{-1} lithium solution, chart divisions
1	15	32
2	15	33
3	16	33
4	16	32
5	13	32
6	13	33

In a separate experiment, the telephoto lens was deliberately moved from its optimum position in order to defocus the image and allow increasing amounts of tube-wall background signal into the monochromator. In Table III the variation in detection limit for lithium is shown as the relative background signal is increased. The entrance and exit slit widths were kept constant at 0.3 and 0.5 mm, respectively. As expected, the detection limit is considerably degraded as the background signal is increased.

TABLE III

EFFECT OF MAGNITUDE OF BACKGROUND SIGNAL ON THE DETECTION LIMIT FOR LITHIUM

Relative background signal	Detection limit* for lithium/μg ml^{-1}
10	0.000 16
100	0.000 65
800	0.002
3 000	0.011

* Defined as in Table I.

These experiments indicate the importance of reducing the background from the tube in carbon furnace atomic-emission spectrometry. The commercial instrument systems were used essentially without modification and in some instances their performance could be improved fairly easily if routine operation in the emission mode was required. Careful optical separation of tube-wall emission from atomic emission from the vapour phase in the centre of the tube is an essential prerequisite of sensitive carbon furnace atomic-emission spectrometry and the optical requirements are more stringent than in carbon furnace atomic-absorption spectrometry, in which source modulation copes satisfactorily with moderate background light levels.

Nature of the Background Signal in Carbon Furnace Atomic-emission Spectrometry

Despite the most careful optimisation of optical conditions in the Monospek 1000 - telephoto lens system, some background radiation still entered the monochromator during the atomisation stage of the HGA-70. As this background radiation was evidently emanating from the vapour phase in the centre of the tube and it was continuous over the visible region, it seemed probable that it was tube-wall radiation scattered into the monochromator by atoms, molecules or small particles present in the furnace atmosphere.

This hypothesis was tested by using Rayleigh's law for the scattering of radiation. Rayleigh[16],[17] found that the intensity of light scattered by small particles (including atoms or molecules) was inversely proportional to the fourth power of the wavelength. Rayleigh's law is expressed as

$$I = I_0 \frac{\pi^2 \, V}{2\lambda^4 L^2} \times \frac{(\epsilon - 1)^2}{N_L} \quad .. \quad .. \quad .. \quad .. \quad (6)$$

where I_0 is the intensity of the incident radiation, I is the intensity of scattered radiation, L is the distance between the scattering volume and the observation point, V is the scattering volume, N_L is Loschmidt's number and λ is the wavelength of the radiation. For a gas, the optical dielectric constant, ϵ, is close to unity and $(\epsilon-1)^2$ can be replaced with the expression $4(n-1)^2$, where n is the refractive index.[18] This modifies Rayleigh's law to

$$I = I_0 \frac{2\pi^2 \, V}{\lambda^4 \, L^2} \times \frac{(n-1)^2}{N_L} \quad .. \quad .. \quad .. \quad .. \quad (7)$$

If I_0 was constant with respect to wavelength, then the scattered light intensity would increase with decreasing wavelength, all other terms being constant under a given set of experimental conditions. In the carbon furnace, I_0 represents the tube-wall radiation, and as the furnace is acting as a black-body radiator, I_0 will increase with increase in wavelength up to a maximum in the region of 1 000 nm. If radiation coming from the vapour phase in the centre of the tube is indeed scattered radiation, it will show a relatively higher proportion of short-wavelength radiation than the incident tube-wall radiation.

To test this hypothesis, the intensities of both tube-wall and vapour-phase radiation were measured over the wavelength range from 360 to 730 nm using the Monospek 1000. It was not possible to make a continuous scan over this wavelength region because the intensity of light emitted by the carbon tube during the atomisation stage increases as the temperature increases. Intensity measurements were therefore made point by point at 10-nm intervals at a fixed time of 15 s after the start of atomisation at the maximum power setting of 10 V. Tube-wall radiation was measured by focusing part of the image ring on to the entrance slits of the monochromator and tube-centre radiation was measured by focusing the image ring around the entrance slit, as shown in Fig. 1. A typical set of results is illustrated in Fig. 5. The intensity scale in Fig. 5 is arbitrary and comparisons cannot be made between the tube wall and tube centre. The intense radiation from the tube wall was measured at a much lower photo-multiplier gain voltage than that used to measure the radiation from the centre of the tube. In both instances only part of the radiation was measured and the fraction measured was selected arbitrarily for convenience.

The results shown in Fig. 5 exhibit an apparent maximum in intensity from both the tube wall and tube centre but there is a significant shift in the curve to short wavelengths from

I_0(wall) to I(centre), consistent with the scattering hypothesis. The apparent maximum is a function of the spectral efficiency of the experimental system, which decreases very rapidly at short and particularly at long wavelengths. When these results are corrected for the variation in spectral response of the system, the theoretical variation for a black body radiator is obtained for I_0 and is shown in Fig. 6, and the relatively higher proportion of scattered radiation from the centre of the tube can be observed more clearly. These results suggest that Rayleigh scattering of tube-wall radiation is taking place and that it will constitute the background signal in carbon furnace atomic-emission spectrometry when the optics of the spectrometer adequately prevent tube-wall radiation from reaching the detector directly.
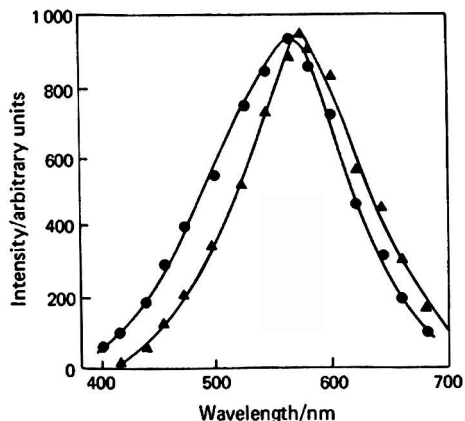
Fig. 5. Measured variation of tube-wall (▲) and tube-centre (●) radiation with wavelength using argon as purge gas.
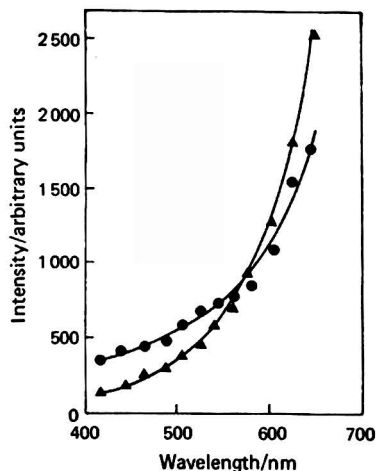
Fig. 6. Variation of tube-wall (▲) and tube-centre (●) radiation with wavelength using argon as purge gas, corrected for the variation in spectral response of the apparatus.

The results shown in Fig. 5 and 6 were obtained when argon was used as the purge gas. It is possible to consider that scattering of radiation takes place on argon atoms or on carbon atoms, molecules or sub-micron particles containing carbon released from the carbon tube. Although the scattering effect of carbon-containing molecules or particles may be much greater, the relative concentration of argon atoms in the 2 300–2 700 K range is very much higher and this would appear to be the more significant factor. Theoretical consideration[18] of Rayleigh's law has shown that the intensity of scattered radiation is dependent on the square of the volume or the sixth power of the radius of the scattering particle. However, it is clear from the theoretical relationship that a change of purge gas from helium (atomic diameter 2.3×10^{-10} m) to argon (2.9×10^{-10} m) or nitrogen (molecular diameter 3.15×10^{-10} m) will have an insignificant effect on the scattered light intensity and similar background intensities were obtained in the presence of any of the three gases. The gases had a much more profound effect on I_0 owing to changes in observed tube temperatures. At present, the effective scattering species cannot be definitely identified.

Under the conditions of carbon furnace atomisation with no sample, the terms V, L, n and N_L in Rayleigh's law [equation (7)] are constant, and therefore a plot of I/I_0 versus $1/\lambda^4$ should be linear with positive slope if the law is obeyed. As a ratio of I/I_0 is calculated, it is unnecessary to correct intensity readings for variations in spectral efficiency. As both the tube-wall (I_0) and tube-centre (I) intensities vary considerably with wavelength, it was necessary, however, to correct each set of readings separately for the variations in photomultiplier gain control necessary to measure intensities over the wavelength range 360–720 nm. The absolute value of the intensity ratio is arbitrary for the same reasons as those given with respect to Fig. 5. Separate graphs of I/I_0 versus $1/\lambda^4$ are shown in Figs. 7 and 8 for argon and nitrogen, respectively. Although there is some scatter of points, particularly when the light intensity
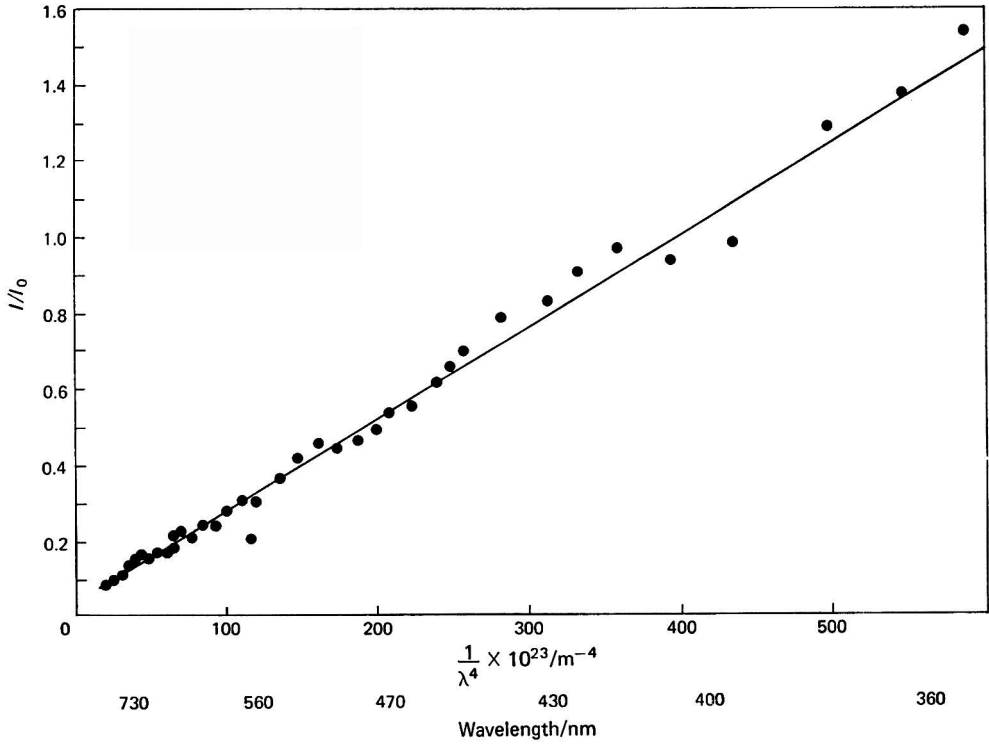
Fig. 7.   Plot of I/I_0 *versus* $1/\lambda^4$ in the range 360–730 nm.   Argon used as purge gas.
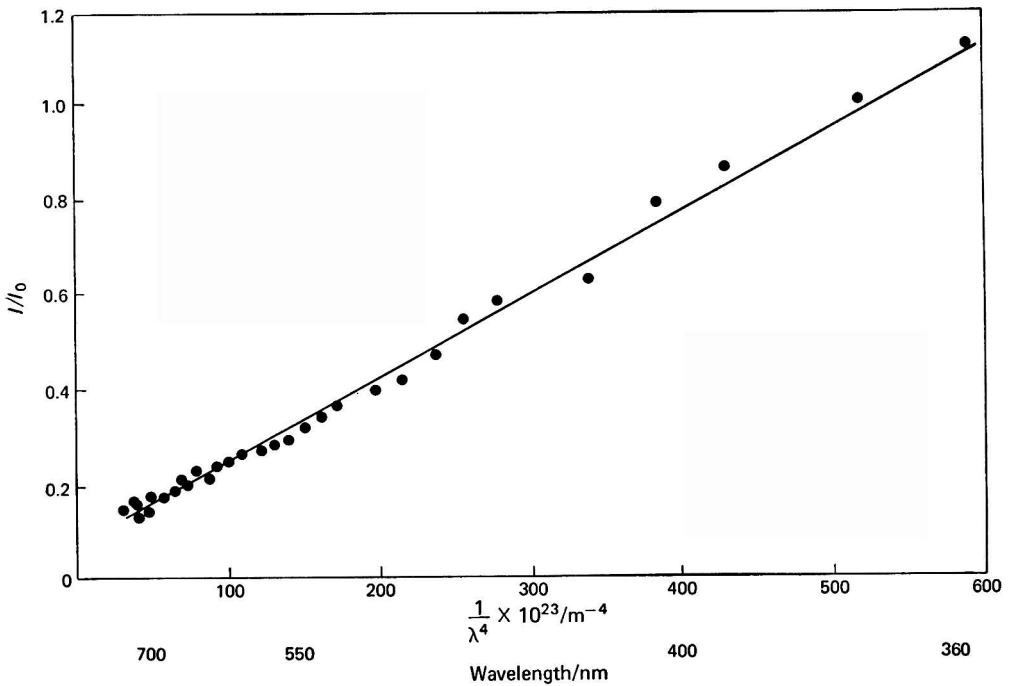
Fig. 8.   Plot of I/I_0 *versus* $1/\lambda^4$ in the range 360–730 nm.   Nitrogen used as purge gas.

readings were relatively small, a linear relationship is given in each instance, indicating that Rayleigh's law is obeyed under these conditions.   It is evident that the value of I/I_0 increases with decrease in wavelength, that is, there is a relative increase in scattered radiation at short wavelengths consistent with Rayleigh's law.   If tube-wall radiation were reaching the detector through imperfect focusing or optical alignment, the slopes in Figs. 7 and 8 would be zero. Changes in intensities were observed when different optical parameters were chosen but for each of the image diameters (6, 9 and 12 mm) and slit widths (0.5–1.5 mm) examined, similar linear relationships of I/I_0 to $1/\lambda^4$ were found.

The results presented here lead to the conclusion that, with careful optical design, the background in carbon furnace atomic-emission spectrometry can be reduced but only until the level of Rayleigh scattering of tube-wall radiation is reached.

Further evidence in support of these conclusions can be obtained by substitution of Wien's law for the intensity of black-body radiation into Rayleigh's law.   Substitution of B_0 from equation (4) for I_0 in equation (7) gives

$$I = \frac{4hc^2\pi^2 V\,(n-1)^2 \exp(-hc/\lambda kT)}{\lambda^9 L^2 N_L} \qquad \cdots \qquad \cdots \qquad \cdots \qquad (8)$$

At a constant tube temperature, a graph of $\ln I\lambda^9$ *versus* $1/\lambda$ should be linear if the radiation from the centre of the tube (I) is scattered black-body tube-wall radiation.   Tube-centre intensity measurements were obtained between 400 and 700 nm and corrected for variations in spectral efficiency.   A linear relationship was obtained, as shown in Fig. 9.   As with Wien's law, the slope in Fig. 9 is equal to $-hc/kT$ and will indicate the tube-wall temperature. Using nitrogen as the purge gas, and assuming an emissivity factor for carbon of unity, the temperature measured with an optical pyrometer was 2 573 K, in close agreement with the value of 2 534 K obtained from Fig. 9.   Again, slight non-linearity at the extremities of the graph is almost certainly due to inaccuracies in the relatively large correction factors for this wavelength region.
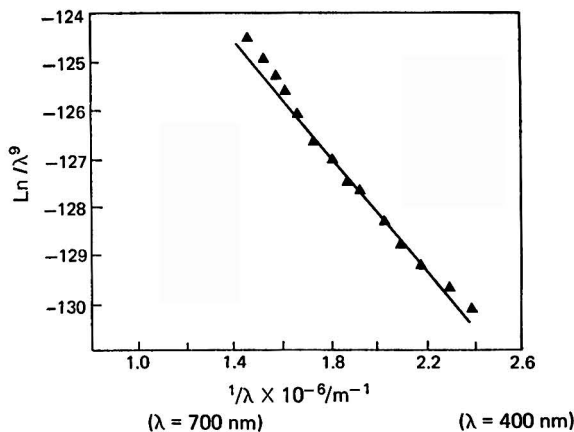
Fig. 9. Plot of $\ln I\lambda^9$ *versus* $1/\lambda$ in the range 400–700 nm. Nitrogen used as purge gas.

The fact that the background radiation from the carbon tube obeys the combined laws of Rayleigh and Wien is further confirmation of the scattering hypothesis and indicates that the source of the radiation is the black-body radiation from the tube wall.

Reduction of Background Signal in Carbon Furnace Atomic-emission Spectrometry

Under conditions in which no tube-wall radiation enters the monochromator, the background signal for carbon furnace atomic-emission spectrometry is due to scattered black-body radiation.   That this condition has been achieved for any particular experimental system can be checked by any of the methods given above.   To keep the scattered radiation to a minimum or to attempt to reduce it further, two possibilities exist, as described below.

(a) Use of a monochromator with higher dispersion

Obviously a wide-aperture, high-dispersion monochromator is required for best detection limits in carbon furnace atomic-emission spectrometry. The aperture must be wide enough to pick up as much atomic radiation from the centre of the tube as possible, without allowing tube-wall radiation to be directly observed. As the background radiation is continuous, the smaller the band width, the less of it will reach the detector and a high-resolution mono-chromator would be preferred, provided that the light-gathering power can be maintained. These desirable features appear to be incorporated in the design of echelle grating spectro-meters.[19] The $f/11$ lens was not a perfect optical match for the monochromator used in this work and the detection limits might be improved slightly by use of a lens system with greater light-gathering power.

(b) Optimisation of parameters in Rayleigh's law to minimise intensity of scattered radiation

Consideration of equation (8) reveals that I might be reduced by reducing I_0, reducing the scattering volume (V) or reducing the number and diameter of scattering centres. An increase in L will decrease the atom line intensity to the same degree as background radiation. Some reduction of background signals can therefore be achieved by alterations of furnace design and composition and purge-gas pressure and nature. Experiments designed to investigate these possibilities are in progress. At present, the species responsible for the scattering of light has not been positively identified and it is hoped that experiments on furnace design will clarify the precise nature of this process. In addition, the nature of the atomic excitation process is not well understood and it is hoped that further developments in research of this type will assist the understanding of the mechanism of excitation in the carbon furnace atomiser.

References

1. Ottaway, J. M., and Shaw, F., *Analyst*, 1975, **100**, 438.
2. Ottaway, J. M., and Hutton, R. C., *Analyst*, 1976, **101**, 683.
3. Epstein, M. S., Rains, T. C., and O'Haver, T. C., *Appl. Spectrosc.*, 1976, **30**, 324.
4. Ottaway, J. M., and Shaw, F., *Appl. Spectrosc.*, 1977, **31**, 12.
5. Shaw, F., and Ottaway, J. M., *Analyt. Lett.*, 1975, **8**, 911.
6. Littlejohn, D., and Ottaway, J. M., *Analyst*, 1977, **102**, 393.
7. Hutton, R. C., Ottaway, J. M., Rains, T. C., and Epstein, M. S., *Analyst*, 1977, **102**, 429.
8. Shaw, F., Ottaway, J. M., and Littlejohn, D., *Proc. Analyt. Div. Chem. Soc.*, 1976, **13**, 264.
9. Massmann, H., and Gücer, S., *Spectrochim. Acta*, 1974, **29B**, 283.
10. Hutton, R. C., Ottaway, J. M., Epstein, M. S., and Rains, T. C., *Analyst*, 1977, **102**, in the press.
11. Strong, B., *MSc Thesis*, University of Strathclyde, 1972.
12. Groves, E. L., *Editor*, "Analytical Emission Spectroscopy," Part II, Marcel Dekker, New York, 1972, p. 428.
13. Larrabee, R. D., *J. Opt. Soc. Am.*, 1959, **49**, 619.
14. Thorne, A. P., "Spectrophysics," Chapman and Hall, London, 1974, p. 87.
15. Adams, M. J., and Kirkbright, G. F., *Analytica Chim. Acta*, 1976, **84**, 79.
16. Lord Rayleigh, "Scientific Papers," Volume I, Cambridge University Press, Cambridge, 1899, p. 87.
17. Lord Rayleigh, "Scientific Papers," Volume IV, Cambridge University Press, Cambridge, 1903, p. 397.
18. Fabelinskii, I. L., "Molecular Scattering of Light," Plenum, New York, 1968, p. 6.
19. Keliher, P. N., and Wohlers, C. C., *Analyt. Chem.*, 1976, **48**, 333A.

Indirect Determination of Uranium by Atomic-absorption Spectrophotometry Using an Air - Acetylene Flame

J. F. Alder and B. C. Das

Department of Chemistry, Imperial College of Science and Technology, London, SW7 2AY

An indirect method has been developed for the determination of uranium by atomic-absorption spectrophotometry using an air - acetylene flame. Use is made of the reduction of copper(II) by uranium(IV) followed by complex formation of the copper(I) ions so produced with neocuproine (2,9-dimethyl-1,10-phenanthroline) and finally the determination of copper in this complex by atomic-absorption spectrophotometry. The results show that the method can be recommended, provided that care is taken to ensure the complete reduction of uranium(VI) to uranium(IV). The sensitivity of the method is 4.9 μg of uranium and the upper limit 500 μg without dilution.

Atomic-absorption spectrophotometry has become popular because of its high sensitivity and rapidity for the determination of a number of important elements in different types of samples. It is, however, insensitive for certain refractory elements, particularly uranium, owing to the high thermal stability of its oxide, UO_2.[1] The direct determination of uranium by atomic-absorption spectrophotometry is possible with only poor sensitivity, even when the high-temperature dinitrogen oxide - acetylene or oxygen - acetylene flames are employed. Amos and Willis,[2] for example, achieved a sensitivity of 120 p.p.m. of uranium by using a pre-mixed dinitrogen oxide - acetylene flame. Martin[3] stated that the determination of uranium is difficult owing to significant interference effects and requires critical control of flame gas composition and burner adjustment; moreover, the sensitivity obtained is poor.

The dissociation energy[4] of UO is 7.76 eV and the temperature of the radiofrequency inductively coupled argon plasma (6 000 K) is sufficiently high to dissociate the UO species. By using this method Scott *et al.*[5] determined uranium by aspirating the solution into the plasma and measuring the optical emission of the U^+ species; they obtained a detection limit of 0.3 p.p.m. X-ray emission spectrometry can be taken as the most rapid analytical method that offers a practical lower limit of detection of 100 p.p.m. of triuranium octaoxide and satisfactory accuracy for the determination of uranium in geological exploration samples.[6]

Many colorimetric reagents, such as arsenazo III [2,7-bis(*o*-arsonophenylazo)-1,8-dihydroxynaphthalene-3,6-disulphonic acid sodium salt],[7] PAN [1-(2-pyridylazo)-2-naphthol],[8] dibenzoylmethane[9] and thiocyanate,[10] have been used for determining uranium, but these methods suffer from serious interferences from many other elements so that prior separation of the uranium is essential.

A simple indirect method developed for the determination of uranium by atomic-absorption spectrophotometry is described that involves the exploitation of the reduction of copper(II) by uranium(IV):

$$U(IV) + 2\ Cu(II) \rightarrow U(VI) + 2\ Cu(I)$$
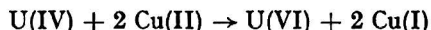
This reaction is stoicheiometric and offers an indirect determination of uranium by determining the copper(I) ion. The copper(I) ions produced by the reaction are complexed with neocuproine (2,9-dimethyl-1,10-phenanthroline).[11] Uranium is then determined by measurement of the copper by flame atomic-absorption spectrophotometry after back-extraction into hydrochloric acid.

Experimental

Apparatus

A Perkin-Elmer Model 303 atomic-absorption spectrophotometer equipped with a copper

hollow-cathode lamp was operated according to the manufacturer's instructions.

Reduction of the uranium(VI) was carried out in a Jones reductor containing amalgamated zinc.[12] The volume of the reductor was 110 cm³ and it held 45 cm³ of solution.

Reagents

All reagents used were of analytical-reagent grade.

Uranium stock solution, 10 000 p.p.m. Dissolve 2.109 g of uranyl nitrate hexahydrate in 97 cm³ of distilled water and add 3 cm³ of hydrochloric acid (36% *m/m*).

Copper solution, 10 000 p.p.m. Dissolve 3.929 g of copper(II) sulphate pentahydrate in 99 cm³ of water and add 1 cm³ of hydrochloric acid (36% *m/m*).

Neocuproine solution, 0.1% *m/V*. Dissolve 0.1 g of neocuproine in 100 cm³ of absolute ethanol.

Preparation of Reduction Column

Fill the column with amalgamated zinc prepared by washing 130 g of granulated zinc in pieces of less than 10 mm with 100 cm³ of 0.5% nitric acid and then several times with water. Activate the surface of the granulated zinc by treating it with 5% sulphuric acid for 10 s and then wash it again three times with water. Treat the zinc for 10 min with 100 cm³ of 2% mercury(II) chloride solution acidified with a drop of 98% sulphuric acid. Pour off the solution, wash the amalgamated zinc several times with 1% sulphuric acid and place it in the column. When not in use, fill the reductor with water to avoid the formation of basic zinc salts which might clog it and wash the column with 5% sulphuric acid before use.

Procedure

Reduction of uranium(VI) to uranium(IV)

Pass the uranium sample solution, containing typically 50 µg of uranium in 45 cm³ of 0.4 N hydrochloric acid, through the reduction column at a flow-rate of 7–10 cm³ min⁻¹. Maintain the volume of the uranium(VI) solution and hydrochloric acid such that the amalgamated zinc in the column is covered fully and the liquid layer lies above the zinc. As the solution passes through the column the uranium(VI) is reduced to uranium(IV) together with a small fraction of uranium(III). Pass the solution through the column for a second time and then wash the column several times with water. Bubble air through this solution for 2 min using a plain glass tube so as to oxidise any uranium(III) to uranium(IV).

Complex formation

Add to the reduced solution 5 cm³ of ammonium acetate buffer (pH 8.5) and adjust the pH of the solution to 8.5 with ammonia if necessary. Add a 5-fold excess of copper(II) and then 10 cm³ of 0.1% *m/V* neocuproine solution in order to form the yellow copper - neocuproine complex and allow to stand for 5 min.

Extraction of the complex

Extract the copper - neocuproine complex[13] from the solution by shaking with 10 cm³ of chloroform for 30 s. Allow the organic layer to settle and then run it off. Carry out a second extraction with 5 cm³ of chloroform and mix the two chloroform extracts. Wash the chloroform solution at least twice with pH 8.5 buffer solution.

Back-extraction of copper from chloroform layer into hydrochloric acid

As aspiration of chloroform into a flame is not recommended, extract the copper into 5 cm³ of 3 N hydrochloric acid. Adjust the final volume of the copper solution to 10 cm³ with distilled water and then determine the copper content by atomic-absorption spectrophotometry against a blank solution using aqueous copper calibration solutions.

Results

Sensitivity

The sensitivity, defined as the mass of uranium in the original solution required to give 1% absorption (due to copper), is 4.9 µg, which compares well with other atomic-absorption procedures (Table I).

TABLE I

COMPARISON OF SENSITIVITIES IN THE ATOMIC-ABSORPTION SPECTROPHOTOMETRY OF URANIUM

Study	Flame	Wavelength/ nm	Sensitivity, p.p.m.
Martin[3]	Dinitrogen oxide - acetylene	356.7	250
Amos and Willis[2]	Dinitrogen oxide - acetylene	358.5	120
Perkin-Elmer Handbook..	Dinitrogen oxide - acetylene	351.5	200
This work	Air - acetylene	324.7*	4.9

* Measurement of copper.

Precision

In order to evaluate the precision of the method, 15 solutions containing 50 μg of uranium(VI) were analysed by the recommended procedure. The relative standard deviation from the mean was 6%. In order to test the applicability of the method to routine laboratory use a set of three solutions containing the same amount of uranium(VI) (50 μg) was analysed by a skilled colleague not familiar with the method. The results obtained by her were within 7% of the mean value obtained in the precision tests.

Effect of Washing

If any of the aqueous phase is included when the complex in the chloroform layer is run off from the bottom of the separating funnel an apparently high recovery of uranium is obtained. Before back-extraction of copper the complex is therefore washed at least twice with a buffer solution having the same pH as that used in the complex formation step. The effect of washing at this stage is shown in Fig. 1.

Effect of High Concentrations of Various Metals and Non-metals

The effect of a number of metals and non-metals on the absorption of copper and hence indirectly on uranium was investigated by observing their influence on the absorption produced in the determination of 50 μg of uranium(VI) (Table II). An ion is considered not to interfere, for the purpose of this study, when less than 12% change in absorption is produced (2 standard deviations).

TABLE II

INTERFERENCE OF METALS AND NON-METALS IN DETERMINATION OF URANIUM

The foreign metals and ions were all present at a mass of 1 000 μg, which is a 20-fold excess over the mass of uranium.

Foreign metals	Relative absorbance*	Foreign ions	Relative absorbance*
None	100	None	100
Na	99	SO_4^{2-}	103
Ba	109	PO_4^{3-}	73
La	95	F^-	77
Pb	91		
Fe(III)	136	CH_3COO^-	94
Mn(II)	94	BO_3^{3-}	91
Mo(VI)	101		
Cd	101	Cl^-	100
Cu(II)	100	NO_3^-	100
Cr(III)	45	NH_4^+	100
Bi	93	Citrate	100
V(V)	36		
Li	102		
Th	90		

* The absorbance values were normalised on the basis that the reading for 50 μg of uranium is 100.

Effect of pH on the Recovery of Uranium

Many workers have reported that copper(I) forms a complex with neocuproine over the pH range 3–10. We have found that in acidic medium the solutions become colloidal, so this method is carried out in alkaline medium. The effect of pH on uranium recovery is shown in Fig. 2.
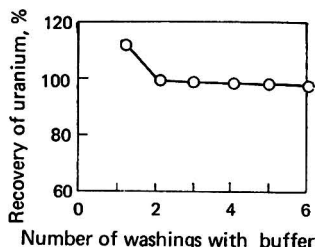
Fig. 1. Effect of number of washings with pH 8.5 buffer on recovery of uranium.
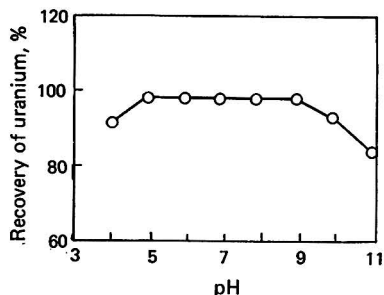
Fig. 2. Effect of pH values on recovery of uranium.

Discussion

In the proposed method the complete reduction of uranium(VI) to uranium(IV) is very important. The reduction efficiency of the column was checked by a titrimetric method and found to be 99% efficient on two passes.[12]

It can be seen from Table II that only a few ions interfere at the 1 000 μg level. The chromium(III) interference is caused by the formation of a colourless complex with neocuproine that interferes with the complexation of copper(I).[14] Vanadium(V) is reduced to vanadium(II) on the column and is re-oxidised to vanadium(IV) on aeration.[12,15] The oxidation of uranium(IV) to uranium(VI) by vanadium(IV) is a possible source of interference although this effect is considered unlikely in view of the relative potentials of the uranium(IV) - uranium(VI) couple ($E_0 = -0.32$ V)[15] and the vanadium(IV) - vanadium(III) couple ($E_0 = -0.36$ V).[15] It is, however, very difficult to predict in theory what would happen when two such species are mixed because of the complex nature of two-electron redox systems involving complex cation species (VO^{2+} and UO_2^{2+}). It is thought more likely that unreduced vanadium(V) is responsible for the re-oxidation of uranium(IV) to uranium(VI) or copper(I) to copper(II). Iron(III) is reduced to iron(II) on the column and the subseqnent reduction of copper(II) to copper (I) by the iron(II) in the presence of neocuproine is almost certainly the cause of the observed enhancement. Addition of iron(II) to copper(II) solution in the presence of neocuproine results in the formation of the yellow colour due to the copper(I) - neocuproine complex.

The effect of phosphate and fluoride is possibly caused by the formation of stable compounds in the column as uranium(IV) is known to give insoluble phosphate and fluoride salts in acid medium[15] and these slow down the reduction of uranium(VI) to uranium(IV).

Iron(III) can form a precipitate during pH adjustments; this precipitation is avoided by adding sodium citrate solution before adding ammonia and this addition was made in all work using iron(III).

It is considered likely that this method will be applicable to the analysis of ore and geochemical samples, although it may require a preliminary separation step to overcome interference problems. The sensitivity of the method will obviously be improved by using an electrothermal atomiser instead of a flame.

Conclusion

The method proposed here for the indirect determination of uranium by atomic-absorption spectrophotometry is much more sensitive than the direct method with the dinitrogen oxide - acetylene flame. With the amplification procedure 1% absorption is given by 4.9 μg of uranium in the original aqueous solution. The copper(I) ions form a complex with a

highly selective reagent, neocuproine, which in turn increases the over-all selectivity of the procedure described.

References

1. Mavrodineanu R., and Boiteux, H., "Flame Spectroscopy," Wiley, New York, 1965, p. 429.
2. Amos, M. D., and Willis, J. B., *Spectrochim. Acta*, 1966, **22**, 1325.
3. Martin, M. J., *Analyst*, 1971, **96**, 843.
4. DeMaria, G., Burns, R. P., Drowart, J., and Inghram, M. G., *J. Chem. Phys.*, 1960, **32**, 1373.
5. Scott, R. H., Strasheim, A., and Kokot, M. L., *Analytica Chim. Acta*, 1976, **82**, 67.
6. Clark, N. H., and Pyke, J. G., *Analytica Chim. Acta*, 1972, **58**, 234.
7. Singer, E., and Matucha, M., *Z. Analyt. Chem.*, 1962, **191**, 248.
8. Cheng, K. L., *Analyt. Chem.*, 1958, **30**, 1027.
9. Yoe, J. H., Will, F., and Black, R. A., *Analyt. Chem.*, 1953, **25**, 1200.
10. Neitzel, O. A., and Desesa, M. A., *Analyt. Chem.*, 1957, **29**, 756.
11. Smith, G. F., and McCurdy, W. H., *Analyt. Chem.*, 1952, **24**, 371.
12. Vogel, A. I., "A Text Book of Quantitative Inorganic Analysis," Third Edition, Longmans, Harlow, 1961, p. 318.
13. Gahler, A. R., *Analyt. Chem.*, 1954, **26**, 577.
14. Schilt, A. A., "Analytical Applications of 1,10-Phenanthroline and Related Compounds," Pergamon Press, Oxford, 1969, p. 72.
15. Cotton, F. A., and Wilkinson, G., "Advanced Inorganic Chemistry," Wiley, London, 1963, p. 897.

Analytical Optoacoustic Spectrometry
Part IV.* A Double-beam Optoacoustic Spectrometer for Use with Solid and Liquid Samples in the Ultraviolet, Visible and Near-infrared Regions of the Spectrum

M. J. Adams, B. C. Beadle and G. F. Kirkbright

Department of Chemistry, Imperial College of Science and Technology, London, SW7 2AY

The design, construction and performance characteristics of a double-beam optoacoustic spectrometer suitable for recording corrected spectra of small solid and liquid samples in the wavelength range 0.25–2.5 μm are described. Typical spectra obtained for rare earth oxides, titanium(IV) oxides, catalase, blood, cystine and kaolinite are presented in order to illustrate the performance of the instrument. The application of the spectrometer to record conventional solution transmittance spectra is also reported.

Keywords: Optoacoustic spectrometry; double-beam optoacoustic spectrometer; thermal diffusivity; absorption spectrometry

The observation of the optoacoustic effect from solid materials, and its application in the technique of optoacoustic spectrometry, has been described by a number of workers.[1-4] The design and performance characteristics of a single-beam optoacoustic spectrometer that is suitable for the examination of small solid samples, and later modifications to provide improved performance and ease of operation, have been described in earlier papers from this laboratory.[3,4] The application of this spectrometer to the direct examination of samples of inorganic, biochemical and phytochemical origin, and the extension of the utility of optoacoustic spectrometry via phase analysis of the resultant signal to provide information concerning the spectra, thermal diffusivity, or thickness of samples composed of distinct layers, has also been reported.[5]

This paper reports the design and performance of a double-beam optoacoustic spectrometer that allows automatic correction of the spectra obtained for the variation in output energy of the source with wavelength. The spectrometer can be employed over a wide range of wavelengths with a single source and detector in order to examine the optoacoustic spectra of both small solid and liquid samples; the application of the double-beam spectrometer in the ultraviolet - visible and near-infrared regions of the spectrum between 0.3 and 2.5 μm to the examination of a number of samples of geochemical, inorganic and biochemical interest is described. The spectrometer can also be used to record transmission spectra of solutions by conventional molecular absorption spectrophotometry.

Experimental

Double-beam Spectrometer

A schematic diagram of the double-beam spectrometer is shown in Fig. 1. The continuum source employed was a 300-W, high-pressure, short-arc xenon illuminator lamp, with integral aluminium parabolic reflector and 25 mm diameter sapphire window (Type VIX300 UV, Varian Associates). The lamp was mounted within a fan-cooled housing (Type R300-1, Varian Associates). Power for this source and cooling system was provided at 15 V and 20 A by a Varian Associates PS300-1 power supply unit. The radiation from the source was focused, by means of a silica lens (25 mm in diameter, with a 70-mm focal length), on to the plane of rotation of a variable-speed rotating sector (Model 9479, Brookdeal Electronics Ltd., Bracknell, Berkshire) placed adjacent to the entrance slit of the $f/4$ grating monochromator that was employed in this work (Metrospec DGO Ltd., Chobham, Surrey).

---

* For details of Part III of this series, see reference list, p. 575.
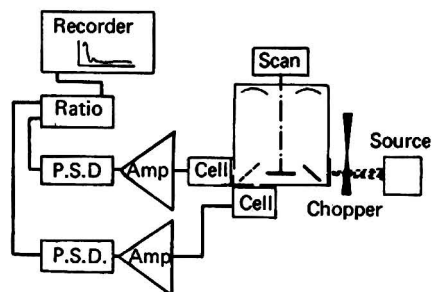
Fig. 1.   Schematic diagram of the double-beam optoacoustic spectrometer.

The monochromator was fitted with either a plane diffraction grating (50 × 50 mm, 1 200 lines mm^{-1}) blazed at 300 nm for use in the ultraviolet - visible region or a similar grating (50 × 50 mm, blazed at 2 μm) for use in the near-infrared region of the spectrum. As is shown in Fig. 1, the monochromator was fitted with two exit slit assemblies, in each of which fixed slits ruled on silica plates could be positioned to provide spectral half-band widths of 1, 2, 5, 10 and 20 nm in the ultraviolet - visible region. For operation in the near-infrared region with the xenon arc source, Chance OX5 filters were used at each exit slit in order to prevent the transmission of radiation at wavelengths less than 0.9 μm from overlapping spectral orders of diffraction. Within the monochromator housing the dispersed radiation beam was split by a 50% plane mirror positioned so as to produce radiation of equal intensity at each exit slit. Radiation emerging from the exit slits was re-focused by using front-surfaced concave mirrors (50 mm in diameter, 200-mm focal length) and directed into the optoacoustic cells as shown in Fig. 2. The mirrors were mounted on springs in housings positioned at the exit slits and their angle to the emerging radiation could be readily arranged for optimum illumination of the samples contained within the cells. The transducers employed were sensitive $\frac{1}{2}$-in capacitor microphones, Type 4166 (Brüel and Kjaer Ltd., Hounslow, Middlesex). Each of the microphone cartridges had a rated sensitivity of 50 mV Pa^{-1} and was fitted with a Type 4169 pre-amplifier (Brüel and Kjaer Ltd.). The polarisation voltage to the microphones (200 V) was supplied from a dry-battery source.

Identical cells were positioned below each exit slit of the monochromator and the design employed is shown in Fig. 2. The cells were constructed from aluminium and were sealed by means of double silica windows to attenuate environmental acoustic noise; they were operated at atmospheric pressure, using air as the filler gas. Samples were positioned on a silica plate (20 mm diameter) mounted in an aluminium tube, which was placed in the cell and sealed by means of three locking nuts. Front-surface illumination of the samples was used throughout.
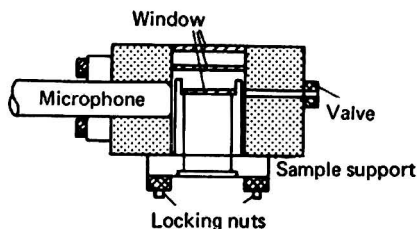
Fig. 2.   Schematic diagram of the optoacoustic cell.

Wavelength scanning of the continuum radiation was achieved by means of a stepping motor connected directly to the cam-drive mechanism of the grating mount within the monochroma-ator. The source, rotating sector, monochromator and optoacoustic cells were mounted together on a single steel plate and the chopper and stepping motor electronic systems, together with the dry cells providing the polarisation voltage for the microphones, were

located inside a steel frame below the optical components.   Pre-selected scanning rates of 200, 100, 50 and 15 nm min^{-1} were available by use of push-button controls, along with forward and reverse selection and modulation frequency controls, all of which were mounted on the front panel of the spectrometer assembly.

The optoacoustic signals from the microphone transducers were led directly, via screened cables, to two lock-in amplifier systems (reference channel, Model 186 amplifier, Princeton Applied Research Corp., New Jersey, USA; sample channel, Model 9502, Brookdeal Electronics Ltd.).   The reference signal for each amplifier was that generated by the variable-speed rotating sector.   The lock-in amplifiers extracted the signal waveforms and presented these as d.c. potentials to a ratiometer unit (Brookdeal Electronics Ltd., Model 5047); the signal from the reference cell was presented directly to the denominator, while the sample signals were taken to the numerator input.   The ratiometer output was shown as a d.c. potential and taken, via a simple resistance - capacitor time-constant circuit (2 s), to a potentiometric chart recorder (Servoscribe, Model RE511, Smiths Industries Ltd.).   Corrected optoacoustic spectra were then obtained by recording the output of the ratiometer against the wavelength of the incident radiation during wavelength scanning at the monochromator.

The optoacoustic spectra of solid and liquid samples were recorded by using carbon black as the reference absorber.   The carbon black was prepared by "smoking" a thin glass microscope slide (19 mm in diameter) and mounting it in the optoacoustic cell on the silica sample plate.

In order to record solution transmission spectra a silica cuvette (50 mm in depth, 20 mm in diameter) was positioned between the sample optoacoustic cell and the exit slit on the monochromator.   Both sample and reference cells were loaded with carbon black samples for these measurements.   The instrument was then operated as described above, *i.e.*, energy transmitted through the sample solution in the cuvette was received at the sample cell and gave an optoacoustic signal for carbon black, the magnitude of which varied depending on the transmittance of the incident radiation at different wavelengths.   Transmission spectra for organic liquid samples (*e.g.*, chloroform) were recorded in this fashion to facilitate wavelength calibration in the near infrared region.

Cell calibration[6] was achieved by employing a low-power neon laser (Metrologic Inc., Bellmawr, N.J., USA).   The radiation from this source was modulated by using the variable-speed chopper and de-focused by using a biconcave lens to fill the sample tray of the optoacoustic cell containing a carbon black sample.   The output power of the laser was determined using a ratiometer and integration of the output energy for a 5-s irradiation period.

Samples and Sample Handling

Solid samples were examined by placing a few milligrams of the material in the sample tray of the optoacoustic cell and recording the spectra in the conventional manner against a carbon black reference cell or, if differential spectra were required, against the necessary reference sample placed in the reference optoacoustic cell.   Liquid materials and solutions were examined by pipetting about 100 μl of the solution into the sample tray.   Transmission spectra of solutions were obtained as described above, using a silica cuvette outside the optoacoustic cell.

The rare earth oxides studied (holmium oxide and erbium oxide) were obtained as fine powders (Johnson Matthey Ltd., London).   Catalase was examined as both the solid, purified powder, obtained from bovine liver, and as crude, sterile solution from bovine liver (Sigma Chemicals Co., St. Louis, Mo., USA).   The titanium(IV) oxide samples, both rutile and anatase powders, were sub-micrometre in particle size (Tioxide International Ltd., Stockton-on-Tees) and the kaolinite was a typical geochemical sample of inhomogeneous particle size.   The solution transmittance spectrum of blood was obtained with fresh, whole blood diluted (1 + 199) with distilled water.

Results and Discussion

Cell Calibration

The major practical difference between optoacoustic spectrometry and the more conventional optical techniques of transmission and reflectance spectrometry is in the use of a microphone transducer to monitor indirectly the absorption of incident electromagnetic radiation by the sample under study.   The design of the optoacoustic cell and the transducer employed is,

therefore, a critical feature of any optoacoustic system. With the great interest currently being shown in optoacoustic spectrometry a means of comparing cell efficiencies is required; the design of optoacoustic cells has been discussed by several workers.[3,5–8] The method of calibrating the optoacoustic cells used in this laboratory is that described by Monroe and Reichard.[6]

The output power of the laser employed for calibration purposes was determined radiometrically and found to be 0.4 mW; with a modulation frequency of 30 Hz the magnitude of the optoacoustic signal from a carbon black sample in a cell of the type shown in Fig. 2 was about 0.80 mV (r.m.s.). When using a microphone with a rated sensitivity of 50 mV Pa^{-1} the cell efficiency was therefore determined as 40 Pa W^{-1}. This efficiency value, which is independent of wavelength, was approximately twice the value determined for the optoacoustic cell described in an earlier publication from this department.[5] The reason for this improvement lies in the reduced volume of air contained within the cell, achieved by mounting the sample tray closer to the entrance window of the cell.

Instrument Performance

Corrected optoacoustic spectra in the wavelength range 0.3–2.5 μm were determined with the double-beam spectrometer by taking the ratio of the amplitude of the optoacoustic spectrum at different wavelengths to the power emitted by the xenon arc continuum source at these wavelengths. The power spectrum of the source was obtained by measuring the optoacoustic spectrum of the carbon black, assuming this to approximate to a black-body absorber.

The emitted power spectra of the lamp in the ultraviolet - visible region and in the near-infrared region, obtained by single-beam operation of the instrument, are shown in Figs. 3 (A) and 4 (A), respectively. The efficiency of the beam splitting arrangement, used with the spectrometer in order to produce a uniform response with respect to wavelength for identical sample and reference cells, was determined by mounting carbon black samples in both cells and examining the ratio of the output from each when obtained by double-beam operation as described above. The flatness responses for the ultraviolet - visible and near-infrared regions are shown in Figs. 3 (B) and 4 (B), respectively. The results obtained were considered satisfactory for the double-beam spectrometric examination of samples.
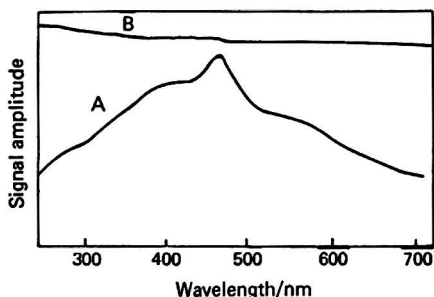
Fig. 3. A, Single-beam ultraviolet and visible optoacoustic spectrum of carbon black. Half-band width 10 nm, scan rate 50 nm min^{-1}, instrument time constant 3 s. B, Typical flatness response curve for double-beam, carbon - carbon, operation in the ultraviolet and visible region. Instrument characteristics as A.
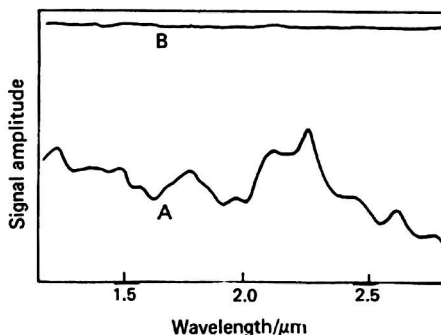
Fig. 4. A, Single-beam near-infrared optoacoustic spectrum. Half-band width 30 nm, scan rate 150 nm min^{-1}, instrument time constant 3 s. B, Typical flatness response curve for double-beam, carbon - carbon, operation in the near-infrared region. Instrument characteristics as A.

Fig. 5 (*a*) and (*b*) shows the ultraviolet - visible spectra of two rare earth oxides, holmium oxide and erbium oxide, respectively. The relatively sharp band absorption spectra of these materials are characteristic of the rare earth oxides and these materials provide good test samples with which to evaluate the spectral resolution and signal to noise ratios obtainable with the optoacoustic spectrometer and small solid samples in the ultraviolet - visible region.
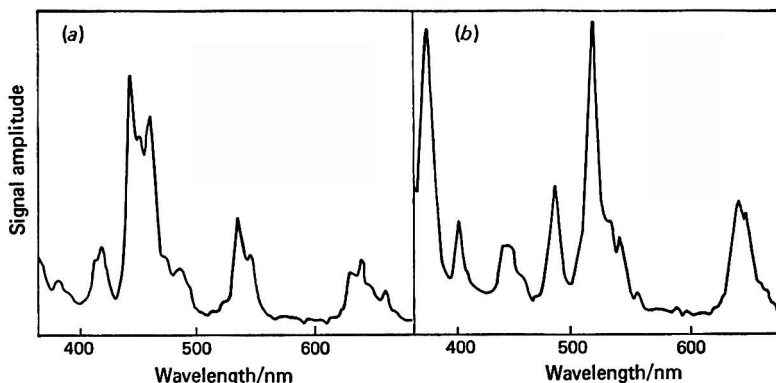
Fig. 5.   Corrected ultraviolet and visible optoacoustic spectra of (a) holmium oxide and (b) erbium oxide.   Half-band width 2 nm, scan rate 15 nm min⁻¹, instrument time constant 3 s.

Both solid samples and solutions can be examined directly by optoacoustic spectrometry, as is illustrated in Fig. 6 (a) and (b).   Fig. 6 (a) shows the corrected optoacoustic spectrum obtained from a few milligrams of purified catalase powder and the characteristic absorption bands at about 400 and 550 nm are evident.   Figure 6 (b) shows a similar optoacoustic spectrum of a suspension of catalase, obtained by pipetting 100 μl of the solution into the sample tray of the optoacoustic cell.
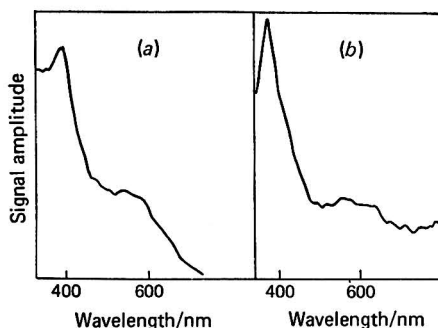
Fig. 6.   Corrected optoacoustic spectra of catalase (a) as a powder and (b) as a crude solution of a suspension of catalase.   Half-band width 10 nm, scan rate 50 nm min⁻¹, instrument time constant 3 s.

An important advantage of a two-cell, double-beam spectrometer is that difference spectra can be studied with relative ease.   This technique is illustrated in Fig. 7, where the optoacoustic spectrometer is used to record the spectra of the rutile and anatase forms of titanium(IV) oxide.   The reference cell sample tray is filled with the powdered rutile sample and the sample cell with the anatase powder.   Uncorrected difference spectra can be recorded by employing an (A—B) technique at the input of one of the lock-in amplifiers or, as with Fig. 7 (c), the ratio of the amplitudes of the optoacoustic signals for each sample and the variation of this ratio with the wavelength of the incident radiation can be monitored; while the latter does not provide a true difference spectrum it does enable corrected spectra to be obtained.   The difference in the location of the edge of the absorption peak of the two samples is clear in Fig. 7 (c).

The double-beam optoacoustic spectrometer was also used for solution transmission studies. The optoacoustic sample cell filled with a carbon black sample served as the detector of the transmitted radiation and an example in which the instrument was operated in this mode is

shown in Fig. 8. Oxygenated whole blood was diluted with distilled water and placed in a silica cuvette; the transmission spectrum obtained was characteristic of oxyhaemoglobin. This technique of examining transmission data was found to be useful for wavelength calibration purposes, and was used for this purpose in the near-infrared region.
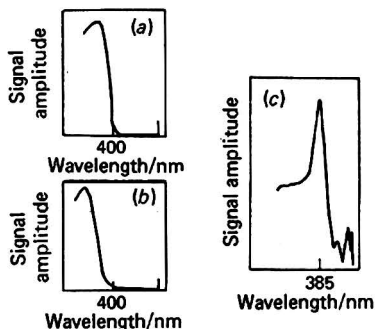
Fig. 7. Uncorrected optoacoustic spectra of (*a*) rutile and (*b*) anatase titanium(IV) oxide, and (*c*) their difference spectrum. Half-band width 10 nm, scan rate 50 nm min⁻¹, instrument time constant 3 s.
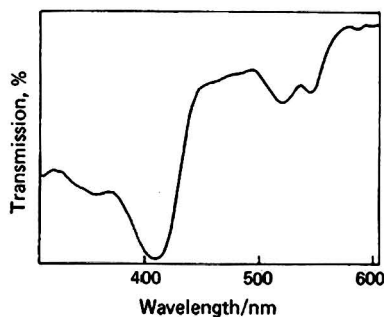
Fig. 8. Transmission spectrum of diluted (0.5% V/V) whole blood employing carbon black optoacoustic cells as radiation detectors. Half-band width 10 nm, scan rate 50 nm min⁻¹, instrument time constant 3 s.

No results appear to have been reported previously for the examination of small, solid samples by optoacoustic spectrometry in the near-infrared region of the spectrum. One of the advantages of optoacoustic spectrometry over conventional techniques employing photocell detectors is that no change in detector is required for spectroscopic studies in various regions of the spectrum provided that the energy output of the source employed is sufficient in the wavelength region of interest. Fig. 4 (A) shows the single-beam carbon black absorption spectrum in the near-infrared region and Fig. 4 (B) the flatness response of the double-beam system in this spectral region. A variety of sample types have been examined by use of near-infrared optoacoustic spectrometry using the double-beam spectrometer and Fig. 9 shows the spectra for a sample of geochemical interest, kaolinite, and a biochemical sample, in the form of a powdered sample of the amino acid cystine. Almost all of the absorption bands in this spectral region, whether overtones or combination bands, involve hydrogenic stretching vibrations. The near-infrared spectrum of kaolinite was determined as part of a study of rocks and minerals. The absorption bands at about 1.4 and 1.9 μm are characteristic of free, undissociated water (*e.g.*, water of hydration), while the bands at about 2.2 μm indicate combination bands from the hydroxyl ion.[9] Fig. 9 (*b*) shows the optoacoustic spectrum of cystine in the near-infrared region. Again, the 1.4- and 1.9-μm absorption bands are present and are
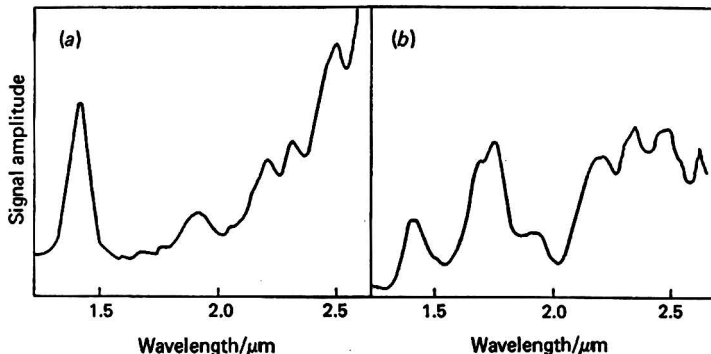
Fig. 9. Near-infrared optoacoustic spectra of (*a*) powdered kaolinite and (*b*) cystine. Half-band width 30 nm, scan rate 150 nm min⁻¹, instrument time constant 3 s.

probably caused by water impurities in the sample or cell. The absorption bands in the 1.7-μm region are characteristic of –NH or –CH stretching vibrations.

Conclusion

This paper describes the construction of a double-beam optoacoustic spectrometer so as to enable the spectra of solid and liquid samples to be studied in the ultraviolet - visible and near-infrared regions of the spectrum. Corrected optoacoustic spectra have been obtained by other workers by digital recording of a reference spectrum prior to examination of the sample material[2] and by employing a thermopile black-body detector.[6] However, the use of a twin-cell arrangement, as discussed here, provides the opportunity of recording difference spectra; this is an important function for a great deal of quantitative work. The versatile spectrometer constructed permits spectra to be obtained over a wide wavelength range (0.25–2.5 μm) with a single source and detector.

The spectrometer described here uses a 300-W, xenon arc continuum source; this unit is of much lower power than that described in our previous papers[3,4] and those used by other workers.[2,6] Because of the integral parabolic reflector of the source, however, the collected radiation output from this source is as great as that available from the 1-kW source used in our earlier studies.

The spectra presented here are provided to illustrate the performance of the spectrometer in its applications to solid- and liquid-sample studies; the use of the instrument for the examination of a variety of sample types, particularly in the near-infrared region, is at present in progress.

References

1. Harshbarger, W. R., and Robin, M. R., *Acc. Chem. Res.*, 1973, **6**, 329.
2. Rosencwaig, A., *Analyt. Chem.*, 1975, **47**, 592A.
3. Adams, M. J., King, A. A., and Kirkbright, G. F., *Analyst*, 1976, **101**, 73.
4. Adams, M. J., Beadle, B. C., King, A. A., and Kirkbright, G. F., *Analyst*, 1976, **101**, 553.
5. Adams, M. J., and Kirkbright, G. F., *Analyst*, 1977, **102**, 281.
6. Monroe, D. M., and Reichard, H. S., Applications Note 147, Princeton Applied Research Corp., Princeton, New Jersey, USA, 1976.
7. McClelland, J. F., and Kniseley, R. N., *Appl. Optics*, 1976, **12**, 2967.
8. Rosengren, L.-G., *Appl. Optics*, 1975, **14**, 1960.
9. Hunt, G. R., and Salisbury, J. W., *Mod. Geol.*, 1970, **1**, 283.

NOTE—References 3, 4 and 5 are to Parts I, II and III of this series, respectively.

Determination of Residues of the Herbicides Bromacil, Lenacil and Terbacil in Soils by Gas Chromatography

David J. Caverly

Ministry of Agriculture, Fisheries and Food, Agricultural Development and Advisory Service, Olantigh Road, Wye, Ashford, Kent, TN25 5KL

and Ronald C. Denney

School of Chemistry, Thames Polytechnic, Woolwich, London, SE18 6PF

A rapid and sensitive procedure for the determination of residue levels of three uracil herbicides in soils is described. After addition of calcium hydroxide and Celite to the soil the herbicides are eluted from columns with water. After acidification of the eluate and partition into chloroform these herbicides are determined by gas chromatography using a nitrogen-selective detector. Recoveries from a range of soil types are better than 80%, with a sensitivity limit of 20 μg kg^{-1}.

Keywords: Uracil herbicide determination; soils; gas chromatography

Bromacil (5-bromo-3-*sec*-butyl-6-methyluracil), **I**, lenacil (3-cyclohexyl-5,6-trimethyleneuracil), **II**, and terbacil (5-chloro-3-*tert*-butyl-6-methyluracil), **III**, are widely used herbicides for the control of annual and perennial weeds in fruit and vegetable crops. Procedures[1-4] for the
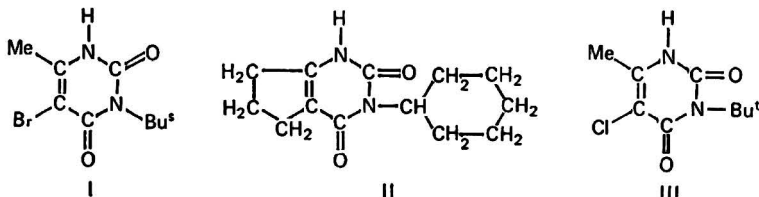
determination of bromacil and terbacil residues in soils using electron-capture gas chromatography have been described but these procedures involve time-consuming clean-up techniques to remove interfering co-extractives. Pease[5] described a flame-ionisation gas-chromatographic procedure for the determination of lenacil residues in soils but this method lacks sensitivity and selectivity at the normal levels found in soils. Micro-coulometric gas chromatography[6,7] has been applied successfully to bromacil residues alone in soils and fruit, but this technique does not possess the simplicity of more standard forms of gas chromatography and has not been applied to residues of lenacil. Thin-layer techniques[8,9] have been used principally for confirmation of the identity of residues found by gas chromatography; they lack the sensitivity for application to normal soil residue levels. Maier-Bode and Riedmann[10] reported comprehensively on the use of the rubidium bromide thermionic detector for the detection of many nitrogen- and phosphorus-containing pesticides; they did not apply their findings to the determination of residues in soils and plants. Recently Jarcjyk[11] has applied the nitrogen-selective detector to the determination of bromacil residues in plants and soils. The procedure uses relatively large volumes of solvents and extracts require a column chromatographic clean-up. The procedure described here is simple, sensitive and can be applied to all three herbicides in a variety of soil types. The sample is mixed initially with calcium hydroxide and Celite and placed in a glass column in which it is eluted with water. The eluate is acidified and extracted with chloroform. After evaporation of the solvent the extract is analysed by gas chromatography, temperature programming being employed for the separation of mixtures of herbicides.

Experimental

Apparatus

A Pye, Series 104, gas chromatograph equipped with a rubidium chloride thermionic detector and a glass column, 0.9 m × 4 mm i.d., packed with 5% high-vacuum silicone grease on 80–100-mesh Gas-Chrom Q, is used [stationary phase as supplied by ICI Ltd. (grade M 494) or BDH Chemicals Ltd.]. Column temperatures corresponding to the elution order terbacil, bromacil and lenacil are 180, 190 and 230 °C, respectively. The temperature programme for the separation of all three herbicides is 180 °C for 1 min, increasing at the rate of 10 °C min^{-1} to a maximum of 230 °C.

Glass columns. 300 × 15 mm i.d. with taps and sintered-glass discs.
Separating funnels. 100-cm^3 capacity.

Reagents

All reagents should be of analytical-reagent grade and checked for impurities and solvents should, if necessary, be re-distilled.

Calcium hydroxide.
Celite. Analytical filter aid (BDH Chemicals Ltd.).
Chloroform.
Hydrochloric acid, concentrated.
Sodium sulphate, anhydrous.
Pesticide standards. Obtained from the Pesticide Residue Analysis and Information Service, Department of Industry, Laboratory of the Government Chemist, Cornwall House, Stamford Street, London, SE1 9NQ. Stock standard solutions were prepared by dissolving a suitable amount of the herbicide in acetone, and the working standard by further dilution of the stock solution with acetone or other suitable solvent to give a concentration of 5 μg ml^{-1}.

The calibration graph was constructed for each herbicide by plotting peak heights against amount injected in nanograms. Fig. 1 shows that straight lines were obtained when working at maximum sensitivity when 30, 25 and 50 ng of terbacil, bromacil and lenacil, respectively, gave 50% full-scale deflection.
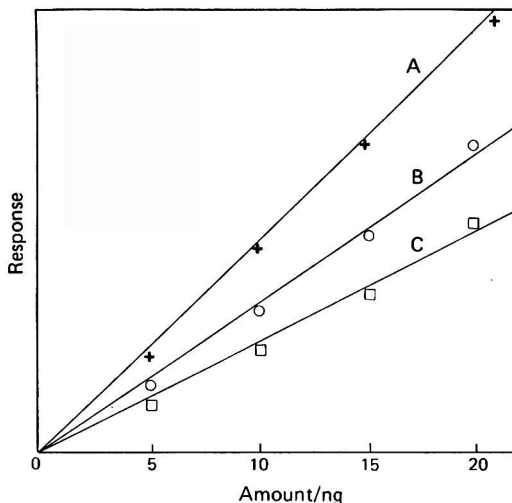
Fig. 1. Response of (A) bromacil, (B) terbacil and (C) lenacil to the nitrogen-responsive detector.

Procedure

To 10 g of air-dried soil add 2 g of calcium hydroxide, 2 g of Celite and sufficient water to produce a slurry; stand for 30 min and transfer to the glass column using the minimum amount of water. Elute the column with 5-cm^3 volumes of water and collect 50 cm^3 of the eluate. Transfer the eluate into a 100-cm^3 separating funnel, add 5 cm^3 of concentrated hydrochloric

acid and 20 cm³ of chloroform and immediately shake vigorously for 30 s. After complete separation of the phases, transfer the lower layer into a small conical flask containing approximately 5 g of anhydrous sodium sulphate. Allow to stand for 10 min with occasional swirling, then decant the chloroform solution into a 150-cm³ flat-bottomed flask. Repeat the extraction with two further 10-cm³ volumes of chloroform, allowing each to stand in the conical flask containing the sodium sulphate before combining with the previous extract.

Under conditions of reduced pressure at 70 °C carefully reduce the volume of solution to approximately 5 ml. Remove the last trace amounts of chloroform by using the minimum of heat. Immediately dissolve the residue in a suitable volume of acetone for examination by gas chromatography.

TABLE I

CHARACTERISTICS OF SOILS STUDIED

Soil number	Texture	pH	Organic matter, %
1	Very fine sandy loam	7.6	2.55
2	Loam	5.1	2.78
3	Calcareous silty loam	7.6	3.57
4	Very fine sandy loam	7.7	4.11
5	Fine sandy loam	6.5	2.37
6	Sandy loam	4.4	2.56
7	Very fine sandy loam	7.2	2.51
8	Clay loam	7.6	5.76
9	Sandy loam	5.7	3.82
10	Very fine sandy loam	7.5	2.24

TABLE II

RECOVERY OF HERBICIDES ADDED TO SOIL SAMPLES

Soil number	Bromacil Added/ mg kg⁻¹	Found/ mg kg⁻¹	Recovery, %	Lenacil Added/ mg kg⁻¹	Found/ mg kg⁻¹	Recovery, %	Terbacil Added/ mg kg⁻¹	Found/ mg kg⁻¹	Recovery, %
1	5.0	4.3	86	5.0	4.8	96	5.0	4.1	82
	1.0	0.76	76	1.0	0.8	80	1.0	0.7	70
	0.2	0.18	90	0.2	0.2	100	0.2	0.18	90
2	5.0	4.7	94	5.0	5.0	100	5.0	4.8	96
	1.0	0.88	88	1.0	0.96	96	1.0	0.9	90
3	5.0	3.7	74	5.0	4.2	84	5.0	4.0	80
	1.0	1.02	102	1.0	1.10	110	1.0	1.0	100
4	5.0	4.2	84	5.0	4.8	96	5.0	3.7	74
	1.0	0.74	74	1.0	0.8	80	1.0	0.8	80
5	5.0	5.0	100	5.0	4.9	98	5.0	4.4	88
	1.0	0.86	86	1.0	0.8	80	1.0	0.98	98
6	5.0	5.0	100	5.0	5.1	102	5.0	5.0	100
	1.0	0.88	88	1.0	1.0	100	1.0	0.88	88
7	1.0	0.86	86	1.0	0.96	96	1.0	0.96	96
	0.2	0.2	100	0.2	0.21	105	0.2	0.19	95
8	1.0	0.86	86	1.0	0.86	86	1.0	0.86	86
	0.2	0.17	85	0.2	0.17	85	0.2	0.17	85
9	5.0	3.6	72	5.0	4.7	94	5.0	3.6	72
	1.0	0.8	80	1.0	0.96	96	1.0	0.96	96
10	5.0	4.3	86	5.0	5.0	100	5.0	4.7	94
	1.0	0.7	70	1.0	0.8	80	1.0	0.82	82

Results

The recovery of these herbicides was checked by adding known volumes of standard solutions to 10-g portions of the ten air-dried soil types (Table I) followed by removal of solvent by a gentle stream of air. The soils were allowed to stand for 24 h and then treated as described under Procedure. The results obtained are shown in Table II. Blank determinations carried out on these soils showed that any herbicide present was below the limit of detection.
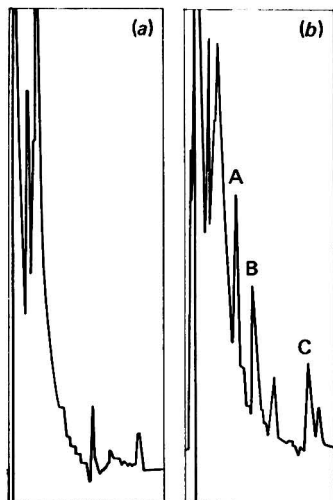
Fig. 2. Gas-chromatographic comparison of (A) terbacil, (B) bromacil and (C) lenacil recovered from (a) untreated soil and (b) spiked soil.
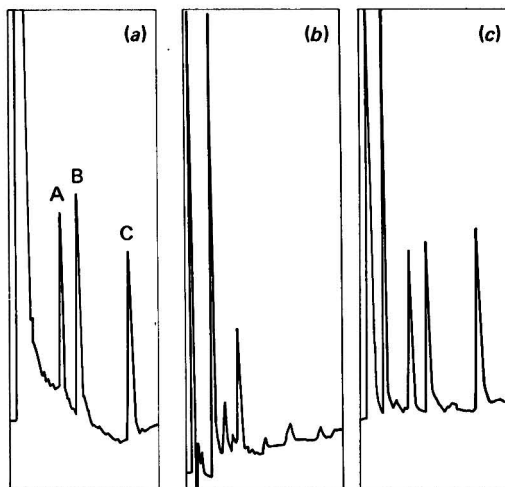
Fig. 3. Gas chromatograms of (a) standard containing (A) terbacil, (B) bromacil and (C) lenacil, (b) extract from soil containing terbacil and (c) extract of soil in (b) after addition of standards at the 1 mg kg^{-1} level, showing coincidence of terbacil peak.

Fig. 2 shows recoveries at the 0.2 mg kg^{-1} level for all three herbicides compared with the gas-chromatographic response for the untreated soil. Fig. 3 shows the response of a field-treated soil containing 0.07 mg kg^{-1} of terbacil together with the recovery of 1 mg kg^{-1} of terbacil, bromacil and lenacil added to this soil and a standard mixture of the three herbicides. The retention times for these compounds were approximately 4, 6 and 10 min, respectively.

References

1. Wheeler, W. B., Thompson, N. P., Ray, B. R., and Wilcox, M., *Weed Res.*, 1971, **19** (3), 307.
2. Jolliffe, U. A., Day, B. E., Jordan, R. S., and Mann, J. D., *J. Agric. Fd Chem.*, 1967, **15**, 174.
3. Gutamann, W. H., and List, D. J., *J. Ass. Off. Analyt. Chem.*, 1971, **54**, 975.
4. Bevenue, A., and Ogata, J. N., *J. Chromat.*, 1970, **46**, 110.
5. Pease, H. L., *J. Sci. Fd Agric.*, 1966, **17**, 121.
6. Pease, H. L., *J. Agric. Fd Chem.*, 1966, **14**, 94.
7. Gawronski, S., and Skapski, H., *Zesz. Nauk. Akad. Roln. Warsz., Ogrodnictwo*, 1974, **8**, 59.
8. Hamilton, D. J., *J. Agric. Fd Chem.*, 1968, **16**, 142.
9. Von Stryk, F. G., and Zajacs, G. F., *J. Chromat.*, 1969, **41**, 125.
10. Maier-Bode, H., and Riedmann, M., *Residue Rev.*, 1975, **54**, 113.
11. Jarcjyk, H. J., *PflSchutz-Nachr. "Bayer,"* 1975, **28**, 319.

Determination of Ronidazole in Pig and Turkey Feeding Stuffs by Gas - Liquid Chromatography

J. R. Harris, P. G. Baker and Geraldine Alliston

Laboratory of the Government Chemist, Cornwall House, Stamford Street, London, SE1 9NQ

A gas - liquid chromatographic method with flame-ionisation detection has been developed for the determination of ronidazole in complete feeding stuffs. The method is based on the formation of a volatile silyl derivative of ronidazole by reaction with *NO*-bis(trimethylsilyl)acetamide. Recoveries of ronidazole at the level of 60 mg kg⁻¹ were about 95%. No interference was observed from grass meal, fish meal or other drugs.

Ronidazole (1-methyl-5-nitroimidazol-2-ylmethyl carbamate) is used in pig feeds for the treatment and control of dysentery and as a growth-promoting compound. It is also used in turkey feeds for the treatment and control of blackhead. The normal levels of usage are between 60 and 120 mg kg⁻¹.

A spectrophotometric method for the determination of ronidazole in animal feeds was described by Szalkowski and Kanora.[1] This method is based on the cleavage of the nitro group by alkaline hydrolysis, followed by diazotisation of 4-aminobenzoic acid by the liberated nitrite ion and then coupling with *N*-2-aminoethyl-1-naphthylamine to form a coloured complex. This method is subject to interference from feeds that contain grass meal, fish meal and other drugs that contain nitro groups (*e.g.*, dimetridazole and nitrofurazone).

A method for the determination of ronidazole in tissues by differential pulse polarography was described by Cala *et al.*,[2] and a method for the study of the metabolism of ronidazole using radioactive tracers was described by Rosenblum *et al.*[3] However, neither of these methods is directly applicable to animal feeds.

This paper describes a gas - liquid chromatographic method for the determination of ronidazole in feeding stuffs.

Experimental

Apparatus

A gas - liquid chromatograph fitted with a flame-ionisation detector is required; a Pye, Model G.C.V., fitted for on-column injections was used.

A glass column (1.5 m × 4 mm i.d.) containing 5% OV-17 on Gas-Chrom Q (80–100 mesh) was used, with the following operating conditions: carrier gas (nitrogen) flow-rate, 30 ml min⁻¹; hydrogen flow-rate, 30 ml min⁻¹; air flow-rate, 300 ml min⁻¹; column temperature, 165 °C; injection port temperature, 220 °C; and detector temperature, 300 °C.

A sintered-glass micro-filter, porosity 1, i.d. 2.3 cm (available from Scientific Supplies Co. Ltd., Vine Hill, London, E.C.1) was used.

Reagents

Sodium chloride.
Sodium sulphate, anhydrous (heated overnight at 350 °C).
Ethyl acetate.
Quinoline.
NO-Bis(trimethylsilyl)acetamide (BSA) silylating reagent. Pierce and Warriner, Chester.
Trisodium orthophosphate solution, 5 g per 100 ml.
Internal standard solution. Dissolve 25.0 mg of diethyl phthalate in quinoline and dilute to 50 ml with quinoline.

Ronidazole standard solution. Weigh to the nearest 0.1 mg approximately 25 mg of pure ronidazole, dissolve it in ethyl acetate and make the volume up to 100.0 ml with ethyl acetate. This solution is stable for 48 h.

Procedure

Once the procedure has been started, it should be completed on the same day.

Extraction

Weigh to the nearest 0.001 g a portion of finely divided and mixed sample expected to contain between 450 and 600 μg of ronidazole (usually 5–20 g of sample). Grind the sample in a mortar with 2 ml of trisodium orthophosphate solution and quantitatively transfer the mixture into an extraction thimble. Extract the mixture in a Soxhlet apparatus with 125 ml of ethyl acetate, allowing about 20 cycles, and then cool it. Reduce the volume of the ethyl acetate extract to about 30 ml, using a rotary evaporator at a temperature of 30 °C, and transfer the solution into a 100-ml separating funnel. Rinse the flask several times with 2-ml portions of ethyl acetate and add the washings to the funnel.

Removal of interfering substances

Extract the ethyl acetate with three 10-ml portions of 1 M hydrochloric acid and combine the extracts in a second 100-ml separating funnel. Add 5 ml of ethyl acetate to the acid extracts, swirl gently and run off the acid layer into a 250-ml separating funnel. Add 10 g of sodium chloride and swirl the funnel to produce a saturated solution. Make the solution alkaline (pH 10) with 5 M sodium hydroxide solution, keeping the time of exposure of ronidazole to the sodium hydroxide as short as possible, and immediately extract with three 40-ml portions of ethyl acetate. Run the extracts through a sintered-glass micro-filter containing 20 g of sodium sulphate into a 250-ml round-bottomed flask. Wash the filter with two 10-ml portions of ethyl acetate and add the washings to the flask.

Silylation

Reduce the volume of the ethyl acetate extract to about 3 ml in the rotary evaporator at 30 °C and quantitatively transfer the remaining extract into a test-tube of capacity about 15 ml, with a number 14 standard ground-glass neck, rinsing the flask with four 2-ml portions of ethyl acetate. Evaporate the mixture to dryness on a water-bath at 50 °C under a stream of nitrogen and add 1.0 ml of the internal standard solution to the residue. Add 250 μl of BSA with a syringe and gently shake the tube. Fit a condenser to the tube and gently heat the solution until it just begins to reflux (5 min). Remove the tube from the heat, allow it to cool to room temperature and inject 5 μl of the solution on to the column. Measure the peak heights of the ronidazole and diethyl phthalate internal standard. The retention times of ronidazole and diethyl phthalate are approximately 12 and 14 min, respectively.

Ronidazole standard

Transfer by pipette 2.0 ml of standard ronidazole solution into a 100-ml separating funnel and make up to a volume of 30 ml with ethyl acetate. Proceed as described above from *Removal of interfering substances.*

Calculation

Calculate the peak-height ratio of ronidazole to diethyl phthalate for the feed sample and ronidazole standard. The amount of ronidazole in the feed is given by the equation

$$\text{Ronidazole/mg kg}^{-1} = \frac{2 \times A \times C}{B \times M}$$

where A = peak-height ratio derived from feed; B = peak-height ratio derived from ronidazole standard; C μg ml^{-1} = ronidazole concentration of standard; and M g = mass of sample taken.

Results

Two pig feeds and two turkey feeds were medicated by the addition of a 5% ronidazole pre-mix (starch-based) and examined by the proposed method; the effects of fish meal and grass meal on the procedure were also examined. The results are given in Table I.

TABLE I

RECOVERY OF RONIDAZOLE ADDED TO FEEDS

Feed			Ronidazole in test portion/μg	Ronidazole found/μg	Recovery, %
Pig feed A	..	..	..	600	590	98
			600	580	97
			600	580	97
Pig feed B	..	..	..	580	540	93
			580	540	93
Turkey feed A ..		..	..	540	540	100
			600	590	98
			600	580	97
Turkey feed B ..		..	..	590	560	95
			590	570	97
Turkey feed B + 5% fish meal		..	590	560	95
Turkey feed B + 5% grass meal		..	590	590	100

The following drugs were added to blank feeds at their normal levels of usage: amprolium (80), carbadox (50), ethopabate (4), nicarbazin (50), nitrovin (10), pyrimethamine (5) and sulphaquinoxaline (125 mg kg^{-1}). None of these drugs gave peaks on the chromatogram.

Dimetridazole (120) and ipronidazole (50 mg kg^{-1}) were added to a feed containing ronidazole (60 mg kg^{-1}). Although both drugs produced well defined peaks on the chromatogram, they were sufficiently well resolved from the ronidazole and internal standard peaks not to interfere.

Halquinol (120 mg kg^{-1}) gave two peaks on the chromatogram corresponding to its two main components, but these peaks did not interfere with the application of the method.

Discussion

When ronidazole standards that had been subjected to the above method were compared with standards silylated directly, it was observed that only about 95% of the ronidazole was being recovered. Detailed examination of the procedure showed that the losses occurred while the ronidazole was in alkaline solution. In order to overcome this problem, it was decided to subject the standard to the clean-up procedure in addition to silylation so that the standard and test portion were treated in the same fashion.

Linearity

Linear peak-height ratios (ronidazole to internal standard) were obtained for amounts of ronidazole ranging from 450 to 700 μg (Table II).

TABLE II

LINEARITY OF PEAK-HEIGHT RATIOS

Amount of ronidazole/μg	Peak-height ratio	$K^* \times 10^{-3}$
470	0.511	9.20
470	0.462	10.17
590	0.637	9.26
590	0.622	9.48
700	0.754	9.28
700	0.759	9.22

* K = Ronidazole (μg)/peak-height ratio.

Silylation

Chromatography of pure ronidazole yields a single peak (A), which shows considerable tailing and neither the height nor the area is sufficiently reproducible for quantitative determinations.   Examination by combined gas chromatography - mass spectrometry suggested that the peak is due to 1-methyl-2-hydroxymethyl-5-nitroimidazole.

If pure ronidazole in chloroform is treated at room temperature with BSA, two peaks are produced, one of which corresponds to peak A above and the other to the silyl derivative of ronidazole.   Heating the reaction mixture gives an increased yield of the silyl derivative.

Solvent

From the above discussion, it is apparent that silylation of ronidazole will be facilitated by carrying out the reaction at an elevated temperature.   The solvent used must be inert towards BSA and, if eluted from the column, must be clearly resolved from the ronidazole derivative.   Several solvents were examined and it was observed that the rate of silylation was dependent on the boiling-point of the solvent (Table III).   Quinoline was selected because it satisfied the requirements and gave quantitative yields with a short reaction time.   3,5-Dimethylpyridine was found to be unsuitable because it gave several peaks that interfered with the peak of the ronidazole derivative.

TABLE III

SOLVENTS FOR SILYLATION

Solvent	Boiling-point/°C	Reaction time
Chloroform ..	61	Incomplete after 16 h
Pyridine ..	114	5 h
3-Methylpyridine ..	141	$1\frac{1}{2}$ h
4-Methylpyridine ..	143	$1\frac{1}{2}$ h
3,5-Dimethylpyridine ..	171	10 min
Quinoline ..	237	5 min

Applicability

Although the method was designed for the assay of ronidazole at the normal levels of inclusion in feeds, its sensitivity is such that acceptable results can be obtained at levels down to about 20 mg kg^{-1}.

References

1.   Szalkowski, C. R., and Kanora, J., *J. Ass. Off. Analyt. Chem.*, 1969, **52**, 101.
2.   Cala, P. C., Downing, G. V., Michielli, R. F., and Wittick, J. J., *J. Agric. Fd Chem.*, 1976, **24**, 764.
3.   Rosenblum, C., Trenner, N. R., Buhs, R. P., Hiremath, C. B., Koniuszy, F. R., and Wolf, D. E., *J. Agric. Fd Chem.*, 1972, **20**, 360.

Acetylation as a Means of End-point Indication in the Catalytic Thermometric Titration of Bases

E. J. Greenhow

Department of Chemistry, Chelsea College, University of London, Manresa Road, London, SW3 6LX

The acid-catalysed acetylation of alcohols and phenols with acetic anhydride is used to indicate the end-point in the titration of tertiary amines and metal carboxylates with 0.1, 0.01 and 0.001 M perchloric acid in acetic acid.

Mixtures of acetic anhydride with butan-1-ol, 2-methylpropan-2-ol, 4-hydroxy-4-methylpentan-2-one, 3,5-dimethylphenol, pyrocatechol, hydroquinone or quinhydrone are all satisfactory end-point indicators for the determination of pyridine and quinoline derivatives, tertiary aliphatic amines and metal carboxylates, but the acetic anhydride - quinhydrone mixture is superior to the other mixtures for the determination of the very weak bases, antipyrine, caffeine, theophylline and urea. A colour change occurs at the end-point when quinhydrone is the hydroxylic component.

The sharpness of the end-point inflection can be improved by adding dichloromethane, nitromethane or propylene carbonate to the sample solution.

Sample sizes down to about 0.000 1 mequiv can be determined with 0.001 M titrant solution. Precisions are usually better than 0.5% with 0.1 M and 1.0% with 0.01 and 0.001 M titrants.

The influence of intra- and intermolecular hydrogen bonding of the hydroxyl groups in the alcohol and phenol reagents on end-point sharpness is discussed.

Keywords: Tertiary amine determination; metal carboxylate determination; non-aqueous thermometric titration; alcohol and phenol acetylation

In their application of the coulometric method of titrant generation to catalytic thermometric titrimetry, Vajgand *et al.*[1] used hydroquinone as a source of hydrogen ions for the titration of bases. The end-point of the titration was indicated by an increase in temperature caused by the acid-catalysed exothermic reaction between acetic anhydride and hydroquinone and/or the benzoquinone formed by its oxidation at the platinum anode in the coulometric cell. The authors suggested that the indicator reaction is the addition of acetic anhydride to the quinoid system, but later in their paper they referred to the "acetic anhydride - hydroquinone indicator reaction." As the amount of quinoid (quinonoid) material, *i.e.*, benzoquinone, produced when the end-point is indicated would be small when the sample is small, it would give rise to small temperature changes only. It seems more likely, therefore, that the unoxidised hydroquinone is the major reactant with acetic anhydride in the indicator reaction.

A brief study of the acetylation of alkyl alcohols and phenol as a thermometric indicator reaction was carried out by Goitzman in 1969.[2] The hydroxyl compound was omitted from the sample solution to avoid a premature reaction, and was added to the solution after most of the sample compound had been neutralised by 0.1 M perchloric acid titrant. A preliminary titration is necessary to determine an approximate titration value. It is suggested that the amount of acetylatable component in the mixture should be at a minimum.

In the present study, 1,4-benzoquinone, hydroquinone, quinhydrone and a range of aliphatic and aromatic hydroxyl compounds were compared as reagents for use with acetic anhydride as thermometric end-point indicators in the titration of weak and very weak bases with solutions of perchloric acid in acetic acid.

In an earlier paper, Vajgand *et al.*[3] pointed out that nitromethane and acetic anhydride are satisfactory solvents for use in the determination of the weak base antipyrine by catalytic thermometric titration with 0.25 M perchloric acid in acetic acid as the titrant, when the exothermic acid-catalysed hydration of acetic anhydride is used to mark the end-point. They noted that the presence of acetic acid has an adverse effect on the temperature change at the end-point and the precision of the determinations. In the present study, acetic acid has been used as a sample solvent only for metal carboxylates that are insoluble in the anhydride.

Experimental

Reagents

Acetic anhydride, acetic acid, hydroquinone, quinhydrone and tris(hydroxymethyl)methyl-amine were analytical-reagent grade materials.   The other amines, solvents, hydroxyl compounds and metal carboxylates were of laboratory-reagent grade, except for cobalt(II) naphthenate, which was a technical-grade material described as containing 10% of cobalt.

The 0.1, 0.01 and 0.001 M solutions of perchloric acid in dry acetic acid were prepared from AnalaR-grade perchloric acid (71.0–73.0%), acetic acid and acetic anhydride by the method of Belcher et al.[4]   The solutions were standardised against solutions of AnalaR-grade potassium hydrogen phthalate in dry acetic acid.

Apparatus

Details of the automatic titration apparatus, in which solvent is introduced by means of a motor-driven micrometer syringe and the temperature is measured by means of a thermistor, and recorded on a potentiometric chart recorder, are given elsewhere.[5]   The titration vessel was a Dewar beaker (14 ml) and solutions were stirred with a magnetic stirrer.

Procedure

Prepare a solution of the base in 1 ml of acetic anhydride, nitromethane, nitroethane, dichloromethane, or 1,2-dichloroethane, or in 2 ml of acetic acid if the sample is insoluble in the former solvents.   The amount of sample will depend on the titrant concentration.   Thus, 0.02–0.2, 0.002–0.02 and 0.000 2–0.002 mequiv of base can be determined conveniently with 0.1, 0.01 and 0.001 M titrants, respectively.   Add to the sample solution in the Dewar beaker sufficient acetic anhydride to make the total volume 5 ml, then add 4 mequiv of the hydroxyl reagent and stir for about 1 min.   Add the titrant at the rate of about 0.2 ml min^{-1}.   It is convenient to operate the chart recorder over the 0–500 mV range.

The end-point of the titration can be measured on the titration graph as the point where the tangent to the main heat rise leaves the curve at its lower temperature end,[6] but the point of inflection on the curve, as shown in Fig. 1, usually gives a more reproducible value, which corresponds more closely to the theoretical value.

Results and Discussion

Titration curves for tripropylamine, 2-methylpyridine, quinoline, antipyrine, caffeine, theophylline, urea and some metal carboxylates are shown in Figs. 1–4.

There is no detectable end-point inflection when a solution of 1,4-benzoquinone in acetic anhydride is used as indicator reagent for the determination of quinoline [Fig. 1(a)].   Quinones undergo an addition reaction with acetic anhydride in acidic media (the Thiele - Winter reaction[7]), but apparently the rate of this reaction is insignificant in the presence of trace amounts of acid.   In contrast, a sharp increase in temperature occurs when a mixture of hydroquinone and acetic anhydride is used as the indicator system [Fig. 1(b)].   However, although the end-point inflection can be detected, there is an increase in temperature during the neutralisation of the quinoline.   This increase is much greater than might be expected from the neutralisation alone, and must be attributed mainly to "uncatalysed" acetylation of the hydroquinone.   More satisfactory end-point inflections are obtained when quinhydrone, butan-1-ol, 2-methylpropan-2-ol, 4-hydroxy-4-methylpentan-2-one (diacetone alcohol) or 3,5-dimethylphenol are used as the hydroxylic components of the thermometric indicator. The temperature increase at the end-point ranges from about 5 to about 15 °C, depending on the hydroxyl compound used in the indicator mixture.

The indicator systems are unsuitable for the determination of primary and secondary amines and benzylamine [Figs. 1(m)–(q)] because acetylation of the amino groups occurs during the titration to yield a non-basic product.   The end-point inflections are not sharp and the titration values obtained depend on the time during which the sample and the indicator system have been in contact.

Indicator systems containing quinhydrone or 4-hydroxy-4-methylpentan-2-one give sharp end-points in the titration of antipyrine ($pK_b = 12.40$) [Figs. 2(b) and (d)], but those containing hydroquinone and butan-1-ol are less satisfactory [Figs. 2(a) and (c)].   The quinhydrone -

acetic anhydride mixture gives the most satisfactory end-point inflection in the titration of the very weak bases, caffeine ($pK_b = 13.39$), theophylline ($pK_b = 13.24$) and urea ($pK_b = 13.80$) [Figs. 2(f), (m) and (p)].

Figs. 2(e), (g), (j) and (k) show that 3,5-dimethylphenol and pyrocatechol are no better than
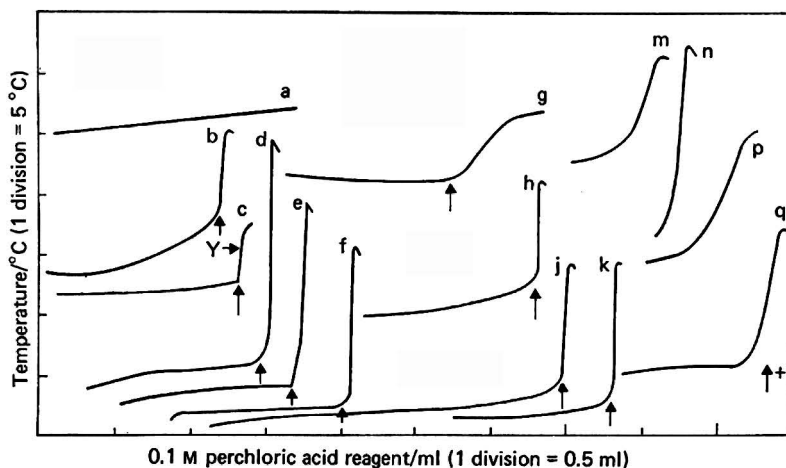
Fig. 1.   Catalytic thermometric titration of aliphatic amines, 2-methylpyridine and quinoline with 0.1 M perchloric acid in acetic acid.   Amine/mg: a–h, quinoline 15.2; j, 2-methylpyridine 23.5; k, tripropylamine 15.2; m, butylamine 13.1; n, tris(hydroxymethyl)methylamine 12.6; p, morpholine 20.0; q, benzylamine 24.7.   Hydroxyl indicator reagent (4 mequiv): a, 1, 4-benzoquinone (included for comparison); b, hydroquinone; c, quinhydrone; d, butan-1-ol; e, 2-methylpropan-2-ol; f, j–q, 4-hydroxy-4-methylpentan-2-one; g, salicylic acid; h, 3,5-dimethylphenol. Acetic anhydride indicator reagent, 5 ml. Arrows indicate end-points (inflection); + indicates theoretical end-point; Y indicates colour change from opaque to clear yellow.

hydroquinone and butan-1-ol as indicator reagents in the titration of caffeine. Although salicylic acid is inferior to quinhydrone as an indicator reagent for the determination of
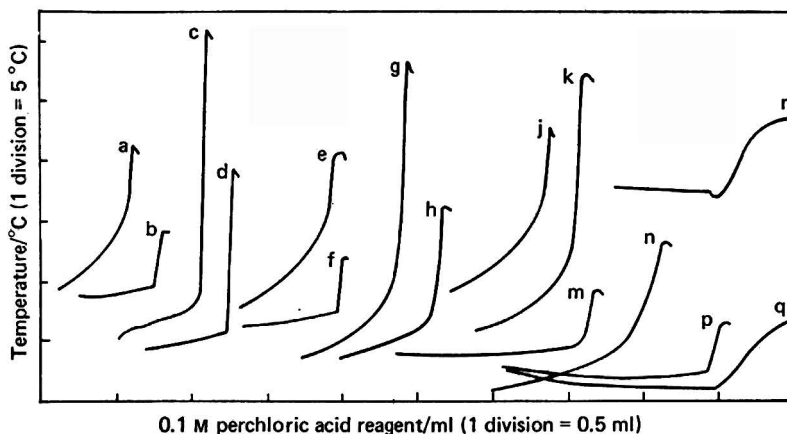
Fig. 2.   Catalytic thermometric titration of antipyrine, caffeine, theophylline and urea with 0.1 M perchloric acid in acetic acid.   Amine/mg: a–d, antipyrine 9.4; e–k, r, caffeine 12.0; m, theophylline 25.0; n, theophylline 22.5; p, urea 9.0; q, urea 8.5.   Hydroxyl indicator reagent (4 mequiv): a, e, hydroquinone; b, f, m, p, quinhydrone; c, g, butan-1-ol; d, h, n, 4-hydroxy-4-methylpentan-2-one; j, 3,5-dimethylphenol; k, pyrocatechol (8 mequiv); q, r, salicylic acid.   Acetic anhydride indicator reagent, 5 ml.

caffeine and urea in terms of end-point sharpness, no "uncatalysed" acetylation is evident when it is used [Figs. 2(q) and (r)].

Sodium, potassium, calcium and cobalt carboxylates can be determined without difficulty when a mixture of acetic anhydride and 4-hydroxy-4-methylpentan-2-one is used as the thermometric indicator (Fig. 3). The other hydroxyl compounds that were satisfactory as indicator reagents for the determination of quinoline can be used instead of the diacetone alcohol in the carboxylate titrations. The titration value found for the technical-grade cobalt naphthenate corresponds to a cobalt content of 10.3%, and this value is in good agreement with the claimed content of 10%.
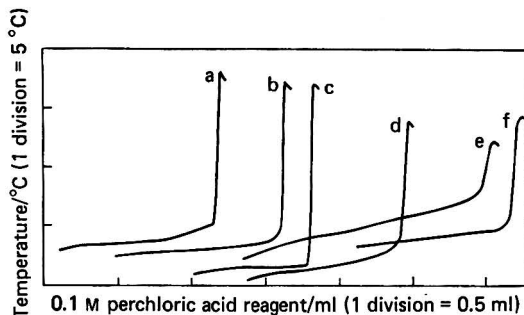
Fig. 3. Catalytic thermometric titration of metal carboxylates with 0.1 M perchloric acid in acetic acid. Carboxylate/mg: a, potassium acetate 10.6; b, sodium benzoate 16.2; c, potassium hydrogen phthalate 15.2; d, sodium salicylate 17.5; e, calcium acetate 14.6 in 2 ml of acetic acid; f, cobalt(II) naphthenate 31.1 in 2 ml of acetic acid. Indicator reagent, 0.46 g of 4-hydroxy-4-methylpentan-2-one + 5 ml of acetic anhydride.

Sharp end-point inflections have been obtained by using 0.01 M perchloric acid as the titrant for the determination of quinoline, antipyrine, caffeine, potassium acetate and potassium hydrogen phthalate [Figs. 4(a)–(j)]. The indicator reagents used with the 0.1 M titrant were satisfactory with the weaker titrant. The end-point inflections were much less sharp when a
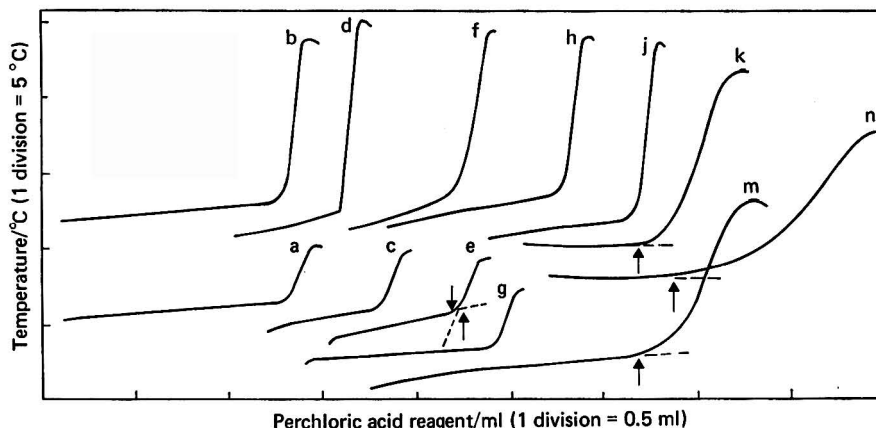
Fig. 4. Catalytic thermometric titration of bases with 0.01 and 0.001 M perchloric acid in acetic acid. Base/mg: a, b, quinoline 1.52; m, quinoline 0.152; c, d, antipyrine 0.94; k, antipyrine 0.094; e, f, caffeine 1.20; n, caffeine 0.12; g, h, potassium acetate 0.93; j, potassium hydrogen phthalate 1.52. Hydroxyl indicator reagent (4 mequiv): a, c, e, g, quinhydrone; b, d, f, h–n, 4-hydroxy-4-methylpentan-2-one. Titrant molarity: a–j, 0.01; k–n, 0.001. Acetic anhydride indicator reagent, 5 ml. Arrows indicate end-points.

0.001 M titrant was used [Figs. 4(k)–(n)], but the titration values were reproducible when the end-point was located by drawing a tangent to the horizontal part of the titration graph, as shown in Fig. 4.   Sample sizes down to about 0.000 1 mequiv, *e.g.*, 13 µg of quinoline, can be determined conveniently by using the 0.001 M titrant.

Table I summarises the results obtained in an evaluation of the precision of the method when it is used for the determination of weak and very weak bases.   The coefficients of variation are of the order of 0.5% when the 0.1 M titrant is used and less than 1% with the 0.01 and 0.001 M titrants.   In the determination of caffeine with the 0.01 M titrant, more reproducible titration values were obtained by taking as the end-point the point where the tangent to the temperature increase leaves the curve at its lower temperature end, although in most other determinations the point of initial temperature increase, as shown in Fig. 1, gave the more reliable results.

TABLE I

RESULTS FOR PRECISION FROM THE THERMOMETRIC TITRATION OF ORGANIC BASES AND POTASSIUM ACETATE WITH 0.1, 0.01 AND 0.001 M SOLUTIONS OF PERCHLORIC ACID

Indicator system: acetic anhydride (5 ml) + hydroxyl reagent (4 mequiv).

Compound	Hydroxyl indicator reagent*	Base taken/mg	Titrant concentration/M	n†	Mean titre/ml	Standard deviation/ml	Coefficient of variation, %
Quinoline	A	16.1	0.1	4	1.226	0.005 9	0.48
Quinoline	A	1.52	0.01	4	1.137	0.006 2	0.55
Quinoline	A	0.152	0.001	4	1.49	0.010	0.67
Antipyrine	A	0.094	0.001	3	0.572	0.003 5	0.61
Caffeine	Q	12.0	0.1	4	0.618	0.003 0	0.49
Caffeine	Q	1.20	0.01	4	0.666	0.006 3	0.95‡
Potassium acetate	A	0.93	0.01	4	0.930	0.005 9	0.63

* A = 4-Hydroxy-4-methylpentan-2-one; Q = quinhydrone.
† n = Number of determinations.
‡ 0.39% when determined from the end-points measured by the tangents to the curve of temperature increase (see Procedure).

In all of these determinations the ideal titration curve is one in which no "uncatalysed" acetylation occurs during the neutralisation of the base, and the catalysed acetylation occurs rapidly with the minimum amount of perchloric acid following the neutralisation of the base. The hydroxyl compounds found to be the least satisfactory as indicator reagents in the determination of caffeine, namely hydroquinone, butan-1-ol and 3,5-dimethylphenol, differ from the more effective reagents, namely quinhydrone and 4-hydroxy-4-methylpentan-2-one, in the strength of the inter- or intramolecular hydrogen bonding of their hydroxyl groups. Thus, quinhydrone is a strongly hydrogen-bonded complex of 1,4-benzoquinone and hydroquinone, while 4-hydroxy-4-methylpentane-2-one has a structure that favours intramolecular hydrogen bonding of the hydroxyl with the carbonyl group.

Quinhydrone appears to resist acetylation until free perchloric acid becomes available to catalyse the reaction.   At the end-point of the titrations, the dark green, opaque, quinhydrone solution suddenly becomes clear yellow, as shown in Fig. 1(c).   Presumably, the hydrogen bonds of the molecular complex undergo fission rapidly at the onset of acetylation and the resulting yellow colour is that of 1,4-benzoquinone.   The quinhydrone reagent is, therefore, suitable as a visual, as well as a thermometric, indicator.

When hydrogen bonding in the hydroxylic reagent is weak, "uncatalysed" acetylation would be more likely to occur.   On the other hand, compounds in which the hydroxyl groups are very strongly hydrogen bonded may be less suitable or unsuitable for use in acetylation indicator systems.   For example, no end-point can be detected when 2-nitrophenol is used as the hydroxylic component of the indicator system but the 3- and 4-isomers are satisfactory reagents.   The gradual increase in temperature at the end-point when salicylic acid is used as an indicator [Figs. 1(g) and 2(q)] suggests that this reagent is more strongly hydrogen bonded than is quinhydrone.

Acetylation reactions that occur during the neutralisation of very weak bases are unlikely to be true uncatalysed reactions because the protonated bases themselves will show some catalytic activity, the magnitude of which will depend on the acid strengths of the BH^+ species as indicated by the pK_a values.

From the rates of the "uncatalysed" and catalysed acetylation reactions, as represented by the slopes of the titration curves before and after the end-point inflection, it should be possible to evaluate, or at least to compare, the reactivities of different hydroxyl reagents used in the indicator system.   Other acylating reagents, in addition to acetic anhydride, could also be evaluated in this way.   This possibility, with particular reference to the relationship between the reactivity and the molecular environment of the hydroxyl and acyl groups, is now being investigated.

The effect on the shape of the titration curve of replacing acetic anhydride with mixtures of acetic anhydride with nitromethane, nitroethane, dichloromethane, 1,2-dichloroethane, carbon tetrachloride, chloroform, propylene carbonate (4-methyl-1,3-dioxolan-2-one) and acetonitrile, in the sample solution, has been investigated.   Solutions of caffeine in the acetic anhydride mixtures, to which was added 4-hydroxy-4-methylpentan-2-one as the hydroxyl reagent, were titrated with 0.1 M perchloric acid. This sample - hydroxyl reagent combination was chosen because an unsatisfactory end-point is obtained when acetic anhydride alone is the other constituent. Fig. 5 summarises the results obtained when solvent mixtures containing acetic anhydride and the solvents listed above, in different proportions, were used. There was no clear improvement in the sharpness of the end-point when the proportions of acetic anhydride and solvent were $4 + 1$, but the use of solvents containing acetic anhydride and dichloromethane, nitromethane or propylene carbonate in the proportions $3 + 3$, $2 + 4$ and $1 + 5$, instead of acetic anhydride alone, led to sharper end-points.   There appears to be no simple relationship between the dielectric constants (ϵ) of the added solvents and the shape of the titration curves, as dichloromethane ($\epsilon = 9.1$), nitromethane ($\epsilon = 36.0$) and propylene carbonate ($\epsilon = 69.0$) are almost equally effective.
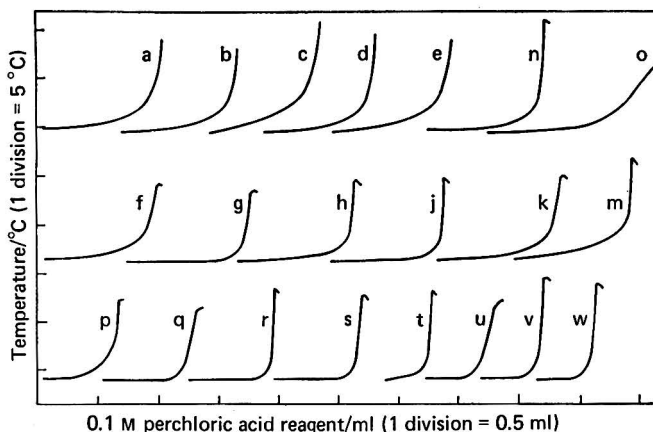
Fig. 5.   Catalytic thermometric titration of caffeine in different solvent mixtures with 0.1 M perchloric acid in acetic acid.   Caffeine/mg: a–e, 18.0; f–o, 17.6; p–s, 11.7; t–w, 5.9.   4-Hydroxy-4-methylpentan-2-one, 0.46 g.   Acetic anhydride/ml + solvent/ml: a–e, $4 + 1$; f–o, $3 + 3$; p–s, $2 + 4$; t–w, $1+5$.   Solvents: a, f, p, t, acetic anhydride only; b, g, q, u, nitromethane; c, h, nitroethane; d, j, r, v, dichloromethane; e, k, 1,2-dichloroethane; m, carbon tetrachloride; n, chloroform; o, acetonitrile; s, w, propylene carbonate.

As a method of thermometric end-point indication, esterification offers two advantages over the hydrolysis of anhydrides, the method evaluated by Vajgand and Gaál.[8]   Firstly, alcohols and phenols are much less basic hydroxylic reagents than is water, and they are therefore more suitable as solvents in the titration of very weak bases.   Secondly, much

larger amounts of alcohols and phenols can be tolerated in the sample solution when organic bases are determined because, unlike water, they are good solvents in general for organic compounds, and consequently greater increases in temperature at the end-point can be achieved conveniently.

References

1. Vajgand, V. J., Gaál, F. F., and Brusin, S. S., *Talanta*, 1970, **17**, 415.
2. Goitzman, M. S., *Dokl. Akad. Nauk SSSR*, 1969, **184**, 599.
3. Vajgand, V. J., Kiss, T. A., Gaál, F. F., and Zsigrai, I. J., *Talanta*, 1968, **15**, 699.
4. Belcher, R., Nutten, A. J., and Macdonald, A. M. G., "Quantitative Inorganic Analysis," Third Edition, Butterworths, London, 1970.
5. Greenhow, E. J., and Spencer, L. E., *Analyst*, 1973, **98**, 98.
6. Vaughan, G. A., and Swithenbank, J. J., *Analyst*, 1970, **95**, 890.
7. Thiele, J., and Winter, E., *Justus Liebigs Annln Chem.*, 1900, **311**, 341.
8. Vajgand, V. J., and Gaál, F. F., *Talanta*, 1967, **14**, 345.

Kinetic Micro-determination of Manganese in Natural Waters and of Iridium, Nitrilotriacetic Acid and 1,2-Diaminocyclohexane-*NNN'N'*-tetraacetic Acid

D. P. Nikolelis and T. P. Hadjiioannou*

Laboratory of Analytical Chemistry, University of Athens, Athens, Greece

An automatic kinetic spectrophotometric method is described for the ultra-micro determination of manganese and iridium, based on their catalytic effect on the periodate - phosphinate reaction. The method is also used for the determination of nitrilotriacetic acid (NTA) and 1,2-diaminocyclohexane-*NNN'N'*-tetraacetic acid (DCTA), on the basis of their activating and inhibiting effect, respectively, on the manganese-catalysed periodate - phosphinate reaction. The time required for the reaction to consume a fixed amount of periodate is measured automatically and related directly to the concentration of catalyst, activator or inhibitor. Manganese and iridium at the 10^{-8}–10^{-7} M level and NTA and DCTA at the 10^{-6} M level were determined with average errors of about 2%. The method has been applied to the determination of manganese in natural waters.

Keywords: Manganese determination; iridium determination; nitrilotriacetic acid; 1,2-diaminocyclohexane-NNN'N'-tetraacetic acid; natural waters

Kinetic methods have been widely used for the detection and determination of various catalytically active species.[1] In the instance of metal-ion catalysis, complexing agents that form highly stable metal complexes with such catalysts act as inhibitors and they can be determined on the basis of their inhibiting effect on the metal-ion catalysed reactions.[2] On the other hand, small amounts of certain substances, called activators, can increase significantly the rate of a catalytic reaction, thus improving the sensitivity and detectability of the determination of the catalyst[3] or permitting the determination of the activator.[4,5]

In a study of periodate reactions we found that the periodate - phosphinate reaction, which proceeds at a very slow rate at room temperature, is highly accelerated by trace amounts of manganese and iridium ions. In this paper, a kinetic spectrophotometric method for the ultra-micro determination of manganese(II) and iridium(III) is described, based on their catalytic effect on the periodate - phosphinate reaction. The method has also been used for the determination of trace amounts of nitrilotriacetic acid (NTA) and 1,2-diaminocyclo-hexane-*NNN'N'*-tetraacetic acid (DCTA), on the basis of their activating and inhibiting effects, respectively, on the manganese-catalysed periodate - phosphinate reaction. In all determinations, the time required for the periodate - phosphinate reaction to consume a fixed amount of periodate and thus for the absorbance to decrease by a pre-selected amount is measured automatically with a solid-state "double-switching" network[6,7] and related directly to the concentration of catalyst (manganese or iridium), activator (NTA) or inhibitor (DCTA).

The automatic procedure is accurate, precise, rapid and simple. The sample is added by pipette into the reaction cell containing the required reagents, sodium periodate or phosphinate is injected to start the reaction, the start button on the instrument is pressed and the elapsed time is read on a dial shortly after the start. Ultra-micro amounts of manganese in the range 12–400 ng (5.5×10^{-8}–1.8×10^{-6} M) and of iridium in the range 40–400 ng (5.2×10^{-8}–5.2×10^{-7} M) were determined with average errors and relative standard deviations of about 2% and reaction times of 20–200 s. The method has been applied to the determination of manganese in natural waters and the results obtained compare favourably with those obtained by activation analysis.[8] Microgram amounts of NTA and DCTA were determined with average errors and relative standard deviations of about 2–3%.

Experimental

Apparatus

The apparatus was the same as previously described.[6,7] The "double-switching" network

* To whom correspondence should be addressed.

was adjusted to measure the time required for the recorder pen to cross pre-selected positions on the chart, corresponding to 0.89 and 0.82 absorbance unit.

Reagents

Water was purified by doubly distilling de-ionised water through an all borosilicate-glass still. This water passed the dithizone test[9] and was used throughout this work.

Sodium metaperiodate stock solution, 0.100 M. Dissolve 21.4 g of sodium metaperiodate (G. F. Smith Co., Columbus, Ohio) in water and dilute to 1 l. Prepare more dilute solutions daily by dilution of the stock solution. Keep all periodate solutions in amber-glass bottles.

Sodium phosphinate stock solution, 0.100 M. Dissolve 1.06 g of sodium phosphinate $(NaH_2PO_2.H_2O)$ in water in a 100-ml calibrated flask and make the volume up to the mark with water.

Phosphate buffers, 2 and 1 M, pH 6.60. Dissolve 276 and 138 g, respectively, of sodium dihydrogen orthophosphate $(NaH_2PO_4.H_2O)$ in water, neutralise with 5 M sodium hydroxide solution to pH 6.60 and dilute to 1 l with water.

Phosphate buffer, 0.5 M, pH 7.80. Dissolve 69 g of sodium dihydrogen orthophosphate $(NaH_2PO_4.H_2O)$ in water, neutralise with 5 M sodium hydroxide solution to pH 7.80 and dilute to 1 l with water.

Manganese standard solutions. Dissolve 2.002 g of reagent-grade manganese (better than 99.9%) in 40 ml of dilute hydrochloric acid $(1 + 1 \ V/V)$ and dilute to 1 l with water; this solution contains 2.0 g l^{-1} of manganese. Prepare working solutions containing 1, 4 and 8 p.p.m. of manganese from the 2.0 g l^{-1} solution by dilution. Prepare working standards containing 3, 10, 15, 30, 50 and 100 p.p.b. (parts per 10^9) of manganese from the 1 p.p.m. solution by dilution.

Iridium standard solution. Dissolve 0.2482 g of ammonium hexachloroiridate(III) $[(NH_4)_3IrCl_6.H_2O]$ in 1 l of water; this stock solution contains 100 p.p.m. of iridium.

Nitrilotriacetic acid stock solution, 0.0500 M. Dissolve 9.958 g of NTA which has been recrystallised from hot water in water, neutralise with 5 M sodium hydroxide solution to pH 6.60 and dilute to 1 l with water. Prepare working standards of concentrations 1.20×10^{-6}, 6.00×10^{-6} and 1.20×10^{-5} M from the stock solution by dilution.

1,2-Diaminocyclohexane-NNN'N'-tetraacetic acid stock solution, 0.010 00 M. Dissolve 3.643 7 g of DCTA monohydrate in water, neutralise with 5 M sodium hydroxide solution to pH 6.60 and dilute with water to 1 l. Prepare working standards of concentrations 2.50×10^{-7}, 12.5×10^{-7} and 25.0×10^{-7} M from the stock solution by dilution.

Prepare the very dilute DCTA and NTA solutions (less than 10^{-5} M) just before use. Keep all working standards, reagent solutions and samples in a water-bath at 32.5 ± 0.1 °C, except when required for iridium determination, when they are kept at 30 ± 0.1 °C.

Procedure

Preparation of equipment

The equipment was prepared as previously described.[7]

Preparation of water samples

When using the method of standard addition, measurements are made on three solutions, solution A being the unknown water sample and solutions B and C containing in addition 8 and 4 p.p.b. of manganese, respectively. To prepare solution B, transfer 0.050 ml of the 4 p.p.m. manganese solution into a 25-ml calibrated flask using a 0.05-ml Hamilton microlitre syringe and dilute to the mark with solution A. To prepare solution C, mix solutions A and B $(1 + 1)$. For the determination of manganese, only 4-ml volumes of solutions B and C are needed; however, larger volumes are prepared so as to permit sedimentation of suspended impurities and to have sufficient solution for rinsing the pipettes.

Preparation of iridium standards and samples

These preparations are as previously described.[10] Three standards containing 10, 50 and 100 p.p.b. of iridium, prepared by dilution from 1 p.p.m. iridium solution that has been boiled for 0.5 h, are used for the construction of the calibration graph.

Determination of manganese

Into the reaction cell kept at 32.5 °C thermostatically, transfer by pipette 1.00 ml of 2 M phosphate buffer, pH 6.60, and 4.00 ml of sample or standard manganese solution and inject 0.100 ml of 0.100 M sodium phosphinate solution. Start the reaction by injecting 0.100 ml of 0.015 0 M sodium periodate solution into the cell using a 0.1-ml Hamilton microlitre syringe. Close the compartment and immediately press the start button on the universal digital instrument (UDI).[6]

The measurement is completed automatically and the number shown on the timer is recorded. Press the re-set button and empty the cell by suction. Repeat the procedure for each determination.

Determination of manganese in the presence of NTA activator

Follow the procedure for the determination of manganese, but use the 1 M phosphate buffer, pH 6.60, and after adding the sample, inject 0.100 ml of 0.050 0 M NTA solution.

Determination of blank

Carry out determinations on standard solutions containing 3, 15 and 30 p.p.b. of manganese according to the procedure and plot the reciprocals of the times against the concentration of the standards. The intercept of the straight line on the abscissa gives the amount of blank.

Determination of NTA

Into the reaction cell kept thermostatically at 32.5 °C, transfer by pipette 1.00 ml of the 2 M phosphate buffer, pH 6.60, and 4.00 ml of sample or standard NTA solution and inject 0.100 ml of 4 p.p.m. manganese solution. Continue as described for the determination of manganese from the point of sodium phosphinate addition.

Determination of DCTA

Into the reaction cell kept thermostatically at 32.5 °C, transfer by pipette 1.00 ml of the 2 M phosphate buffer, pH 6.60, and 4.00 ml of sample or standard DCTA solution and inject 0.100 ml of 8 p.p.m. manganese solution. Continue as described for the determination of manganese from the point of sodium phosphinate addition.

Determination of iridium

Into the reaction cell kept thermostatically at 30 °C, transfer by pipette 1.00 ml of 0.5 M phosphate buffer, pH 7.80, and 4.00 ml of sample or standard iridium solution, and inject 0.100 ml of 0.015 0 M sodium periodate solution. Start the reaction by injecting 0.100 ml of 0.050 M sodium phosphinate solution into the reaction cell and continue as described for the determination of manganese.

Calculations

Calibration graphs are obtained by plotting the reciprocal of the read-out (time in hundredths of a second) *versus* concentration of manganese, NTA, DCTA or iridium. The graphs are drawn to read molar concentration for NTA and DCTA but in the graphs for manganese and iridium the sample concentration is read in parts per billion. For the determination of manganese in water by the standard additions method, the figure for sample A (the water sample without added manganese) is plotted as 0 p.p.b. of manganese and its actual concentration is obtained from the intercept of the calibration graph on the abscissa. The blank should be subtracted from this value.

Results and Discussion

Basic considerations concerning reducing and oxidising agents, contamination, control of experimental conditions, and preparation of calibration graphs are similar to those previously reported.[11]

Both the manganese- and the iridium-catalysed periodate - phosphinate reactions are critically dependent on pH and therefore the pH should be kept constant to better than ±0.1 pH unit. The optimum pH is in the range 6.5–6.6 for manganese and 7.1–7.8 for iridium. A pH of 7.8 was chosen for iridium, because at this pH the interfering effect of manganese, which is present as an impurity in the reagents, is very small.

In both catalysed reactions variation in periodate concentration showed that the reaction rate and the sensitivity increased with increasing concentration of this reagent while the blank remained almost unaffected. Thus, the measurement times decreased by about 60% when the concentration of periodate in the final solution increased from 3.92×10^{-5} to 2.88×10^{-4} M and from 1.18×10^{-4} to 2.88×10^{-4} M for manganese and iridium determinations, respectively. Variation in phosphinate concentration showed that in the manganese-catalysed reaction the reaction rate and the blank increased with increasing concentration of this reagent. Thus, a four-fold decrease in the measurement times and an increase in the blank was obtained as the concentration of phosphinate in the final solution was changed from 1.92×10^{-3} to 3.92×10^{-2} M. In the iridium-catalysed reaction there is better proportionality between reaction rate and iridium concentration when [periodate] $= 0.3$ [phosphinate]. The concentrations chosen are a compromise to ensure small blanks and reaction times in the range 15–250 s.

The reaction can be started by addition of either periodate or phosphinate. The first approach was chosen for manganese determination and the second for iridium because it gave better precision and accuracy.

The rate of the manganese-catalysed reaction and the sensitivity decreased with an increase in ionic strength of the solution. Thus, a two-fold increase in the measurement times and a 2.3-fold decrease in sensitivity were obtained as the concentration of the buffer in the final solution was changed from 0.1 to 0.5 M. Manganese can be determined even in solutions of high ionic strength, provided that the composition of the standard manganese solutions is similar to that of the samples. Otherwise, the standard additions method should be used. In the iridium-catalysed reaction an increase in the ionic strength of the solution from 0.1 to 0.5 M did not affect the blank or the accuracy of the method.

Linear calibration graphs were obtained for manganese and iridium in the temperature range 25–33 °C. Within this range the sensitivity increases with increasing temperature, while the blank remains virtually constant for manganese and increases with temperature for iridium. At temperatures higher than 33 °C there is no proportionality between reaction rate and manganese concentration. For the determination of iridium a temperature of 30 °C was chosen as a compromise between sensitivity and amount of blank.

The catalytic activity of the iridium reagent solutions increases upon ageing, reaching a maximum constant value after several months. However, this maximum catalytic activity is obtained within 0.5 h by boiling the solutions.[10]

It was found that citrates, 2,2'-bipyridyl, ethylenediaminetetraacetic acid (EDTA), NTA, 1,10-phenanthroline and 1,2-di(2-aminoethoxy)ethane-*NNN'N'*-tetraacetic acid (EGTA) enhance the catalytic effect of manganese(II) on the periodate - phosphinate reaction. These results parallel earlier observations by Mottola and co-workers on the activating effect of NTA, EGTA and 1,10-phenanthroline on the manganese-catalysed periodate - malachite green reaction [3–5, 12] and our findings on their activating effect on the manganese-catalysed periodate - triethanolamine reaction. These facts point to the independence of ligand modification from the indicator reaction and suggest that this modification operates via true metal complex catalysis by complexation of, probably, manganese(III).[4,12–14] NTA was chosen as activator for the determination of manganese, because it increased the sensitivity and the detectability of the method to a larger extent than the other tested compounds and because of its lower cost. The activating effect of NTA increased with increasing NTA concentration in the range 10^{-4}–10^{-3} M and remained almost constant at higher NTA concentrations.

In order to investigate the effect of various ions that might interfere in the determination of manganese (in the presence of NTA) and iridium the measurement step was modified as follows: after the addition of a manganese standard (15 p.p.b.) and NTA or of iridium (50 p.p.b.), 0.25 ml of water or of the solution of the ion being examined was injected into the reaction cell. Strongly alkaline solutions were neutralised with sulphuric acid and acidic solutions with sodium hydroxide, before their effect on the reaction rate was studied. Potassium, sodium, calcium and magnesium ions did not affect the rate of the manganese-catalysed reaction even when their concentrations were several thousand times that of the manganese. Tables I and II show the effect of interfering ions on manganese and iridium determinations.
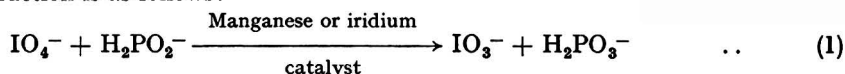
The over-all reaction is as follows:

$$\mathrm{IO_4^- + H_2PO_2^- \xrightarrow[\text{catalyst}]{\text{Manganese or iridium}} IO_3^- + H_2PO_3^-} \qquad .. \qquad (1)$$

TABLE I

EFFECT OF VARIOUS IONS ON MANGANESE DETERMINATION

Concentration of manganese in solution, 2.73×10^{-7} M (15 p.p.b.).

Ion*	Source	Ratio of added ion concentration to Mn concentration	Ion†	Source	Ratio of added ion concentration to Mn concentration
Cr(III)	$Cr(NO_3)_3$	0.25	Cu(II)	$CuSO_4.5H_2O$	17
V(IV)	$VOSO_4$	8	Fe(III)	$Fe(NO_3)_3.9H_2O$	90
Fe(II)	$FeSO_4.7H_2O$	17	Mo(VI)	$(NH_4)_6Mo_7O_{24}.4H_2O$	100
Al(III)	$Al(NO_3)_3.9H_2O$	32	Co(II)	$Co(NO_3)_2.6H_2O$	150
Pb(II)	$Pb(NO_3)_2$	170	Ni(II)	$Ni(NO_3)_2.6H_2O$	500
Cd(II)	$3CdSO_4.8H_2O$	170			
Zn(II)	$ZnSO_4.H_2O$	330			

* These ions in the stated ratio caused a positive relative error of less than 5%.
† These ions in the stated ratio caused a negative relative error of less than 5%.

TABLE II

EFFECT OF VARIOUS IONS ON IRIDIUM DETERMINATION

Concentration of iridium in solution, 2.60×10^{-7} M (50 p.p.b.).

Ion*	Source	Ratio of added ion concentration to Ir concentration	Ion†	Source	Ratio of added ion concentration to Ir concentration
Rh(III)	$(NH_4)_3RhCl_6.1\frac{1}{2}H_2O$	3	Pt(IV)	$(NH_4)_2PtCl_6$	5
Au(III)	NH_4AuCl_4	15	Re(VII)	NH_4ReO_4	5
Ru(III)	$(NH_4)_2RuCl_5.H_2O$	25	Hg(II)	$HgCl_2$	10
Os(IV)	$(NH_4)_2OsCl_6$	250	Pd(II)	$(NH_4)_2PdCl_4$	300
Ag(I)	$AgNO_3$	500	EDTA	Na_2EDTA	1 000

* These ions in the stated ratio caused a positive relative error of less than 5%.
† These ions in the stated ratio caused a negative relative error of less than 5%.

Analysis of aqueous manganese solutions of known concentrations, in the absence and the presence of NTA, gave the results shown in Tables III and IV. The results indicate that ultra-micro amounts of manganese in the range 40–400 ng in the absence of NTA and 12–120 ng (4-ml samples of solutions containing 3–30 p.p.b. of manganese) in the presence of NTA can be determined with average errors of about 2%. The reaction is pseudo-first order with respect to manganese in the range 10–100 p.p.b. of manganese in the absence of NTA and 3–30 p.p.b. in the presence of NTA. At higher manganese concentrations the order of the reaction with respect to manganese becomes greater than unity and therefore the manganese concentration of such samples should be brought into the aforementioned ranges by dilution. The relative standard deviation was 2.2% for a 10 p.p.b. manganese sample in the absence of NTA, and 1.1% for a 3 p.p.b. sample in the presence of NTA ($n = 6$).

TABLE III

DETERMINATION OF MANGANESE IN AQUEOUS SOLUTIONS

Reciprocal time/ $s^{-1} \times 10^3$	Amount of manganese in 4-ml sample/ng		Relative error, %
	Taken	Found*	
4.11, 4.11	40.0	40.0, 40.0	0, 0
7.36, 7.64	100	96, 100	−4.0, 0
13.6, 13.6	200	200, 200	0, 0
24.3, 24.5	400	378, 386	−5.5, −3.5

* From straight-line calibration graph.

TABLE IV

DETERMINATION OF MANGANESE IN AQUEOUS SOLUTIONS WITH NTA AS AN ACTIVATOR

Reciprocal time/ $s^{-1} \times 10^3$	Amount of manganese in 4-ml sample/ng		Relative error, %
	Taken	Found*	
3.94, 3.94	12.0	12.0, 12.0	0, 0
8.04, 7.91	30.0	30.4, 29.6	+1.3, −1.3
14.2, 14.2	60.0	57.2, 57.2	−4.7, −4.7
29.9, 29.9	120.0	124.8, 124.8	+4.0, +4.0

* From straight-line calibration graph.

Analysis of aqueous iridium solutions of known concentrations, which had been boiled,[10] gave the results shown in Table V. It can be seen that ultra-micro amounts of iridium(III) in the range 40–400 ng can be determined with average errors of about 1%. The relative standard deviation was 2.2% for a 50 p.p.b. iridium sample ($n = 6$). Similar results were obtained with iridium solutions that had not been boiled but had stood for 7 d, but the reaction times were longer by a factor of about 2.

TABLE V

DETERMINATION OF IRIDIUM IN AQUEOUS SOLUTIONS

Reciprocal time/ $s^{-1} \times 10^3$	Amount of iridium in 4-ml sample/ng		Relative error, %
	Taken	Found*	
6.11, 6.11	40.0	40.0, 40.0	0, 0
16.6, 16.1	100	100, 104	0, +4.0
32.3, 33.4	200	203, 201	+1.5, +0.5
65.9, 64.3	400	406, 402	+1.5, +0.5

* From straight-line calibration graph.

To check the precision of the complete procedure, six aliquots of a 1 p.p.m. iridium standard sample were boiled and then diluted to the 50 p.p.b. iridium level and measured. The relative standard deviation was 2.9%.

Addition of a complexing agent to a metal-ion catalysed reaction can result in true metal complex catalysis, ligand promotion or inhibition.[15] Figs. 1 and 2 show the effect of various complexing agents on the rate of the periodate - phosphinate reaction. There is a linear relationship between reaction rate and ligand concentration, thereby making possible the determination of several ligands. NTA and DCTA were determined on the basis of their
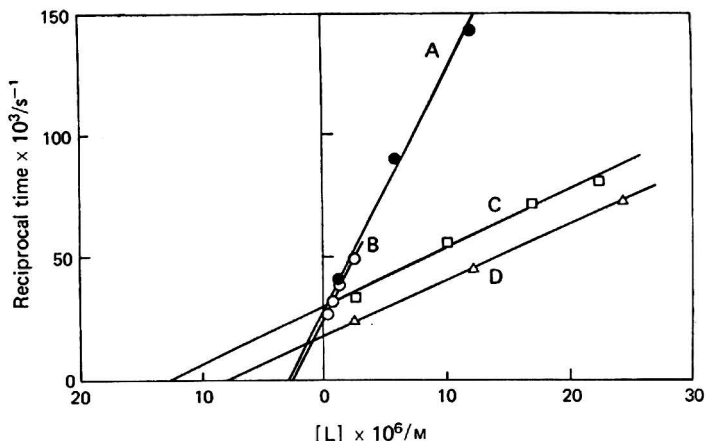

Fig. 1.   Activating effect of complexing agents, L, on the manganese-catalysed periodate - phosphinate reaction. A, Nitrilotriacetic acid; B, EDTA; C, EGTA; and D, citrates.

activating or inhibitory action in order to show the possibilities of the method. For the determination of NTA, variation in manganese concentration showed that the sensitivity increased and the blank decreased with increasing concentration of this reagent. The concentration chosen for the determination of NTA is a compromise to ensure small blanks and measurement times in the range 10–40 s. As shown in Fig. 2, the linear relationship between reaction rate and DCTA concentration extends over a wide concentration range (at least a decade), thereby making possible the determination of DCTA in very dilute solutions (10^{-7}–10^{-6} M). Manganese concentrations lower than 1.4×10^{-7} M were tested but the catalysis was insufficient to give a measurable change in reaction rate under the chosen experimental conditions. On the other hand, for manganese concentrations higher than 2.7×10^{-6} M the reaction becomes too fast to be followed.
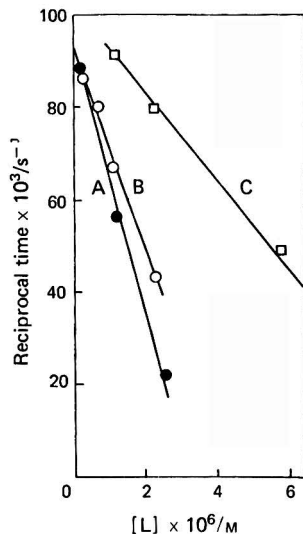

Fig. 2. Inhibitory effect of complexing agents, L, on the manganese-catalysed periodate - phosphinate reaction. A, DCTA; B, DTPA; and C, TTHA.

Analysis of aqueous NTA and DCTA solutions of known concentrations gave the results shown in Table VI. The results indicate that micro amounts of NTA and DCTA in the range 0.9–9 and 0.4–4 μg, respectively (1.2×10^{-6}–1.2×10^{-5} M NTA and 2.5×10^{-7}–2.5×10^{-6} M DCTA), can be determined with average errors of about 2%. The relative standard deviations for 6.0×10^{-6} M NTA and 1.25×10^{-6} M DCTA solutions were 2.4% and 2.9%, respectively ($n = 6$).

TABLE VI

DETERMINATION OF NTA AND DCTA IN AQUEOUS SOLUTIONS

Amount of NTA in 4-ml sample/μg		Relative error, %	Amount of DCTA in 4-ml sample/μg		Relative error, %
Taken	Found*		Taken	Found*	
0.918	0.918, 0.918	0, 0	0.364	0.364, 0.364	0, 0
2.29	2.18, 2.23	−4.8, −2.6	0.911	0.949, 0.949	+4.2, +4.2
4.59	4.41, 4.39	−3.9, −4.4	1.82	1.87, 1.88	+2.7, +3.3
9.18	9.43, 9.47	+2.7, +3.2	3.64	3.55, 3.55	−2.5, −2.5

* From straight-line calibration graph.

NTA and DCTA analogues that can be expected to interfere in their determination on the basis of their stability constants include EDTA, EGTA, diethylenetriaminepentaacetic acid (DTPA) and triethylenetetraminehexaacetic acid (TTHA).   Potential interfering substances including the above compounds, sodium oxalate and citrate and potassium biphthalate were tested and the results are summarised in Table VII.

TABLE VII

EFFECT OF FOREIGN SPECIES ON THE DETERMINATION OF NTA AND DCTA BY THE MANGANESE(II)-CATALYSED PERIODATE - PHOSPHINATE REACTION

Solutions contained 6.00×10^{-6} M NTA or 1.25×10^{-6} M DCTA.

Foreign species	Concentration (M) that gives 5% positive error in the determination of		Concentration (M) that gives 5% negative error in the determination of	
	NTA	DCTA	NTA	DCTA
Nitrilotriacetic acid (NTA)..				2.5×10^{-8}
1,2-Diaminocyclohexane-*NNN'N'*-tetra-acetic acid (DCTA)			1.5×10^{-8}	
Triethylenetetraminehexaacetic acid (TTHA)		7.5×10^{-6}	2.5×10^{-6}	
Diethylenetriaminepentaacetic acid (DTPA)		1.5×10^{-7}	2.5×10^{-8}	
Ethylenediaminetetraacetic acid (EDTA)	2.5×10^{-7}			2.4×10^{-7}
1,2-Di(2-aminoethoxy)ethane-*NNN'N'*-tetraacetic acid (EGTA)..	1.5×10^{-6}			1.5×10^{-6}
Sodium oxalate		7.5×10^{-7}	1.5×10^{-8}	
Sodium citrate	2.5×10^{-5}			1.5×10^{-6}
Potassium biphthalate		2.5×10^{-6}	2.5×10^{-6}	

Table VIII shows the results as read directly from the read-out dial of the automatic system for a typical series of determinations.   Duplicate determinations were run to illustrate the reproducibility of the method.   The values for manganese in water samples obtained by the standard additions method were compared with those obtained by using a calibration graph, as shown in Table IX.   The difference between the values obtained by the two methods varies from 0 to 4.8 p.p.b. of manganese.

TABLE VIII

DETERMINATION OF MANGANESE IN NATURAL WATERS BY USING AUTOMATIC APPARATUS

Sample	Direct time read out/s	$[\text{Mn}]t$
3 p.p.b. manganese	257.80, 253.80	
15 p.p.b. manganese	66.21, 68.00	1 091–1 126
30 p.p.b. manganese	34.50, 35.00	
A*	128.65, 132.78	
A* +4 p.p.b. manganese	85.72, 90.87	1 112–1 150
A* +8 p.p.b. manganese	70.09, 68.40	
B*	212.55, 216.66	
B* +4 p.p.b. manganese	142.28, 139.33	1 415–1 492
B* +8 p.p.b. manganese	96.93, 96.91	
C*	218.83, 225.34	
C* +4 p.p.b. manganese	153.79, 148.43	1 734–1 813
C* +8 p.p.b. manganese	108.43, 108.36	

* Water samples A, B and C were obtained from Kalymnos, Rhodes and Loutraki (Greece), respectively.

The reciprocals of the average read-out values from Table VIII are plotted against concentration in Fig. 3.   If the rate of the reaction in all water samples was the same for the same manganese concentration, the calibration graphs would have the same slope and the product of the manganese concentration in parts per billion (including the blank, which in this series of measurements was equivalent to 1.4 p.p.b.) multiplied by the measurement time in seconds,

<div align="center">TABLE IX</div>

COMPARISON OF RESULTS FOR THE DETERMINATION OF MANGANESE IN WATER BY THE
STANDARD ADDITIONS METHOD, BY CALIBRATION GRAPH AND BY NEUTRON-ACTIVATION
ANALYSIS

Sample No.*	Origin	Amount of manganese, p.p.b.		
		Standard additions method	Calibration graph	Neutron-activation analysis
1	Kalymnos	7.2	7.0	8.1
2	Rhodes	5.2	3.8	5.6
3	Loutraki	6.6	3.6	6.6
4	Katerini	5.4	7.2	5.5
5	Andros	3.6	7.2	3.5
6	Salamis	9.1	6.8	8.9
7	Kastoria	5.1	6.5	5.0
8	Halkis	6.7	1.9	6.2
9	Etoloakarnania	3.0	3.0	2.9
10	Athens	4.7	8.2	4.4

* Greek potable waters: 1–9 = fountain water; 10 = lake water.

[Mn]t would be the same for all samples. However, it can be seen from Fig. 3 and Table VIII that this product is not constant. The difference in slope and the large variation in the value of the product [Mn]t (about 1090–1810) is caused by interfering substances that affect the rate of the reaction. Any substance that oxidises phosphinate or reduces periodate under the conditions of the procedure constitutes a potential interference. In addition, large amounts of salts decrease the rate of the reaction. To compensate for the effect of interfering substances the composition of the standard manganese solutions should be similar to that of the samples. However, as interfering substances may be present in different amounts in the various samples it is not feasible to prepare such standard manganese solutions. It is therefore concluded that the use of a calibration graph obtained with pure solutions of manganese in distilled water can often lead to erroneous results (Table IX) and that the standard additions method described here should be used. By applying the standard additions method it is ensured that the concentration of all substances (except manganese) will be the same in all of the manganese solutions used in each analysis.
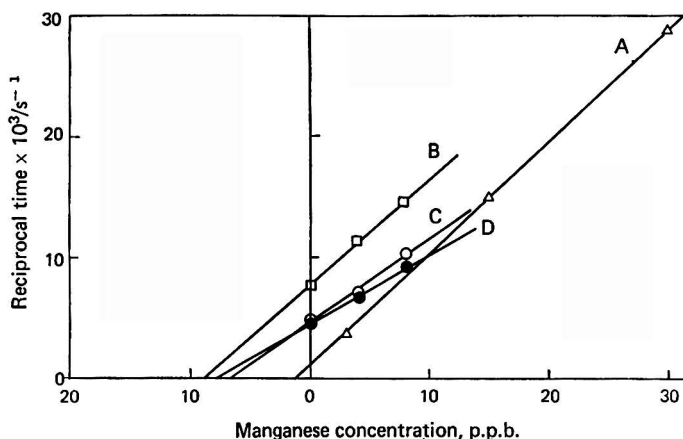

Fig. 3. Graphs of reciprocal time *versus* manganese concentration.
A, Determination of blank; B–D, potable water samples.

The values for manganese in water samples obtained by the automatic kinetic method are compared with those obtained by neutron-activation analysis in Table IX. The results for 10 samples do not indicate a consistent difference between results obtained by the two methods.

Because standard reference samples were not available the accuracy of the method was further checked by carrying out recovery experiments. The recovery of manganese based on the amount added (2–10 μg l^{-1}) to 10 samples of natural waters (mainly potable waters) ranged from 90 to 110%, with an average of 99.1%.

Conclusion

A method for the determination of trace amounts of iridium based on the iridium-catalysed periodate - phosphinate reaction, and of trace amounts of NTA and DCTA on the basis of their activating or inhibiting effects on the manganese-catalysed periodate - phosphinate reaction, has been developed. Although the application reported here deals with the determination of manganese in water, the scope of the method is intended to be more general. A basic procedure and general considerations for the determination of manganese are given so that the method can be adapted for its determination in many specific samples, e.g., tissues, bones and blood.

References

1. Yatsimirskii, K. B., "Kinetic Methods of Analysis," Pergamon Press, Oxford, 1966.
2. Mottola, H. A., and Freiser, H., *Analyt. Chem.*, 1967, **39**, 1294.
3. Mottola, H. A., and Harrison, C. R., *Talanta*, 1971, **18**, 683.
4. Mottola, H. A., and Heath, G. L., *Analyt. Chem.*, 1972, **44**, 2322.
5. Chlapowski, E. W., and Mottola, H. A., *Analytica Chim. Acta*, 1975, **76**, 319.
6. Efstathiou, C. E., and Hadjiioannou, T. P., *Analytica Chim. Acta*, 1977, **89**, 55.
7. Nikolelis, D. P., and Hadjiioannou, T. P., *Mikrochim. Acta*, 1977, 125.
8. Grimanis, A. P., Pantazis, G., Papadopoulos, C., and Tsanos, N., *Proc. Int. Conf. Peaceful Uses Atom. Energy, Geneva*, 1964, **15**, 854.
9. Sandell, E. B., "Colorimetric Determination of Traces of Metals," Third Edition, Interscience, New York, 1965, pp. 17–18.
10. Hadjiioannou, T. P., and Siskos, P. A., *Chim. Chron., N.S.*, 1973, **2**, 107.
11. Hadjiioannou, T. P., and Kephalas, T. A., *Mikrochim. Acta*, 1969, 1215.
12. Mottola, H. A., *Analyt. Chem.*, 1970, **42**, 630.
13. Mottola, H. A., *Analytica Chim. Acta*, 1974, **71**, 443.
14. Mottola, H. A., *CRC Crit. Rev. Analyt. Chem.*, 1975, **4**, 229.
15. Martell, A. E., *Pure Appl. Chem.*, 1968, **17**, 129.

Determination of Citrate as Its Iron(III) Complex by Differential Pulse Polarography

R. Prasad

Inco Europe Limited, European Research and Development Centre, Wiggin Street, Birmingham, B16 0AJ

A method for determining citrate as its complex with iron(III) by differential pulse polarography is described. The method is sensitive to 5 μg ml^{-1} of citrate, without any interference from equimolar propan-2-onedicarboxylate and propenetricarboxylate ions and 10% of oxalate and tartrate ions. The limits of error in citrate concentrations determined by the proposed method are better than $\pm 2.5\%$.

The feasibility of determining oxalate, succinate and tartrate by means of differential pulse polarography was also explored and the method was found to be applicable to the determination of oxalate.

Keywords: Citrate determination; citrate - iron(III) complex; differential pulse polarography

In recent years differential pulse polarography has become a very popular technique for determining trace amounts of electroactive species in biological, inorganic and organic materials, owing to its high sensitivity and the minimum of interference experienced from excesses of species reduced at more positive potentials and at slightly different half-wave potentials. While Zuman[1] has reviewed theoretical and practical aspects, Heijne and Van der Linden[2] have recently established the current - potential relationship for differential pulse polarography.

The difficulty of obtaining an electrode reduction step for saturated carboxylate ions in aqueous systems is well known, and no polarographic method for the determination of citrate ions has previously been reported.

The proposed method is based on the fact that the half-wave potential of a metal ion is shifted by the formation of a complex and this shift is a function of the stability of the metal complex. The wave produced by the iron(III) - citrate complex is a well defined, reversible wave,[3] which in the present method is used for the indirect determination of the citrate ion.

Experimental

Apparatus

Polarographic waves were recorded on an X - Y recorder, Model 26000 A3, manufactured by Bryans Southern Instruments. They were obtained by using a Polarographic Analyzer 174A, incorporating a dropping mercury electrode fitted with a mechanical drop timer, a saturated calomel reference electrode and a polarographic cell, which was manufactured by Princeton Applied Research, Princeton, New Jersey, USA.

Reagents

All of the solutions were prepared from analytical-grade reagents.
Buffer solution, pH 4.5. Prepared from sodium acetate (1.0 M) and acetic acid.
Iron(III) sulphate solution, 1 mM, *in* 0.01% *V/V sulphuric acid.*
Trisodium citrate solution, 0.1 mM.

Procedure

An appropriate amount of the sample is transferred into the polarographic cell. About 20 ml of the buffer solution and an amount of iron(III) solution that is about twice the suspected citrate content of the sample are added. The solution is then de-aerated with nitrogen for about 5 min and polarograms are recorded between -0.10 and -0.85 V *versus* S.C.E.

The peak current is measured and related to the concentration of citrate ion from the appropriate calibration graph, which is obtained by using standard solutions.

Results and Discussion

A detailed polarographic study of the iron(III) - citrate/iron(II) - citrate redox system was made in order to evaluate its reversibility before assessing its use for the determination of citrate.

Polarograms of 1 mg ml^{-1} of citrate and of iron(III) sulphate, obtained by use of classical d.c. and differential pulse polarography, are presented in Figs. 1 and 2, respectively.   Points on the classical d.c. polarogram for the iron(III) - citrate complex (Fig. 1, A) were used to construct a graph of $\log i/(i_d - i)$ *versus* applied potential in the range from -0.15 to -0.35 V with respect to S.C.E.   The graph was found to be linear, with a slope of 58.3 mV, and crossed the line $\log i/(i_d - i) = 0$ at -0.250 V $= E_{\frac{1}{2}}$, in close agreement with the theoretical value of 58.1 mV for a reversible, one-electron redox process at 20 °C.
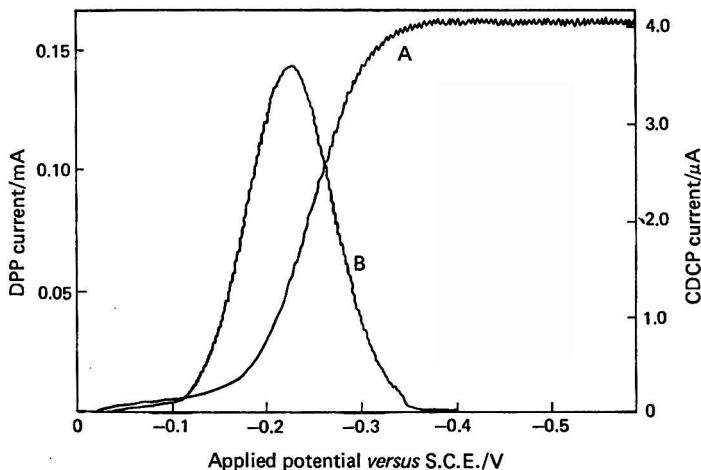
Fig. 1.   Iron(III) - citrate polarograms.   A, Classical d.c. polarogram; B, differential pulse polarogram.

The value of the peak potential from the differential pulse polarogram of iron(III) - citrate (Fig. 1, B) was related to the half-wave potential of a classical d.c. polarogram according to a theoretically derived equation[2] as follows:

$$E_p = E_{\frac{1}{2}} - \Delta E/2 \qquad \text{..} \qquad \text{..} \qquad \text{..} \qquad \text{..} \qquad (1)$$
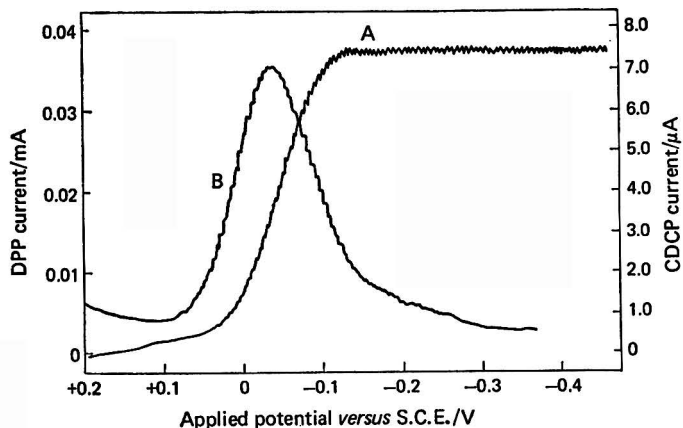
Fig. 2.   Iron(III) sulphate polarograms.   A, Classical d.c. polarogram; B, differential pulse polarogram.

where E_p is the peak potential, $E_{\frac{1}{2}}$ the half-wave potential and ΔE the applied pulse amplitude (-50 mV).

A differential pulse polarogram of the iron(III) - citrate complex in the presence of an excess of iron(III) sulphate is shown in Fig. 3. There was no shift in peak potential B at -0.225 V *versus* S.C.E. as a result of the iron(III) - citrate/iron(II) - citrate redox process. Peak A, at -0.0375 V *versus* S.C.E., corresponds to the peak potential due to the reduction step of iron(III) sulphate (Fig. 2).
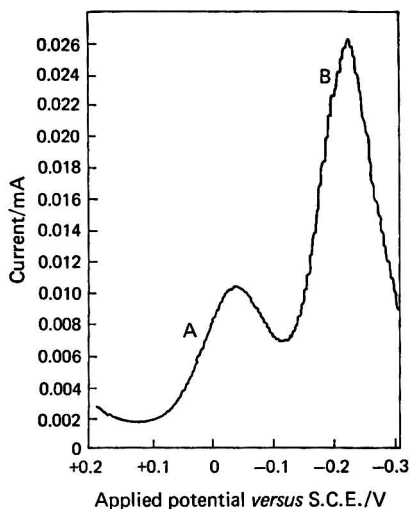
Fig. 3. Differential pulse polarogram of iron(III) - citrate in excess of iron(III) ions. A, Peak due to free iron(III) ions; B, peak due to the complexed iron(III) ions.

The peak potential -0.225 V *versus* S.C.E. was independent of the citrate concentration (Fig. 4). The peak current was found to increase linearly with increasing citrate concentration (Fig. 5), giving a further check on the reversibility of the iron(III) - citrate reduction wave.

The effects of other functional groups on the determination of citrate by the proposed
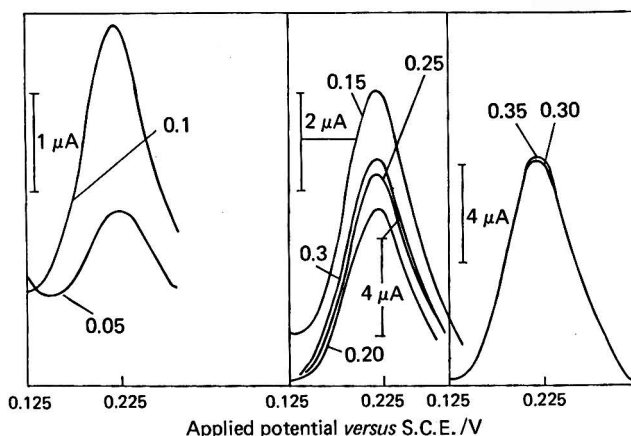
Fig. 4. Effect of concentration of citrate on the peak potential and diffusion current for iron(III) - citrate in an excess of free iron ions. Values represent milligrams of citrate.
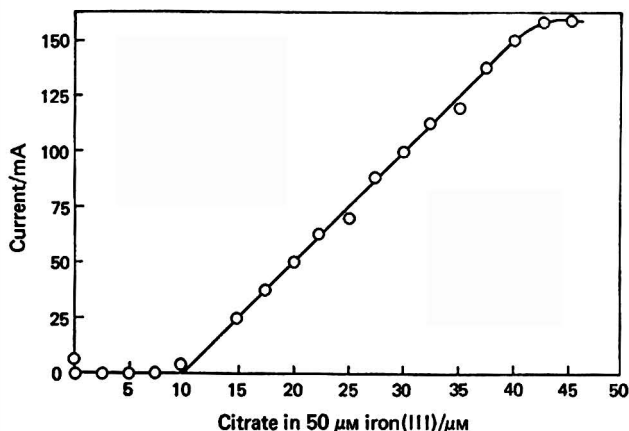
Fig. 5. Relationship between peak current and citrate concentration for iron(III) - citrate.

method were studied by adding various dibasic and polybasic carboxylate ions. Standard solutions containing different amounts of foreign carboxylate ions were added to 100-ml flasks containing 1.0 and 5.0 ml of the proposed iron(III) and citrate reagent solutions, respectively, and diluted to 100.0 ml with the acetate buffer. The solutions were de-aerated and polarograms were recorded in the suggested potential range. The dominant polarographic wave due to the reduction step of iron(III) - citrate ion was examined in each instance and it was found that oxalate and tartrate complexes of iron(III), with peak potentials at -0.175 and 0.030 V *versus* S.C.E., respectively, did not interfere at a concentration of 10% m/V of the iron(III) - citrate complex. Propan-2-onedicarboxylate and propenetricarboxylate ions, degradation products of the citrate ion, also did not appear to interfere with the proposed method, even at concentrations equal to that of the iron(III) - citrate complex. Excellent recovery values were obtained when small amounts of citrate (0–1.00 mg) were added to an iron(III) solution containing 20 mg of citrate; these results are given in Table I.

TABLE I

RECOVERY OF CITRATE ADDED TO A 0.01 M IRON(III) SOLUTION
CONTAINING 20.0 mg OF CITRATE

Citrate added/ mg	Citrate found/ mg
—	20.00
0.10	20.09_9
0.20	20.20_0
0.50	20.50_1
0.80	20.79_8
1.00	21.00_0

In order to overcome an interference on the lower range of the calibration graph (Fig. 5) caused by the small separation between peak potentials for iron(III) - citrate and iron(III) sulphate reduction processes the peak potential shift for the copper(II) - citrate system was examined. The polarograms in Fig. 6 were obtained by using copper(II) sulphate and copper-(II) - citrate in 2 M sodium acetate. A peak potential shift from 0.075 V [copper(II) sulphate] to -0.310 V [copper(II) - citrate] *versus* S.C.E. was observed, which was about 20% greater than the shift for the iron(III) - citrate system.

However, when the polarograms for copper(II) - citrate were examined it was found that the electrode reduction step for copper(II) - citrate was irreversible, firstly because the graph of log $i/(i_d - i)$ *versus* applied potential was not linear and the slope was 79 mV, which is higher than expected (58.1 mV) for a one-electron reversible redox process, secondly because the peak
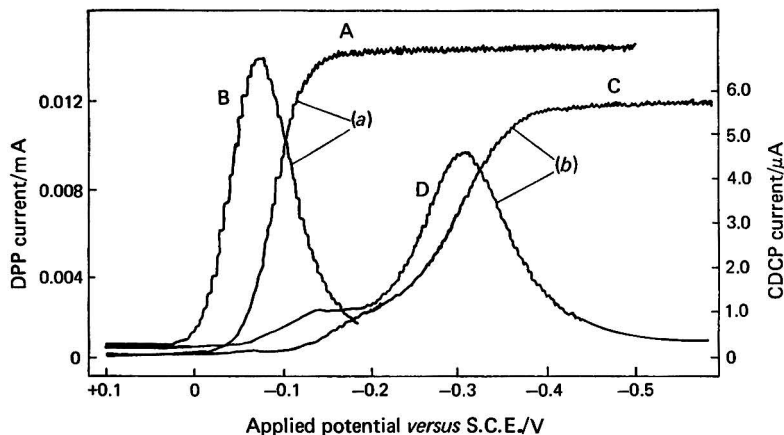
Fig. 6.   (*a*), Copper(II) sulphate: A, classical d.c. polarogram; and B, differential pulse polarogram.   (*b*), Copper(II) - citrate: C, classical d.c. polarogram; and D, differential pulse polarogram.

potential was not related to the half-wave potential according to equation (1), the calculated value of E_p being -0.265 V compared with an observed value of -0.310 V, and thirdly because the peak potential shifted towards a more negative value as the concentration increased (Fig. 7) and the peak current was not directly proportional to the concentration of citrate.
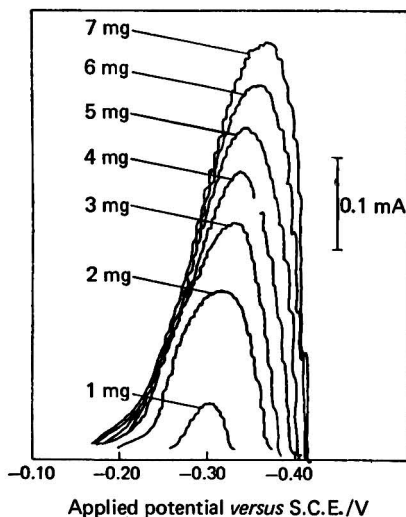
Fig. 7.   Effect of citrate on the peak potential and current of a copper(II) sulphate electrode reduction.

The possibility of determining oxalate, succinate and tartrate as their iron(III) complexes was also explored. Attempts to determine succinate failed completely because of the low stability of the iron(III) - succinate complex. The results of classical d.c. and differential pulse polarographic studies on the iron(III) - tartrate system (Fig. 8) revealed that the redox couple was not reversible. The non-linear graph of log $i/(i_d-i)$ *versus* applied potential had a slope of 86 mV and the observed peak potential (0.0375 V *versus* S.C.E.) did not agree with the calculated value (0.048 V *versus* S.C.E.).
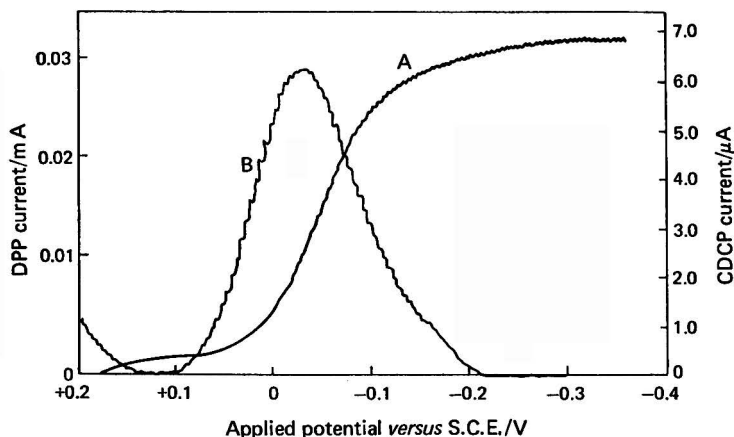
Fig. 8.   Iron(III) - tartrate polarograms.   A, Classical d.c. polarogram;
B, differential pulse polarogram.

Oxalate ions gave results similar to those of the successful iron(III) - citrate system. Polarograms of iron(III) - oxalate obtained by classical d.c. polarography and differential pulse polarography are shown in Fig. 9; the graph of $\log i/(i_d - i)$ *versus* applied potential for the classical d.c. polarogram is linear with a slope of 58.4 mV, in agreement with the theoretical value of 58.1 mV for a one-electron reversible redox system at 20 °C.   The peak potential of the differential pulse polarogram (0.175 V *versus* S.C.E.) is also in good agreement with the value of 0.200 V *versus* S.C.E. required by the relationship indicated in equation (1), reported by Heijne and Van der Linden.[2]
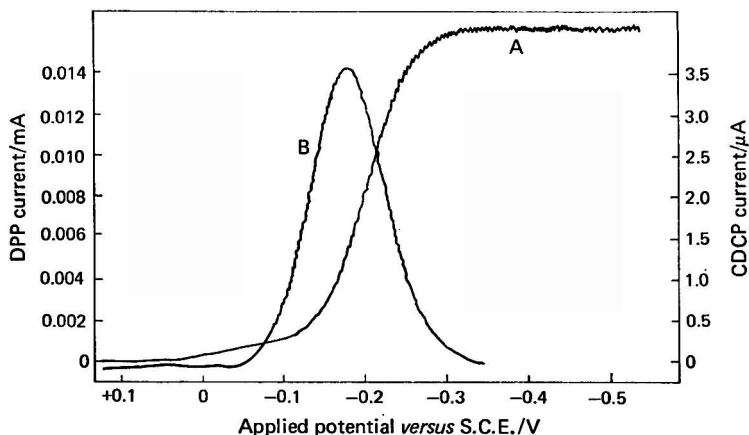
Fig. 9.   Iron(III) - oxalate polarograms.   A, Classical d.c. polarogram;
B, differential pulse polarogram.

References

1.   Zuman, P., *Proc. Analyt. Div. Chem. Soc.*, 1975, **12**, 199.
2.   Heijne, G. J. M., and Van der Linden, W. E., *Analytica Chim. Acta*, 1976, **82**, 231.
3.   Lingane, J. J., *J. Am. Chem. Soc.*, 1946, **68**, 2448.

Analytical Methods Committee

REPORT PREPARED BY THE ESSENTIAL OILS SUB-COMMITTEE

Application of Gas - Liquid Chromatography to the Analysis of Essential Oils

Part V.* Determination of 1,8-Cineole in Oils of Lavender and Lavandin

The Analytical Methods Committee has received and approved for publication the following Report from its Essential Oils Sub-Committee.

Report

The constitution of the Sub-Committee responsible for the preparation of this report was: Mr. A. M. Humphrey (Chairman), Mr. J. H. Greaves, Mr. B. E. Kent, Mr. W. S. Matthews, Mr. D. A. Moyler, Mr. R. G. Perry, Mr. J. Ridlington, Mr. R. A. Stocks and Mr. G. Watson, with Mr. P. W. Shallis as Secretary and Mr. J. J. Wilson as Assistant Secretary.

Introduction

The oxide 1,8-cineole is a constituent of many essential oils. In some, such as cardamom, eucalyptus, rosemary, sage and spike lavender, it is a major constituent, while in others, such as lavender and lavandin, it is only a minor constituent. A previous report[1] by the Analytical Methods Committee presented a method for the determination of 1,8-cineole in oils of cardamom, rosemary, sage and spike lavender but specifically excluded its application to the determination of 1,8-cineole in oils of lavender and lavandin. Previous collaborative work had shown that these oils contained an unidentified compound which was not separated from the 1,8-cineole by the conditions recommended for its analysis in the other four oils.

The determination of 1,8-cineole in oils of lavender and lavandin has assumed some importance as oils adulterated with spike lavender have a higher content of 1,8-cineole. Its determination at low levels by gas - liquid chromatography was therefore studied.

Experimental

When gas - liquid chromatography is applied to the determination of a minor component in essential oils, the possibility of interference from other minor components becomes important. This interference can occur with cineole in oils of lavender and lavandin and the first requirement in order to establish a method is the selection of a suitable stationary phase. As previous collaborative work had shown that PEG 400 stationary phase was unsuitable for lavender oil, various other stationary phases were examined. The results of this exercise showed that a column of fluorosilicone oil QF1 gave an apparently better separation for cineole than the other stationary phases tried, although a 5-m column was required. On such a column the peak for cineole did not show any base broadening and quantitative results showed that analysis on the QF1 column gave a significantly lower result than that obtained on a PEG 400 column (Table I). The implication of this was that the peak for cineole when a PEG 400 column was used contained an additional, interfering component. Indeed, this had previously been noted in some instances as a peak base broadening beyond that normally expected from pure cineole.

In the work reported in Table I, cyclohexyl acetate was used as the internal standard with the PEG 400 columns and *n*-butyl *n*-butyrate with the QF1 column. No interference with the internal standard peaks was found.

A collaborative exercise was arranged in which the cineole contents of several commercial samples of lavender and lavandin oils were to be determined gas chromatographically on QF1

* For Part IV of this series, see *Analyst*, 1975, **100**, 593.

columns under agreed conditions. Most of the collaborators had to prepare or obtain the non-standard QF1 columns, and it was soon evident that the members were not achieving the quality of separations obtained in the original experiment. The peaks were non-gaussian, the HETP values were high and the resolutions poor. The original work on the QF1 column, the results of which are given in Table I, was carried out by a member who had previous experience of this particular analysis.

<div align="center">

TABLE I

DETERMINATION OF CINEOLE ON DIFFERENT COLUMNS

</div>

	QF 1 column	PEG 400 (column 1)	PEG 400 (column 2)	PEG 400 (column 3)
Cineole in lavender 40/42, %	0.46	1.6	2.0	2.0
Cineole in lavandin supra, %	3.4	5.5	5.6	5.9

During subsequent discussions the effects of column ageing were considered and various ageing techniques were tried. These techniques resulted in proposals for a further collaborative exercise for which precise details for the preparation of the column were laid down. These details were as follows.

1. Pack an 18-ft column with Chromosorb W, acid washed, dimethyldichlorosilanised, 80–100 mesh, impregnated with 15% of QF1.
2. Programme the temperature to rise at 2 °C min^{-1} from ambient to 250 °C with a carrier gas flow-rate of 30 ml min^{-1} and the column disconnected from the detector.
3. Stop the carrier gas flow and maintain the column at 250 °C for 2 h.
4. Cool the column to 150 °C and re-start the carrier gas flow.
5. Programme the temperature to rise at 2 °C min^{-1} to 250 °C.
6. Cool to ambient temperature and connect the column to the detector.
7. Heat the column to 125 °C and inject 5-μl amounts of water until there is no appreciable detector response.
8. Check that satisfactory resolution is obtained for cineole in lavender oil. If not, repeat the heating to 250 °C as from stage 5, followed by injection of water until the resolution is satisfactory.

Reports of the success of the preparation of the columns varied but although all members found that the heating and water injection technique improved the performance of the columns, none of them achieved the degree of efficiency obtained by the one member in the first experiment. Unfortunately, this particular column had a lengthy and obscure history and the exact details of its preparation were unknown.

The material of the column itself next received consideration but none of the collaborating members reported that their columns induced any apparent degradation of samples of linalyl acetate when run under the proposed conditions for the analysis of cineole. This observation was the same for both glass and stainless-steel columns as well as for on-column or flash injections.

While the disappointing results of this exercise were being considered a highly relevant paper was published[2] in which evidence was presented that fluorosilicone phases readily decompose in acetone solution. This is the normally recommended solvent for these phases and had been used exclusively by the collaborating members. Accordingly, a new set of conditions for preparation of the column and analysis for cineole in lavender oils was prepared, taking into account the recommendations made in the paper for preparation of the column packing. The significant details of this were to use OV 210 instead of QF1 and to use ethyl acetate instead of acetone as the solvent.

The gas - liquid chromatographic conditions to be used in the collaborative work were:

Stationary phase ..   ..   OV 210
Support   ..   ..   Chromosorb W, acid washed, dimethyldichlorosilanised, 80–100 mesh
Stationary phase loading   ..   ..   5% *m/m*
Column   ..   ..   Glass, 12–18 ft (4–6 m), diameter $\frac{1}{4}$ in or 4 mm

Column temperature	..	..	..	110 °C (maximum)
Internal standard	..	..	..	*n*-Butyl *n*-butyrate
Solvent	..	..	..	..	Propan-2-ol

The cineole contents of three samples of lavender oil were determined and the results are given in Table II. All of the collaborators achieved satisfactory resolution and peak shapes and no apparent decomposition of a sample of linalyl acetate put on the column was reported

TABLE II

DETERMINATION OF 1,8-CINEOLE IN OILS OF LAVENDER

| | Cineole, % | | | Column | Column | |
Laboratory	Lavender 40/42	Lavender Barreme	Lavender Vaucluse	length/ ft	temperature/ °C	Measurement
A	0.69	1.20	0.85	15	90	PH × RD
B	0.72	1.17	0.82	15	100	PH × RD
C	0.57	1.00	0.62	18	80	PH × RD
D	0.53	1.03	0.56	18	100	PH × RD
E			0.65	18	110	PH × RD
F	0.68	1.19	0.77	15	90	PH × RD
Mean	0.64	1.12	0.71			
B	0.87	1.56	1.14	15	100	Integrator
C	0.69	1.24	0.80	18	80	Integrator

Six sets of results in Table II were calculated from the product of peak height and retention distance measurements and a further two sets were calculated from integrated areas. The results were considered to be satisfactory in view of the low levels of cineole present in the samples, although it had been noted that the results calculated from the integrated areas were significantly higher than the others. A further collaborative test was then undertaken on two samples of lavandin oil; the results are given in Table III.

TABLE III

DETERMINATION OF 1,8-CINEOLE IN OILS OF LAVANDIN

| | Cineole, % | |
Laboratory	Lavandin abrialis	Lavandin supreme
A	8.8	2.8
B	9.0	2.7
C	8.7	2.7
D	8.7	2.9
F	9.2	3.0
Mean	8.9	2.8

The results in Table III were considered to be satisfactory and a final collaborative test was arranged in order to determine the recovery of a known amount of cineole added to a sample of English lavender oil. The oil used in this test was known to contain a considerably higher percentage of cineole than did the oils used for the work reported in Table II. The results of this recovery test are given in Table IV; the known addition of cineole to the oil was 6.79% and the average recovery was 103%.

Discussion

The collaborative experiments have shown that fluorosilicone stationary phases (in particular OV 210) can be used satisfactorily provided the support material is coated with a solution of the phase in ethyl acetate. The solution should be prepared and used as rapidly as possible, the solvent being removed from the support without delay. It was not found necessary to specify any particular process for artificially ageing the columns in order to achieve the required resolution. However, a wide variation of retentions were reported from different laboratories who adjusted the operating temperatures of their columns to give reasonable retention times for the cineole and internal standard peaks.

TABLE IV

RECOVERY OF ADDED CINEOLE FROM OIL OF LAVENDER

Laboratory	Cineole found in sample, %	Cineole found in sample + added cineole, %	Cineole recovered, %
A	19.1	24.4	7.0
B	18.9	23.8	6.4
C	18.5	24.2	7.5
D	18.8	23.9	6.7
Mean	18.8	24.1	7.0

A further variation occurred as a result of the different lengths of commercially available columns. These varied according to the type of instrument being used, but lengths of 12–18 ft (4–6 m) have been found satisfactory, and one laboratory achieved satisfactory results with a 9-ft column. Continued experience with the OV 210 columns suggested that they continue to "age" progressively, even when operated at temperatures well below their recommended maximum and it is to be expected that a column in continuous use will need to be operated at progressively lower temperatures over a period of time.

Both on-column and flash injections were found to be satisfactory and flash temperatures up to 150 °C did not give any degradation of samples of linalyl acetate.

Experiments on the preparation of column packings carried out since the original preparation of this report have shown that the difficulties experienced with OV 210 can be readily explained. Polar stationary phases have difficulty in wetting the surface of the support, particularly if it has been silanised. The procedure described above for the preparation of the columns aims to produce an even coating of the stationary phase, but this can be improved by adopting a modified version of the usual slurry coating process. In this modification the volume of solvent, in millilitres, used to dissolve the stationary phase should be about equal to the mass, in grams, of the support. When the support is added to the solution of the stationary phase, complete absorption takes place, and the mixture is then "tumbled" to achieve complete mixing in the semi-dry state. The mixture is then allowed to stand in a closed container for 12 h before the solvent is removed by evaporation. A packing prepared in this way should be conditioned overnight at 200 °C; if heating is continued above 200 °C the stationary phase desorbs from the surface and the resolution of the column decreases as a result.

Note on Dimensions

The Sub-Committee members are aware of the progress of metrication and where lengths and diameters are stated these are in line with contemporary commercial practice at the time the experiments were carried out.

Conclusions

Gas - liquid chromatography can be used for the quantitative determination of cineole in oils of lavender and lavandin provided that suitable columns are prepared for use. The recommended method affords a means of determining the cineole content of the stated oils without apparent interference from other components, which gives a determination hitherto unattainable.

APPENDIX

Recommended Method for the Determination of 1,8-Cineole in Oils of Lavender and Lavandin by Gas - Liquid Chromatography

Operating Conditions

It is essential that, throughout a determination, the operating conditions are maintained as constant as is practicable. It is also essential to use the detector - amplifier system within its linear range.[3]

Detector	..	..	..	Flame ionisation
Stationary phase	..	..	..	OV 210
Support	..	..	..	Chromosorb W, acid washed, dimethyldichloro-silanised, 80–100 mesh
Stationary phase loading	..		..	5% *m/m*
Column	..	..	..	Length 4–6 m (12–18 ft); outside diameter 4 mm (¼ in); glass
Column temperature		..	..	Isothermal, 80–100 °C, according to degree of resolution required
Injection	..	..	..	On-column or, if a flash heater is used, maximum temperature 150 °C
Gas flow-rates	..	..	..	To give satisfactory instrument performance
Chart speed ..	..	..	..	15 in h⁻¹ (minimum)
Peak heights (internal standard and cineole)	..	..	..	Within 40–75% of full-scale deflections
Internal standard	..	..	..	*n*-Butyl *n*-butyrate (purity by gas - liquid chromatography not less than 99.0%)
Cineole	..	..	..	Purity by gas - liquid chromatography not less than 99.0%
Solvent	..	..	..	Propan-2-ol
Injection volume	..	..	..	Such that the internal standard and cineole peaks fall within the linear range

Preparation of the Column Packing

Weigh 1 g of the OV 210 into a 250-ml conical flask, add 15 ml of ethyl acetate and swirl the flask to dissolve the stationary phase.   Weigh 19 g of the support into a beaker and add it to the solution of the stationary phase in the conical flask through a powder funnel.   Stopper the flask and "tumble" to achieve uniform mixing.   The packing will be damp at this stage but should not show signs of congealing.   Set the mixture aside in the stoppered flask for at least 12 h.   After this time, transfer the packing to a flat open dish and allow the solvent to evaporate, turning the mixture carefully at intervals during the evaporation.   When all the solvent has been removed, sieve the packing to remove any fines and then use it for packing the columns.   Maximum resolution will be maintained only if the temperature of the columns is kept below 200 °C.

Determination of the Factor, *f*, for the Internal Standard (Cineole = 1)

Make all weighings to an accuracy of 0.2 mg.   Weigh about 0.1 g of cineole and 0.2 g of *n*-butyl *n*-butyrate (or such other mass as will give about equal heights for the two peaks) and dilute the mixture with 25 ml of solvent.   Inject 1.0 µl or such other volume as will ensure response within the linear range and calculate to three decimal places the factor, *f*, from the equation

$$f = \frac{h \times d \times m_c}{h_c \times d_c \times m}$$

where h_c is the height of the cineole peak; d_c the retention distance of the cineole peak; h the height of the *n*-butyl *n*-butyrate peak; d the retention distance of the *n*-butyl *n*-butyrate peak; m the mass of *n*-butyl *n*-butyrate; and m_c the mass of cineole.   Repeat twice on the same solution and use the average of the three values of *f* in the calculation of the cineole content of the sample.

Determination of the Cineole Content of the Sample

Weigh about 0.2 g of *n*-butyl *n*-butyrate and an adequate amount of the sample (1–5 g according to whether more or less cineole is present) that will give about equal heights for the two peaks and dilute with 25 ml of solvent.   Inject about 1.0 µl or such other volume as will

ensure response within the linear range on the instrument and calculate the cineole content of the sample to four significant figures from the equation

$$\text{Cineole, \%} = \frac{f \times h_c \times d_c \times m \times 100}{h \times d \times m_s}$$

where f is the factor determined as described above; h_c the height of the cineole peak; d_c the retention distance of the cineole peak; h the height of the n-butyl n-butyrate peak; d the retention distance of the n-butyl n-butyrate peak; m the mass of the n-butyl n-butyrate; m_s the mass of the sample.

Repeat the operation twice with the same solution and report the average of the three results to three significant figures.

References

1. Analytical Methods Committee, *Analyst*, 1973, **98**, 616.
2. Hanneman, L. F., and Klimisch, H. M., *J. Chromat.*, 1972, **70**, 81.
3. Primavesi, G. R., McTaggart, N. G., Scott, C. G., Nelson, F., and Wirth, M. M., *J. Inst. Petrol.*, 1967, **53**, 367 (Appendix II, p. 377).

NOTE—Reference 1 is to Part II of this series.

SHORT PAPERS

Some Difficulties Encountered in Speciation Studies of Arsenic

B. I. Diamondstone and R. W. Burke

Institute for Materials Research, National Bureau of Standards, Analytical Chemistry Division, Washington, DC 20234, USA

A paper by Aggett and Aspell[1] was published in this journal recently on the determination of arsenic(III) and total arsenic by means of atomic-absorption spectrophotometry. At the time that their paper appeared studies were being carried out at the National Bureau of Standards on a speciation procedure, which involved a pre-extraction of arsenic(III) and the subsequent spectrophotometric measurement of the coloured product formed from the reaction between arsine and silver diethyldithiocarbamate (AgDDC). These studies were carried out on a variety of organic materials, which are currently available as Standard Reference Materials (SRMs).

Although the final measurement techniques are different, the dissolution procedures studied included the one that Aggett and Aspell have recommended. In their paper, those authors stated that the dissolution procedure which they were recommending would not alter the valence state of the arsenic present in the original sample.

A summary of methods using two different acid systems to digest spinach samples is shown in Table I. Spinach was chosen as a low-arsenic biological matrix for this study, although a similar effect was seen when bovine liver or tomato leaves were used. It can be seen from the table that when the nitric acid-sulphuric acid system suggested by Aggett and Aspell was used, some arsenic(III) was oxidised to the arsenic(V) form regardless of whether or not an organic matrix was present. Similarly, in the sulphuric acid system some arsenic(V) was reduced to arsenic(III) when organic material was present. Except for the first experiment listed in Table I, all of the samples were pre-extracted into benzene from 9–10 N hydrochloric acid and back-extracted with water before arsine generation was carried out.[2] The arsine was collected in 4 ml of AgDDC-pyridine solution and spectrophotometric measurements were made at a wavelength of 535 nm. The values obtained for arsenic(III), with and without pre-extraction, are included to show the efficiency of the extraction into benzene.

TABLE I

ABSORBANCE OF COLOURED ARSINE - SILVER DIETHYLDITHIOCARBAMATE PRODUCT AFTER BENZENE EXTRACTION OF ARSENIC(III)

	Concentrated H_2SO_4	$HNO_3 - H_2SO_4$*
5 μg of arsenic(III)	0.226† $\pm$ 0.003	0.075† $\pm$ 0.003
5 μg of arsenic(III)	0.224 $\pm$ 0.003	0.070 $\pm$ 0.003
0.5 g of spinach‡ + 5 μg of arsenic(III) spike	0.230 $\pm$ 0.010	0.052 $\pm$ 0.010
5 μg of arsenic(V)	0.001 $\pm$ 0.003	0.005 $\pm$ 0.003
0.5 g of spinach + 5 μg of arsenic(V) spike	0.166 $\pm$ 0.010	0.006 $\pm$ 0.010

* According to instructions given in reference 1.
† Standard added directly to arsine generator after acid treatment.
‡ NBS SRM No. 1570, total arsenic = 0.15 p.p.m.

In addition, Aggett and Aspell have stated that in the AgDDC procedure, pre-reduction of arsenic(V) to arsenic(III) with tin(II) chloride is not necessary when the arsine is generated from a zinc - hydrochloric acid mixture. In Table II our results show that the absorbance obtained for arsenic(V), in the absence of tin(II) chloride, is about 20% of that obtained when tin(II) chloride is used. In both instances generation and collection were carried out for 1 h.

<div align="center">

TABLE II

EFFECT OF REDUCTION WITH TIN(II) CHLORIDE ON ABSORBANCE

Average of at least six determinations.

</div>

Reduction with SnCl$_2$		No reduction	
As(III)	As(V)	As(III)	As(V)
0.193 ± 0.003	0.192 ± 0.003	0.192 ± 0.003	0.039 ± 0.003

In conclusion, the results of this study indicate that the use of a pre-extraction procedure in conjunction with arsine generation will permit the accurate determination of arsenic(III) in aqueous samples containing mixtures of arsenic(III) and arsenic(V). As the AgDDC procedure can be used, without extraction, to determine total arsenic, arsenic(V) can subsequently be determined by difference. However, to date no suitable acid system has been found in this laboratory that will effectively digest organic and biological materials without altering the original valence states of the arsenic.

<div align="center">

References

</div>

1. Aggett, J., and Aspell, A. C., *Analyst*, 1976, **101**, 341.
2. Fischer, W., and Harre, W., *Angew. Chem.*, 1954, **66**, 165.

Determination of Acetone Vapour in the Atmosphere

J. E. Scott

Analytical Laboratory, Philips Hamilton, Wellhall Road, Hamilton, Lanarkshire, Scotland, ML3 9BZ

A method for the determination of acetone vapour in air, from 10 to 2 000 p.p.m., has been developed and evaluated. The usual problems associated with sorption of the organic vapour on the walls of sampling vessels, polythene bags and syringes, with consequent loss of acetone from the air sample, are avoided with this method, in which the acetone vapour is collected in an active-carbon adsorption tube and subsequently thermally desorbed into a gas chromatograph.

The technique should be adaptable to the determination of other volatile compounds in the atmosphere, provided that the correct combination of adsorbent and gas-chromatographic column packing is used.

<div align="center">

Experimental

</div>

Apparatus

Adsorption tube. The adsorption tube consists of a glass tube, 14 cm long by 0.62 cm o.d., with a wall thickness of 0.1 cm. A bulb is blown in the tube 4.5 cm from one end, and

a section of the tube is packed with activated charcoal (0.25 g of 60–80-mesh material). Two adsorption tubes joined in series by means of a short polythene sleeve are used for sampling (Fig. 1).

Desorption - injection system. The apparatus used is easily constructed and is similar to that described by Ellis *et al.*,[1] but it is more easily manipulated by being directly coupled to the gas chromatograph and thus the use of a hypodermic needle and a rubber injection septum is avoided.

The system is used in conjunction with an external-loop gas injection valve and replaces the loop normally used with this valve. In this work, a Pye Unicam 792082 injection valve was used.

In use, the injection valve is left in the "inject" position and the by-pass on the desorption system used to maintain a continuous flow of carrier gas. This arrangement permits the adsorption tube to be heated without carrier gas flowing through the tube and hence allows more rapid injection of the sample, thus preventing the peak broadening that usually occurs with slow heating systems.

Stainless-steel tubing is used in the construction of the system, with Nupro bellows-sealed valves fitted with Swagelok couplings (available from Techmation Ltd.). The adsorption tube is fitted into the system by using Nupro O-ring couplings, which provide good gas-tight seals (Fig. 2).
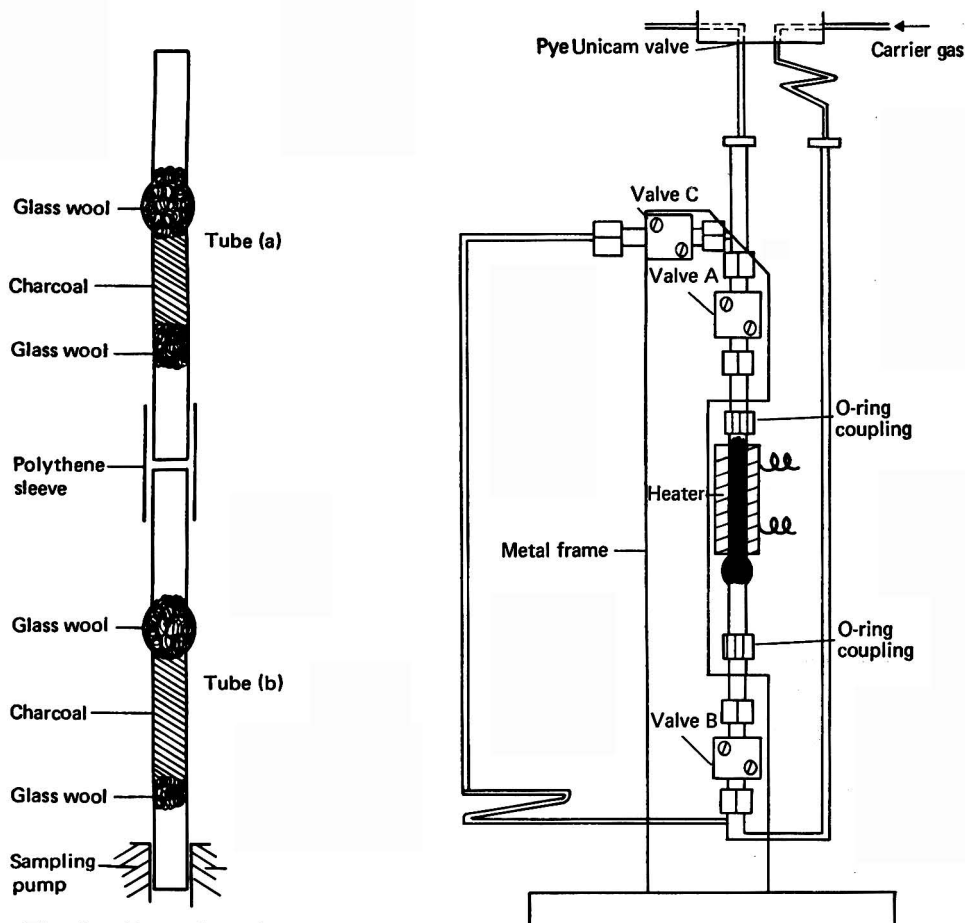
Fig. 1.   Two adsorption tubes joined in series.
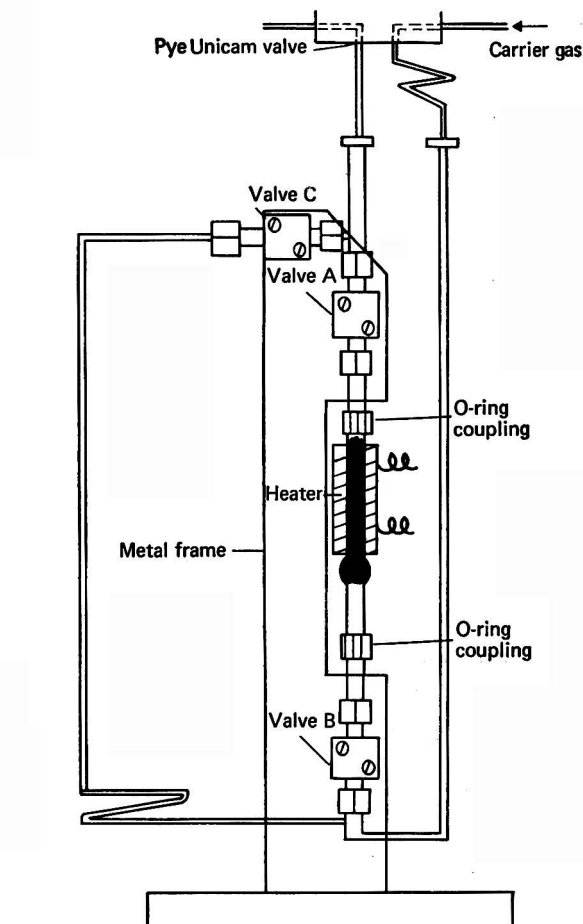
Fig. 2.   The desorption - injection system.

Heater. The heater is constructed by winding 30 turns of 1.5 mm diameter 80 + 20 nickel - chromium wire around a ceramic tube 6 cm long by 1.2 cm o.d., with a wall thickness of 0.2 cm, and encasing the windings in a refractory cement.

A mains-isolating transformer with a 10–15-V tapping should be used to power the heater. In this work we used the 10.5-V tap, which raised the temperature of the adsorption tube from 20 to 300 °C in 4 min.

Procedure

Activation of adsorption tubes

Connect the desorption system to the sample loop ports on the injection valve (Fig. 2). Close valves A and B (Fig. 2), open valve C and turn the injection valve to the "inject" position. Carrier gas will now flow through the by-pass on the desorption system. Remove the two bolts that secure valve B to the frame and fit the lower end of the adsorption tube into the O-ring coupling attached to this valve.

Place the heater in position over the adsorption tube, and fit the upper end of the adsorption tube into the O-ring coupling attached to valve A. Secure valve B on to the frame by means of the two small bolts and tighten all couplings. Next open valve B, then A, and close valve C; switch on the heater and heat the tube for 15 min. Then switch off the heater and allow the tube to cool, maintaining the flow of carrier gas through the adsorption tube. When the tube has cooled, close valves A and B, open valve C and detach the adsorption tube from the system. Finally, fit rubber stoppers to the open ends of the tube; two tubes are required per sample.

Sampling

When used to determine acetone concentrations of about 10 p.p.m. the adsorption tube serves to concentrate the sample and an air volume of 1 l is adequate. With higher concentrations of acetone smaller samples will give adequate sensitivity with most gas-chromatographic detectors, but it should be borne in mind that a small, local sample may not accurately represent the acetone concentration in a large chamber. The advantage of the adsorption tube method of sampling is that the atmosphere can be sampled slowly (intermittently if necessary) at different points in the room if required.

Any suitable means of drawing a measured volume of air through the adsorption tube at flow-rates of up to 100 ml min^{-1} can be used for sampling. In areas where a fire risk precludes the use of electrically driven vacuum pumps, a Dräger hand-operated sampling pump, when calibrated, is suitable.

Two adsorption tubes are used in series (Fig. 1), the second tube serving as an indicator that the analytical tube has not been overloaded. The ends of the two tubes should meet inside the polythene connector, which should fit tightly around both tubes. The composite adsorption tube should be fitted into the pumping system with the bulb ends away from the pump.

When the required volume of air has been drawn through the adsorption tube the open ends of each tube should be stoppered and both tubes retained for analysis.

Desorption and injection

With valve C open and valves A and B closed, fit the analytical adsorption tube [(a) in Fig. 1] into the system with the heater in place over the tube. Note that carrier gas will flow through the tube in the same direction as the air sample.

Close valve C and open valve B, then A, and allow the carrier gas to sweep the residual air from the tube for 1 min. Open valve C, close valves A and B and switch on the heater; heat the adsorption tube for 4 min. Next close valve C, open valve A and then B; the carrier gas will sweep the acetone vapour into the column.

Repeat the desorption and injection procedure using the second tube (b) in place of the analytical tube. A zero reading should be obtained from the analysis of the contents of this tube. If this is not the case, the sampling procedure should be repeated, using a smaller air sample.

Calibration

By use of a reliable hypodermic syringe inject appropriate calibration volumes of acetone or acetone in solution in water into the bulb end of an activated adsorption tube.

Desorb and inject the calibration sample by using the same technique as was used in the analysis of the sample.

Chromatographic conditions

The analysis was carried out on a Pye Unicam, Model 104, gas chromatograph fitted with a flame-ionisation detector. A 2 m by 6 mm column packed with 80–100-mesh Porapak Q and operated at 200 °C was used in order to separate the acetone from other organic vapours known to be in the atmosphere at the time of sampling. Argon, at a flow-rate of 60 ml min^{-1}, was used as the carrier gas.

Comparison of Results

Atmospheres of acetone vapour in air were prepared by vaporising the liquid in a sealed fume cupboard and allowing the vapour mixture to reach equilibrium. The atmosphere was sampled and analysed by the method described in this paper and simultaneously sampled and analysed by the modified 2,4-dinitrophenylhydrazine method of Smith and Wood.[2] The results are given in Table I.

TABLE I

DETERMINATION OF ACETONE BY USE OF TWO DIFFERENT METHODS

Acetone, p.p.m.		
2,4-Dinitrophenylhydrazine method	Charcoal-adsorption method	Difference, %
280	290	+ 3.6
310	330	+ 6.5
620	600	− 3.2
560	570	+ 1.8
1 250	1 190	− 4.8
1 090	1 150	+ 5.5
1 620	1 700	+ 4.9
1 600	1 700	+ 6.3
1 970	2 150	+ 9.1
2 060	2 300	+11.7

The results show reasonable agreement between the two methods at acetone concentrations up to 1 700 p.p.m. The efficiency of absorption of acetone vapour in the double absorption vessels used in the 2,4-dinitrophenylhydrazine method appeared to decrease at concentrations of about 2 000 p.p.m.

Samples of the acetone atmospheres were further diluted with clean air by means of a flow-mixing technique, and the resulting atmospheres sampled and analysed by the charcoal-adsorption method. The results are given in Table II, and show good agreement over the range of concentrations examined.

TABLE II

COMPARISON OF CALCULATED RESULTS WITH THOSE OBTAINED BY
USING THE CHARCOAL-ADSORPTION METHOD

Acetone,	Calculated	..	11	20	60	119	170
p.p.m.	Measured	..	10	23	57	125	165

As a measure of the precision of the technique, ten samples from a large chamber (constant concentration of acetone vapour) were collected and analysed by each of the two methods and the results compared (Table III). It can be seen that the standard deviation of the charcoal-adsorption technique compares favourably with that of the 2,4-dinitrophenylhydrazine method.

TABLE III

DETERMINATION OF A CONSTANT CONCENTRATION OF ACETONE IN AN ATMOSPHERE

2,4-Dinitrophenylhydrazine method, p.p.m.	Charcoal-adsorption method, p.p.m.
450	450
430	450
450	440
440	430
460	460
430	450
450	440
430	450
440	440
430	430
Standard deviation: 11.0	Standard deviation: 9.7

References

1. Ellis, C. F., Kendall, R. F., and Eccleston, B. H., *Analyt. Chem.*, 1965, **37**, 511.
2. Smith, A. F., and Wood, R., *Analyst*, 1970, **95**, 683.

Communication

Material for publication as a Communication must be on an urgent matter and be of obvious scientific importance. Rapidity of publication is enhanced if diagrams are omitted, but tables and formulae can be included. Communications should not be simple claims for priority: this facility for rapid publication is intended for brief descriptions of work that has progressed to a stage at which it is likely to be valuable to workers faced with similar problems. A fuller paper may be offered subsequently, if justified by later work.

Manuscripts are not subjected to the usual examination by referees and inclusion of a Communication is at the Editor's discretion.

Determination of Phosphorus in Steel by Atomic-absorption Spectrophotometry with Electrothermal Atomisation

There appears to be a continued and considerable interest in the possibility of determining phosphorus by atomic-absorption spectrophotometry. In the "wet" laboratory at present, for example, most metallic elements can be determined by atomic-absorption spectrophometry, and sulphur and carbon by combustion methods, leaving phosphorus as the only element that has to be measured colorimetrically.

The availability of electrodeless discharge lamps for phosphorus has much improved the situation. Such lamps provide a phosphorus line at 213.6 nm of adequate intensity and good stability. Unfortunately the strongest absorbing lines of phosphorus occur at 177.5, 178.3 and 178.8 nm, and for routine work would require a spectrometric system in which the whole light path is purged with argon or nitrogen. The sensitivity of the available line at 213.6 nm has only one hundredth[1] of their reported sensitivity.

The sensitivity of the phosphorus 213.6 nm line in the dinitrogen oxide - acetylene flame is about 80–100 p.p.m., which is equivalent to 0.16–0.2% of phosphorus in a steel sample that has been dissolved and made up to a 5% solution.

As typical phosphorus levels being determined in steel and copper alloys are from 0.01 to 0.1%, we were prompted to investigate the possibility of measuring phosphorus in such samples using the

electrothermal method of atomisation. A further encouraging factor in this context is the present availability of electrothermal atomisation furnace tubes of a new design (Profile tubes*), which are known to improve the sensitivity of many elements by a factor of 3–5 over that of the standard cylindrical tube.

Experimental

Equipment

The following instruments were used: a Pye Unicam SP2900 atomic-absorption spectrophotometer with simultaneous background correction; a Pye Unicam SP9-01 digital electrothermal atomiser with graphite Profile tubes; a Pye Unicam SP9-20 EDL radio-frequency power supply; and a phosphorus electrodeless discharge lamp.

Operating Procedure

Dissolution method

Weigh 1.000 g of sample into a 25-ml beaker. Add 2.5 ml of hydrochloric acid (sp. gr. 1.18) and 2 ml of nitric acid (sp. gr. 1.42). When the initial reaction has subsided, add 1.5 ml of perchloric acid (sp. gr. 1.54) and warm the mixture gently until the perchloric acid refluxes down the sides of the beaker. Cool, add 5 ml of de-ionised water and filter through a Whatman 541 paper into a 20-ml calibrated flask. Wash with 5 ml of de-ionised water, then dilute the filtrate plus washings to volume.

Calibration and sample injection

Calibration is easily carried out by the method of standard additions. Prepare standards of 10, 20 and 30 p.p.m. of phosphorus from a stock solution of ammonium dihydrogen orthophosphate (these concentrations are equivalent to 0.02, 0.04 and 0.06% of phosphorus in the original sample). The injection procedure consists in the following steps:

1. inject 20 μl of sample solution into the electrothermal atomisation furnace tube, carry out "dry" and "ash" phases as detailed below, then stop the programme;

2. inject 20 μl of de-ionised water, carry out the complete programme from the beginning, monitoring the atomic-absorption peak during the "atomise" phase;

3. repeat steps 1 and 2 for each standard, injecting 20 μl of standard instead of de-ionised water in step 2;

4. plot absorbance peak height against concentration of added phosphorus and derive the phosphorus concentration of sample.

Instrumental settings

The following conditions were used.

Electrothermal atomiser:

			Phase			
	Dry	Ash	Delay	Atomise	Delay	Clean
Temperature/°C	100	300	—	2 750	—	2 850
Time/s	20	30	10	4.0	10	6.0

Spectrophotometer: Wavelength, 213.6 nm; band pass, 0.8 nm; and electrodeless discharge lamp power, 8 W.

* Patent applied for.

Results

The results in Table I were obtained using British Chemical Standard steel samples.

TABLE I

RESULTS FOR ANALYSIS OF BCS STEELS

The duplicate values quoted are from separate sample weighings.

Steel	Sample	Phosphorus content, %	
		Certificate value	Duplicate results
Carbon steel	BCS 152/3	0.062	0.062, 0.059
	BCS 240/2	0.025	0.026, 0.026
Mild steel	BCS 456	0.010	0.010, 0.012
Low alloy steel	BCS 408	0.043	0.045, 0.044

The atomisation temperature used was that which gave the maximum absorbance peak height. It is our intention to extend this type of method to copper alloys and also to examine the whole procedure for possible improvements. There would seem to be no reason why an aliquot of the sample solution remaining after the above analysis should not be diluted and used for the determination of the metal constituents by a flame atomic-absorption method such as that already in use.[1,3]

References

1. L'vov, B. V., in Dagnall, R. M., and Kirkbright, G. F., *Editors*, "Atomic Absorption Spectroscopy," Butterworths, London, 1970, p. 28.
2. Thomerson, D. R., and Price, W. J., *Analyst*, 1971, **96**, 825.
3. "Atomic Absorption Methods: Elements in Steels," Pye Unicam, Cambridge, 1975.

P. J. Whiteside
W. J. Price

Pye Unicam Ltd,
York Street,
Cambridge, CB1 2PX

Book Reviews

ELECTROTHERMAL ATOMIZATION FOR ATOMIC ABSORPTION SPECTROMETRY. By C. W. FULLER. *Analytical Sciences Monographs, No.* 4. Pp. viii + 127. London: The Chemical Society. 1977. Price £6.75; CS Members £5.

This small book represents the first monograph completely devoted to atomic-absorption spectrometry with electrothermal atomisation. Because the design of atomic-absorption spectrometers, light sources, optics, radiation measurement, etc., has already been adequately discussed in some monographs on atomic-absorption spectrometry with flames, the author refrained from repeating these aspects.

After a brief outline of the historical development of electrothermal atomisers, the commercial versions of carbon furnaces, cups, rods and metal filaments are used to illustrate atomiser design features, and in a further section theoretical aspects of atomisation processes are discussed. For more detailed study, the reader can easily find useful hints and references.

The major part of the book, consisting of 70 pages, deals in three sections with general experimental conditions, analytical conditions for the determination of 50 elements and analytical applications to special sample matrices. This part will prove useful for beginners interested in developing analytical procedures in their laboratories. However, it must be pointed out that the figures quoted for sensitivity, detection limit, pyrolysis and atomisation temperature that are given in the section treating the analytical determination of elements can be only guide values. Exact numerical values are relevant only if the operating conditions and the analytical problem are accurately defined. For the same reason, the wavelengths for background measurements, *e.g.*, by the two-line technique, are useless. On the other hand, the last section, on applications to special sample matrices, is very useful. Numerous analytical procedures for the determination of elements in metals, oils, biological samples, water, etc., are surveyed in short sub-sections accompanied by extensive tables. For more detailed information about the procedures in question references to the original literature are given.

This book reflects the present status of atomic-absorption spectrometry with electrothermal atomisation and will serve as a useful guide to analytical chemists interested in the development of new analytical procedures.   H. MASSMANN

THERMAL ANALYSIS. Edited by W. W. WENDLANDT and L. W. COLLINS. *Benchmark Papers in Analytical Chemistry, Volume* 2. Pp. xiv + 338. Stroudsburg, Pennsylvania: Dowden Hutchinson & Ross, Inc. Distributed by Halsted Press. 1976. Price £26.20; $43.20.

This book consists of a collection of original papers concerned with the development of two of the techniques of thermal analysis, viz., differential thermal analysis (DTA) and thermogravimetry (TG), and the papers deal solely with the analytical aspects of these techniques.

The Editors state that they hope that their choices represent the most important papers in the development of DTA and of TG in analytical chemistry. To some extent their hopes are fulfilled, as several of the papers are universally accepted as classic examples of, say, DTA, DSC and TG, but others are not so easily accepted. One of the criteria for inclusion in a book of this nature must be that a particular paper was the first significant step forward in the technique, either in the application under acceptable analytical conditions, or in the development of the technique—in theory or practice. Some of the papers in the volume do not meet this criterion.

One may question the purpose of books such as this. Is the intention to make available to the beginner a series of papers presented so that the development of the techniques is obvious, or to give to the experienced worker a piece of dilettantism with which to beguile the hours between heating the sample and obtaining the computer print-out of the relevant results? Whatever the main purpose, it could have been achieved more successfully by better presentation.

An article by Le Chatelier has been translated expressly for this volume; there seems to be merit in this course since the original paper is not readily available and the article is certainly worthy of inclusion. However, there are several papers which have been reproduced from journals which are generally available, and which will need to be so if the reader is to read the article with ease and visual comfort. One such paper, by Vold (*Analyt. Chem.*, 1949), is so poorly reproduced that one wonders if the printing process has gone awry as the lines of print are curved

and the density of the print varies across the page. This is not an isolated example as several papers from the same journal have suffered a similar fate. The diagrams are not usable, and yet in other papers the Editors have noted that they have not been able to reproduce certain diagrams because of their poor photographic texture in the original publication. Space in books and in libraries is always at a premium, and a short monograph by the same authors, giving a critical appraisal of these and other papers with, if appropriate, an appendix containing a reading list, would have been, at least for the present reviewer, a more worthwhile venture.   L. S. BARK

NEW DEVELOPMENTS IN SEPARATION METHODS. Edited by ELI GRUSHKA. Pp. x + 246. New York and Basle: Marcel Dekker. 1976. Price SwFr.85.

Separation methods are an integral part of almost every branch of the physical and biological sciences, and consequently it is necessary for scientists from the various disciplines to meet, exchange ideas, compare the various applications of similar techniques and try to arrive at some common understanding of the field of separation methods. Indeed, it is necessary to have such meetings to create "separation sciences" out of separation methods.

This book consists of eleven of the papers contributed at a symposium on "New Methods of Separation" held in Los Angeles in 1974. The papers cover a very wide range of subjects and techniques, from anion separation using foams, to zonal centrifugation for some selected bioseparations. Several papers deal mainly with theoretical problems while others have a more pragmatic approach to the problems of separation. The standard of the work is generally high and there will be few readers who will not gain some insight into the field from this book.   L. S. BARK

ISOELECTRIC FOCUSING. Edited by NICHOLAS CATSIMPOOLAS. Pp. xii + 265. New York, San Francisco and London: Academic Press. 1976. Price £16.70; $23.50.

Isoelectric focusing (IEF) is a technique whereby proteins can be separated according to their different isoelectric points (pI) in a stabilised pH gradient. Proteins migrate under the influence of an applied electric field through the pH gradient until they reach a point at which the pH equals their pI. At this point they have no over-all charge and are "focused" into extremely narrow bands. The pH gradient is established by amphoteric buffers termed ampholytes and can be stabilised in several ways, for example by a gel or sucrose density gradient, and a variety of apparatus can be used. All afford extremely high resolution of proteins.

This book consists of nine chapters by prominent workers in the field of IEF. Kolin gives an interesting but limited account of his early experiments with the technique while Rilbe presents a rigorous explanation of the basic theory. Vesterberg's comprehensive chapter on ampholytes covers the topic in depth, discussing their synthesis, properties and separation from protein in detail. In comparison, Chrambach and Baumanns' contribution on focusing in polyacrylamide gels treats this important aspect rather superficially. An explicit treatment would have been more useful for those intending to make use of this technique. Wrigley, on the other hand, gives just such an account of isoelectric focusing combined with electrophoresis. It is well written and is most informative, as is the chapter by Radola on focusing in granulated gels. Both chapters will be of great value to workers wishing to separate proteins by these methods. The last three chapters by Fawcett, Bours and Catsimpoolas, on continuous flow, focusing in free solution and transient-state focusing, respectively, describe variations of the technique that have not yet found extensive application. The continuous flow system has possibilities for use as a large-scale separation process, but transient-state focusing, while giving an interesting insight into the kinetics and mechanism of focusing and pH gradient formation may, as the author says, be "possibly labelled a laboratory curiosity."

The book tends to be repetitive, a common trait in works that consist of chapters by different authors. For example, Fig. 8 on p. 46 re-appears as Fig. 1 on p. 55 in the chapters by Rilbe and Vesterberg, respectively, and the characteristics of ampholytes are described by several contributors.

Catsimpoolas states in the preface that the "volume is intended to serve in some useful way all those workers who need to know what isoelectric focusing is all about." The book does not fulfil this intention entirely, as it would be of only limited use to newcomers to the field. It is, however, interesting but not essential reading for those who already have some knowledge of IEF.   J. W. LLEWELLYN

METHODS OF BIOCHEMICAL ANALYSIS. Volume 23. Edited by DAVID GLICK. Pp. x + 435. New York, London, Sydney and Toronto: John Wiley. 1976. Price £19.20; $31.

This volume deals with several analytical procedures of particular interest to the protein chemist or enzymologist and several which, although based in physical chemistry, will soon find more general application in biology.

C. H. Spink and I. Wadsö present a timely review of calorimetry as an analytical tool in biochemistry and biology. An exhaustive account is given of the design principles and types of calorimeter (including commercial designs), the selection of the design for a particular application (*e.g.*, measurement of small heat changes, fast or slow processes) and of the errors inherent in the measurements. The applications of the method to biochemical processes (thermodynamic studies, binding reactions, transition studies and analytical applications such as kinetic measurements) and in biology (bacterial systems, yeasts and algae and the erythrocyte) are discussed.

The article is too long, general and detailed to be easily readable but will be an invaluable stimulus to biologists venturing into calorimetric measurement and a useful reference guide to those familiar with the method.

W. R. F. Seitz and M. P. Neary provide a brief account of recent advances in bioluminescence and chemiluminescence assay. The article is intended to update and supplement the chapter by B. L. Strehler, devoted to firefly ATP assay, in Volume 16 of the series. Consequently the ATP assay gets cursory attention and the authors are concerned with the extension and more general application of the technique.

Their approach is straightforward and just sufficient theoretical detail is given to acquaint a novice with the principle of the method. Sections are included which deal with instrumentation, firefly bioluminescence (as ATP assay, particularly in the determination of biomass), bacterial luminescence [in FMN and NAD(P)H assay] and chemiluminescence detection of hydrogen peroxide (in glucose and NADH determination). Miscellaneous examples of the measurement of potentially carcinogenic *N*-nitrosoamines and trace metals are also given.

The article provides a good, practical account of the methodology and application of luminescence without too many theoretical frills.

C. A. Burtis, T. O. Tiffany and C. D. Scott give an account of a centrifugal fast analyser for biochemical and immunological analyses. This account describes the instrument concept and design in addition to the theory and practice of its application, and is authoritative and easily comprehensible. However, the concept is simple and does not break any really new ground. In view of this, I find the article rather long, particularly in the section descriptive of the instrument. Fast analysers are now commercially available and most readers will be interested in the application of the technique to their problem rather than in the innards of the machine.

A. McPherson, Jr., describes the growth and preliminary investigation of protein and nucleic acid crystals for X-ray diffraction analysis in an article that will help to bridge the gap between crystallographers and protein chemists. The author deliberately avoids discussion of the technical points of X-ray diffraction but provides the necessary bibliography and encouragement for those who wish to undertake crystallographic analyses. The article contains a comprehensive review of procedures of crystallisation with plenty of practical detail and many instances of minor variation of method. A very full table of procedures applied to particular macromolecules which have undergone analysis is provided and should prove useful in the selection of a method.

The article is well written and could be the answer to many an enzymologists prayer. It was particularly well received in my own laboratory.

M. Wilchek and C. S. Hexter describe approaches to the purification of biologically active compounds by affinity chromatography. Although this method of purification has been with us for a decade, many technical problems still hamper its application. The present authors have been associated with affinity chromatography since its inception and are well qualified to review it. In general, this good, concise article is refreshingly objective and points out the drawbacks as well as the advantages of the method.

The main advantage seen for the technique is its specificity, while almost all of the disadvantages stem from the method of covalent attachment of the ligand to its solid support. For steric reasons a flexible spacer must usually be interposed between ligand and carrier matrix before the macromolecule can bind. The chemical coupling of the spacer to the matrix often introduces charged groups and the spacers are generally hydrocarbon molecules. These factors introduce non-specific ion-exchange and hydrophobic interaction between macromolecule and matrix, thus

largely destroying the specificity of binding. Additionally the chemical modification of the ligand during the immobilisation procedure may itself preclude binding of the ligand to the selective macromolecule and the limited capacity of the matrix often necessitates substantial preliminary purification of the macromolecule by conventional techniques. The authors describe the proper choice of matrix, spacer and coupling reaction to minimise these effects. I must note, however, that they have a predilection for hydrazide coupling procedures which help to eliminate ion-exchange effects. These effects they believe to be the most important in contributing to lack of specificity.

Most of the review deals with the purification of proteins and brief sections deal with nucleic acids and peptides. A list of several enzymes already purified is provided but must be approached with caution. Because of the non-specific binding described, the number of claims for affinity chromatography far outweighs the number of properly established examples. The clue to the usefulness of the method is contained in the first paragraph of the article ". . . affinity chromatography shows the promise of becoming the pre-eminent method for the isolation of macromolecules present biologically at extremely low concentration." It is not the method for more commonplace or abundant substances.

This review, as explained by the authors, was written early in 1974 and the great body of recent literature is not considered. Nevertheless, it is a readable and useful article.

The volume as a whole will make a useful addition to any library.　　　　J. S. Easterby

Quadrupole Mass Spectrometry and its Applications. Edited by Peter H. Dawson. Pp. xxii + 349. Amsterdam, Oxford and New York: Elsevier Scientific Publishing Company. 1976. Price Dfl129; $49.75.

The intention of this book is to produce a systematic text rather than a series of reviews in order to provide a broader than usual viewpoint. The book is a definitive text of quadrupole mass spectrometry and the different areas on this subject are so highly specialised it is improbable that any one author could deal adequately with them. The multi-author format adopted has, in general, been successful and it is noteworthy that a lot of repetition has been avoided by the circulation of drafts between authors, something that should be encouraged in books of this type.

The first five chapters deal with the principles of operation, the analytical theory and the imperfections of real instruments in the greatest mathematical detail. For those who are able to digest this material, the next four chapters deal with various practical types of spectrometer, including the mass filter, the monopole, quadrupole ion traps and the time-of-flight mass spectrometer. The remaining four chapters deal with applications of quadrupole mass spectrometry in various fields, *e.g.*, atomic and molecular physics, atmospheric research, gas chromatography and medical and environmental applications.

Quadrupole mass spectrometers are shown to be very versatile devices and of use in many applications where the more conventional magnetic sector instruments could not easily be used. A good example of this for the analytical chemist is in combination with the liquid chromatograph, where the high source pressures obtained can easily be tolerated.

The book holds together well in spite of the multi-author format, although the applications chapters seem to be very self-contained. It is also felt that a book entitled "Quadrupole Mass Spectrometry and Its Applications" could have had a little less mathematical theory and more applications, but this is a minor criticism.

It should be pointed out that this is not a book for the beginner but one for the quadrupole mass spectrometer specialist. There does seem to have been a shortage of books on this subject and this book will surely help to fill that gap, in spite of the excessively high price, which seems to be a characteristic of most specialist books. In summary, it is strongly recommended to all those who wish to explore the field of quadrupole mass spectrometry thoroughly.

K. S. Webb

Erratum

April (1977) issue, p. 317. "Modern Fluorescence Spectroscopy." Volumes 1 and 2. Edited by E. L. Wehry. These two volumes are available in the UK and Europe from Heyden and Son Ltd., London. Price (2 volumes) £35; DM224.

LECTURES AND COURSES

**KINGSTON
POLYTECHNIC**
ANALYSIS
MSc in ANALYTICAL CHEMISTRY
An instrumentally-biased two-year part-time course
LRIC ADVANCED ANALYTICAL CHEMISTRY
LRIC/LIBiol BIOCHEMICAL ANALYSIS

Specialist one-year part-time courses primarily offered to Holders of HND/C in chemistry or appled biology. These courses are also suitable as 'refresher' courses, and applicants who do not hold HND/C will be considered on their merits. Candidates successfully completing the course will be awarded a Certificate of Supplementary Study and, subject to certain additional requirements, may qualify for admission as Licentiates of the Royal Institute of Chemistry, or the Institute of Biology.

Further information can be obtained from the Secretary, School of Chemical and Physical Sciences, Kingston Polytechnic, Penrhyn Road, Kingston upon Thames KT1 2EE 01-549 1366

Kinetic Micro-determination of Manganese in Natural Waters and of Iridium, Nitrilotriacetic Acid and 1,2-Diaminocyclohexane-*NNN'N'*-tetraacetic Acid

An automatic kinetic spectrophotometric method is described for the ultra-micro determination of manganese and iridium, based on their catalytic effect on the periodate - phosphinate reaction. The method is also used for the determination of nitrilotriacetic acid (NTA) and 1,2-diaminocyclohexane-*NNN'N'*-tetraacetic acid (DCTA), on the basis of their activating and inhibiting effect, respectively, on the manganese-catalysed periodate - phosphinate reaction. The time required for the reaction to consume a fixed amount of periodate is measured automatically and related directly to the concentration of catalyst, activator or inhibitor. Manganese and iridium at the 10^{-8}–10^{-7} M level and NTA and DCTA at the 10^{-6} M level were determined with average errors of about 2%. The method has been applied to the determination of manganese in natural waters.

Keywords: *Manganese determination*; *iridium determination*; *nitrilotriacetic acid*; *1,2-diaminocyclohexane*-NNN'N'-*tetraacetic acid*; *natural waters*

D. P. NIKOLELIS and T. P. HADJIIOANNOU

Laboratory of Analytical Chemistry, University of Athens, Athens, Greece.

Determination of Citrate as its Iron(III) Complex by Differential Pulse Polarography

A method for determining citrate as its complex with iron(III) by differential pulse polarography is described. The method is sensitive to 5 μg ml^{-1} of citrate, without any interference from equimolar propan-2-onedicarboxylate and propenetricarboxylate ions and 10% of oxalate and tartrate ions. The limits of error in citrate concentrations determined by the proposed method are better than $\pm 2.5\%$.

The feasibility of determining oxalate, succinate and tartrate by means of differential pulse polarography was also explored and the method was found to be applicable to the determination of oxalate.

Keywords: *Citrate determination*; *citrate - iron(III) complex*; *differential pulse polarography*

R. PRASAD

Inco Europe Limited, European Research and Development Centre, Wiggin Street, Birmingham, B16 0AJ.

Application of Gas - Liquid Chromatography to the Analysis of Essential Oils

Part V. Determination of 1,8-Cineole in Oils of Lavender and Lavandin

Report prepared by the Essential Oils Sub-Committee.

Keywords: *1,8-Cineole determination*; *oils of lavender and lavandin analysis*; *gas - liquid chromatography*

ANALYTICAL METHODS COMMITTEE

The Chemical Society, Burlington House, London, W1V 0BN.

Some Difficulties Encountered in Speciation Studies of Arsenic

Short Paper

Keywords: Arsenic speciation; silver diethyldithiocarbamate method; biological and organic materials; arsenic reduction

B. I. DIAMONDSTONE and R. W. BURKE

Institute for Materials Research, National Bureau of Standards, Analytical Chemistry Division, Washington, DC 20234, USA.

Determination of Acetone Vapour in the Atmosphere

Short Paper

Keywords: Acetone determination; atmosphere; adsorption; gas chromatography

J. E. SCOTT

Analytical Laboratory, Philips Hamilton, Wellhall Road, Hamilton, Lanarkshire, Scotland, ML3 9BZ.

Determination of Phosphorus in Steel by Atomic-absorption Spectrophotometry with Electrothermal Atomisation

Communication

Keywords: Phosphorus determination; steel analysis; atomic-absorption spectrophotometry

P. J. WHITESIDE and W. J. PRICE

Pye Unicam Ltd., York Street, Cambridge, CB1 2PX.

THE ANALYST

THE ANALYTICAL JOURNAL OF THE CHEMICAL SOCIETY

CONTENTS